OPEN ACCESS

ORIGINAL ARTICLE

MicroRNA-21 is a potential link between non-alcoholic fatty liver disease and hepatocellular carcinoma via modulation of the HBP1-p53-Srebp1c pathway

Heng Wu,[1] Raymond Ng,[2] Xin Chen,[3] Clifford J Steer,[1,4] Guisheng Song[1]

▶ Additional material is published online only. To view please visit the journal online (http://dx.doi.org/10.1136/gutjnl-2014-308430).

[1]Department of Medicine, University of Minnesota Medical School, Minneapolis, Minnesota, USA
[2]Agency for Science Technology and Research, Singapore, Singapore
[3]Department of Bioengineering and Therapeutic Sciences, University of California San Francisco, San Francisco, California, USA
[4]Department of Genetics, Cell Biology and Development, University of Minnesota, Minneapolis, Minnesota, USA

Correspondence to
Dr Guisheng Song, Division of Gastroenterology, Hepatology and Nutrition, Department of Medicine, University of Minnesota Medical School, MMC 36, VFW Cancer Research Center, V354, 406 Harvard Street SE, Minneapolis, MN 55455, USA; gsong@umn.edu

Received 19 September 2014
Revised 12 July 2015
Accepted 14 July 2015
Published Online First 17 August 2015

Linked

▶ http://dx.doi.org/10.1136/gutjnl-2015-310044

CrossMark

To cite: Wu H, Ng R, Chen X, *et al*. *Gut* 2016;**65**:1850–1860.

ABSTRACT

Background Non-alcoholic fatty liver disease (NAFLD) is a major risk factor for hepatocellular carcinoma (HCC). However, the mechanistic pathways that link both disorders are essentially unknown.

Objective Our study was designed to investigate the role of microRNA-21 in the pathogenesis of NAFLD and its potential involvement in HCC.

Methods Wildtype mice maintained on a high fat diet (HFD) received tail vein injections of microRNA-21-anti-sense oligonucleotide (ASO) or miR-21 mismatched ASO for 4 or 8 weeks. Livers were collected after that time period for lipid content and gene expression analysis. Human hepatoma HepG2 cells incubated with oleate were used to study the role of miR-21 in lipogenesis and analysed with Nile-Red staining. microRNA-21 function in carcinogenesis was determined by soft-agar colony formation, cell cycle analysis and xenograft tumour assay using HepG2 cells.

Results The expression of microRNA-21 was increased in the livers of HFD-treated mice and human HepG2 cells incubated with fatty acid. MicroRNA-21 knockdown in those mice and HepG2 cells impaired lipid accumulation and growth of xenograft tumour. Further studies revealed that *Hbp1* was a novel target of microRNA-21 and a transcriptional activator of *p53*. It is well established that p53 is a tumour suppressor and an inhibitor of lipogenesis by inhibiting *Srebp1c*. As expected, microRNA-21 knockdown led to increased *HBP1* and *p53* and subsequently reduced lipogenesis and delayed G1/S transition, and the additional treatment of *HBP1*-siRNA antagonised the effect of microRNA-21-ASO, suggesting that *HBP1* mediated the inhibitory effects of microRNA-21-ASO on both hepatic lipid accumulation and hepatocarcinogenesis. Mechanistically, microRNA-21 knockdown induced *p53* transcription, which subsequently reduced expression of genes controlling lipogenesis and cell cycle transition. In contrast, the opposite result was observed with overexpression of microRNA-21, which prevented *p53* transcription.

Conclusions Our findings reveal a novel mechanism by which microRNA-21, in part, promotes hepatic lipid accumulation and cancer progression by interacting with the *Hbp1-p53-Srebp1c* pathway and suggest the potential therapeutic value of microRNA-21-ASO for both disorders.

Significance of this study

What is already known on this subject?

- miR-21 is upregulated in human hepatocellular carcinoma.
- p53 is a transcriptional repressor of *Srebp1c*.

What are the new findings?

- miR-21 is highly expressed in hepatocytes, and its expression is significantly increased in livers of dietary obese mice and human HepG2 cells incubated with fatty acid.
- Antagonising miR-21 in liver prevents hepatic lipid accumulation and growth of xenograft tumour.
- miR-21 knockdown prevents G1/S transition and cancer cell proliferation.
- *HBP1* is a novel target of miR-21 and a transcriptional activator of *p53*.
- *HBP1* mediates the inhibitory effects of miR-21-anti-sense oligonucleotide on hepatic lipid accumulation and hepatocarcinogenesis.
- miR-21 is a potential association between non-alcoholic fatty liver disease (NAFLD) and hepatocellular carcinoma (HCC) via interacting with the *Hbp1-p53-Srebp1c* pathway.

How might it impact on clinical practice in the foreseeable future?

- Our data suggest that miR-21 is a potential therapeutic target for both NAFLD and HCC.

INTRODUCTION

The incidence of hepatocellular carcinoma (HCC) worldwide nearly matched its mortality, demonstrating the aggressive nature of this malignancy and limited therapeutic options.[1] Although HBV and HCV are major risk factors of HCC, non-alcoholic fatty liver disease (NAFLD) remains a common underlying pathology to the majority of patients with HCC in the Western world.[2] The incidence of NAFLD is growing rapidly due to the prevalence of obesity.[3] It is estimated that 90% of obese patients have some form of fatty liver, ranging from simple steatosis to more severe forms of non-alcoholic steatohepatitis (NASH) and cirrhosis with its associated high risk of HCC. In addition, given limited effects of chemotherapy and the relative insensitivity of HCC to radiotherapy, complete tumour extirpation represents the only choice for a long-term cure. Unfortunately, the

majority of patients are not eligible for surgical resection because of tumour extent or underlying liver dysfunctions including NAFLD. As described above, despite the strong association between NAFLD and HCC, the underlying mechanisms are largely unknown due in part to their complex nature of disease.

The discovery of a class of naturally occurring small non-coding RNAs, termed microRNAs (miRNAs),[4 5] has stimulated a new field of research on NAFLD and HCC. Alterations in miRNA expression have been reported in human individuals with NAFLD/NASH and HCC.[6 7] Reflective of their key roles in lipid metabolism and carcinogenesis,[5 8] miRNAs have been suggested as novel therapeutic targets for both metabolic diseases and human cancers. However, the miRNAs associated with both NAFLD and its potential sequel HCC are poorly described. Our interest in miR-21 arose initially from hepatocyte-specific miRNA profiling studies in mouse livers, in which we showed that miR-21 is highly expressed in hepatocytes. Furthermore, we observed that high fat diet (HFD) treatment significantly induced expression of miR-21 in livers of mice. By antagonising miR-21 in liver, we were able to prevent hepatic lipid accumulation in dietary obese mice. Consistent with our findings, miR-21 expression was significantly upregulated in human patients with NASH.[6] It is also known that miR-21 is a potent promoter of HCC and other human cancers.[7 9] These data led us to hypothesise that miR-21 plays an important role in the pathogenesis of NAFLD and its potential progression to HCC. In the present study, we have investigated the regulatory role of miR-21 in linking NAFLD and HCC in both in vivo and in vitro model systems.

MATERIALS AND METHODS

Bioinformatic analysis

Identification of miR-21 target genes was conducted as previously described with minor revision.[10] In detail, we compiled a list of downregulated genes in livers of patients with NAFLD/NASH by downloading their microarray data from GEO (http://www.ncbi.nlm.nih.gov/geo/).[11] mRNA profiles of six normal liver samples (male) and eight NAFLD/NASH liver samples (male) were compared using GeneSpring (Agilent Technologies Genomics). Differentially expressed genes were defined by a log-scale ratio ≤ 0.3 between paired samples with a $p<0.05$. Based on these criteria, we identified 1219 downregulated probes in NAFLD/NASH samples (see online supplementary table S1). To identify genes with binding motifs for miR-21, we downloaded the target gene databases of miR-21 based on TargetScan,[12] Pictar[13] and Starbase.[14] Only hits from Target or PicTar algorithm that were confirmed by Ago HITS-CLIP (high-throughput sequencing of RNAs isolated by cross-linking immunoprecipitation (HITS-CLIP) from Argonaute protein complex) were selected. These three databases were compared using Microsoft Access 2000, yielding 219 potential targets that have miR-21 binding motif (see online supplementary table S2). We then compared 1219 downregulated probes in livers of patients with NAFLD/NASH with 219 genes that have at least one binding motif for miR-21 using Microsoft Access 2010, which resulted in an overlap of 13 genes between two databases that were considered as potential targets of miR-21 (see online supplementary table S3). Gene ontology (GO) analysis was done using PathwayStudio software (Elsevier).

Animal, diet treatment and sample collection

Male *Dicer1*$^{fl/fl}$ mice on a mixed 129S4, C57Bl/6 strain background[15] were crossed with C57Bl/6 *Alb-Cre*$^{+/-}$ mice[16] to generate *Dicer1*$^{fl/fl}$, *Alb-Cre*$^{+/-}$ mice (mice are from Dr Holger Willenbring's lab at the University of California, San Francisco). To specifically investigate the impact of miRNAs on mature liver function, we initiated Cre recombinase expression in 8-week-old to 10-week-old mice.[17] To restrict *Cre* expression to hepatocytes, we used a hepatocyte-specific *Transthyretin* (*Ttr*) promoter and pseudotyped the vector genome with capsids from AAV8, a serotype that can transduce virtually all hepatocytes in vivo without causing toxicity.[10 17 18]

To determine the effect of hepatic lipid accumulation on miRNA expression, 8-week-old wildtype male C57Bl/6 mice (Jackson Laboratory, n=6) were maintained on either a normal chow diet (Open Source D12450B: 10% Kcal fat) or an HFD (Open Source D12492: 60% Kcal fat) for 4 weeks as described by Vickers *et al*.[19] After 4 weeks of HFD administration, livers were collected for miRNA and gene expression analysis.

To determine the role of miR-21 in NAFLD, we synthesised locked nucleic acid anti-miR-21 anti-sense oligonucleotide (ASO) (Exiqon) specifically targeting miR-21 and also generated miR-21-mismatched-ASO (miR-21-MM-ASO), a control ASO that differs from miRNAs in four mismatched base pairs. The male C57Bl/6 mice kept on HFD for 4 weeks were divided into two groups; one group (n=8) was treated with miR-21-ASO and the other with miR-21-MM-ASO (control, n=8). Mice received a dose of 25 mg/kg miR-21-ASO or miR-21-MM-ASO (0.9% NaCl) weekly for 4 or 8 weeks via tail vein injection. At those times, the mice were anaesthetised, and blood was collected by way of cardiac puncture. Subsequently, the livers were harvested and immediately frozen in liquid nitrogen and stored at −80°C for gene expression and histological analysis.

Fatty acid treatment of HepG2 cells

HepG2 cells were obtained from Dr Xin Chen's laboratory at the University of California, San Francisco. Sodium oleate was obtained from Sigma-Aldrich and was dissolved in Dulbecco's modified Eagle medium (DMEM) with 1% fatty acid free bovine serum albumin (BSA) (Sigma). Oleate treatment of HepG2 cells was carried out as previously described with minor revision.[10 20] Specifically, HepG2 cells were plated in four-well chamber slides with DMEM medium supplemented with 10% fetal bovine serum (Invitrogen). After 24 h, HepG2 cells were treated with either control medium (DMEM supplemented with 1% fatty acid free BSA) or medium containing oleate (0.5 mM). The cells were cultured for another 24 h, then lipid accumulation and miR-21 expression were determined by Nile Red Staining (Sigma-Aldrich) and qRT-PCR, respectively (see online supplementary materials and methods for details).

Cell proliferation analysis

HepG2 cells were transfected with miR-21-ASO, scrambled control or miR-21-ASO plus *HBP1*-siRNA using lipofectamine 2000 (Invitrogen). After 48 h, cell proliferation was determined using a MTT (3-(4,5-dimethylthiazol-2-yl)-2, 5-diphenyltetrazoliumbromide) cell proliferation kit (Cell Biolabs) according to the manufacturer's instruction (see online supplementary material and methods for details).

Focus formation assay and flow cytometry analysis

HepG2 cells were used to determine the effect of miR-21 on focus formation and cell cycle progression (see online supplementary material and methods for details).

Xenograft tumour assay

Male BALB/c athymic nude mice (6 weeks old) purchased from Jackson Laboratory were used to study the role of miR-21 in

promoting growth of xenograft tumour from HepG2 cells (see online supplementary material and methods for details).

Histological analysis

Frozen sections of liver were stained with Oil Red-O staining. Paraformaldehyde-fixed, paraffin-embedded sections of liver were stained with H&E (see online supplementary material and methods for details).

Lipid and lipoprotein analysis

Both plasma and hepatic lipid content were enzymatically measured in liver lysates and plasma via a colorimetric assay using a triglyceride assay kit from Roche Diagnostics, according to the manufacturer's protocols (see online supplementary material and methods for details).

Western blot and Q-RT-PCR

Western blot and qRT-PCR were used to determine expression levels of genes. Primers used for quantitative RT-PCR are listed in online supplementary table S4 (see online supplementary material and methods for details).

Statistical analysis

Statistical analysis was performed using GraphPad Prism Software. Data derived from cell-line experiments were presented as mean±SD and assessed by a two-tailed Student's t test. Statistical difference for cell cycle progression analysis was evaluated using χ^2 test. Mann–Whitney test was used to evaluate the statistical significance for mouse experiments. Each experiment was repeated at least three times; and the error bars represent the SD. $p<0.05$ was considered to be statistically significant.

RESULTS

miR-21 is robustly induced in livers of mice on HFD and HepG2 cells exposed to high levels of fatty acid

Hepatocytes are the major cells that control lipid metabolism and the primary site of NAFLD and HCC. To investigate the role of miRNAs in both disorders, we compiled hepatocyte-specific miRNA profiles by comparing miRNAs expression of livers of hepatocyte-specific *Dicer1* knockout (*DKO*) and wildtype mice (see online supplementary table S5). We observed that miR-21 was the most significantly downregulated miRNA in livers of *DKO* mice (≥39-fold reduced), indicating that hepatocytes represent a main source of its expression in the liver (figure 1A). To assess the role of miR-21 in NAFLD, we fed wildtype C57Bl/6 mice an HFD (see online supplementary figure S1A–C) and measured its hepatic expression. The results showed that miR-21 had a twofold upregulation in the livers of HFD-treated mice (figure 1B), suggesting its potential role in NAFLD.

We also determined whether fatty acids can increase the expression of miR-21 in human hepatoma HepG2 cells. Oleic acids are the most abundant unsaturated fatty acids in liver triglycerides in both normal subjects and patients with NAFLD.[21] In this study, HepG2 cells were used because of their increased sensitivity to fat accumulation.[21] Nile-Red staining revealed that oleic acid treatment led to an increase in intracellular lipids in HepG2 cells (figure 1C, D), which was also associated with upregulation of miR-21 (figure 1E). Taken together, our in vivo and in vitro studies indicated that both HFD treatment of mice and exposure of HepG2 cells to fatty acid were able to induce expression of miR-21.

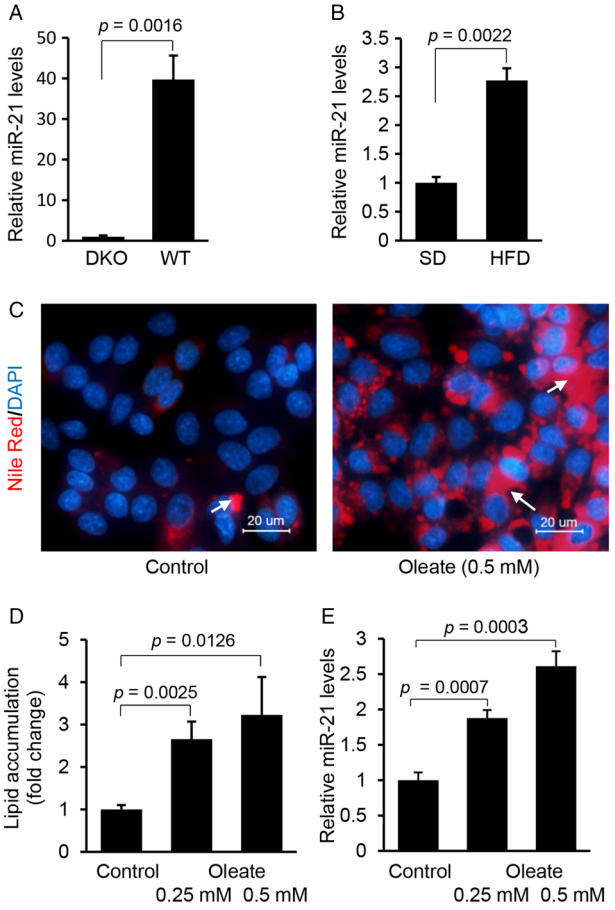

Figure 1 Hepatocyte-specific miR-21 is significantly induced in livers of high fat diet (HFD)-treated mice and HepG2 cells treated with fatty acid. (A) qRT-PCR confirmed that miR-21 was highly expressed in hepatocytes of liver. miR-21 expression in liver was compared between *Dicer1* knockout (DKO) (n=3) and wildtype mice (n=3) using qRT-PCR. Data are presented as mean±SD (p=0.0016, Student's t test). (B) HFD treatment led to higher levels of miR-21 in livers of mice. Briefly, wildtype mice (C57Bl/6) were maintained on HFD for 4 weeks, and then mice were sacrificed and livers collected for miRNA expression analysis. Control mice received standard diet (SD). Data are presented as mean ±SD (p=0.0022, Mann–Whitney test). (C and D) Oleate treatment increased lipid content and subsequently (E) expression of miR-21 in HepG2 cells. HepG2 cells were maintained in Dulbecco's modified Eagle medium containing 0.5 mM oleate. Data are presented as mean±SD. In this multiple-groups experiment, we only performed comparison between two groups and Student's t test was used for statistical analysis. Lipid droplets in human hepatocytes were labelled with arrows.

To further elucidate the role of miR-21 in hepatic lipid accumulation, we began to identify target genes of miR-21 by combining mRNA profiling of livers of NAFLD individuals with the bioinformatic prediction of miR-21 binding motifs within potential target mRNAs. This led us to identify 13 genes including *HBP1*, *SOX7* and *RHOB* that showed reduced expression in human fatty liver and contained a conserved binding motif for miR-21 (see online supplementary table S3). GO analysis of the above 13 genes revealed that *HBP1* was a potent tumour suppressor by preventing G1/S transition of cell cycle.[22 23] In addition, our prediction from in silico algorithms showed that the 3′ UTR of *HBP1* mRNA was 100% complementary to the miR-21 5′ seed region, exhibiting the highest prediction score and binding energy (figure 2A). Therefore, we selected *HBP1* as a potential target of miR-21.

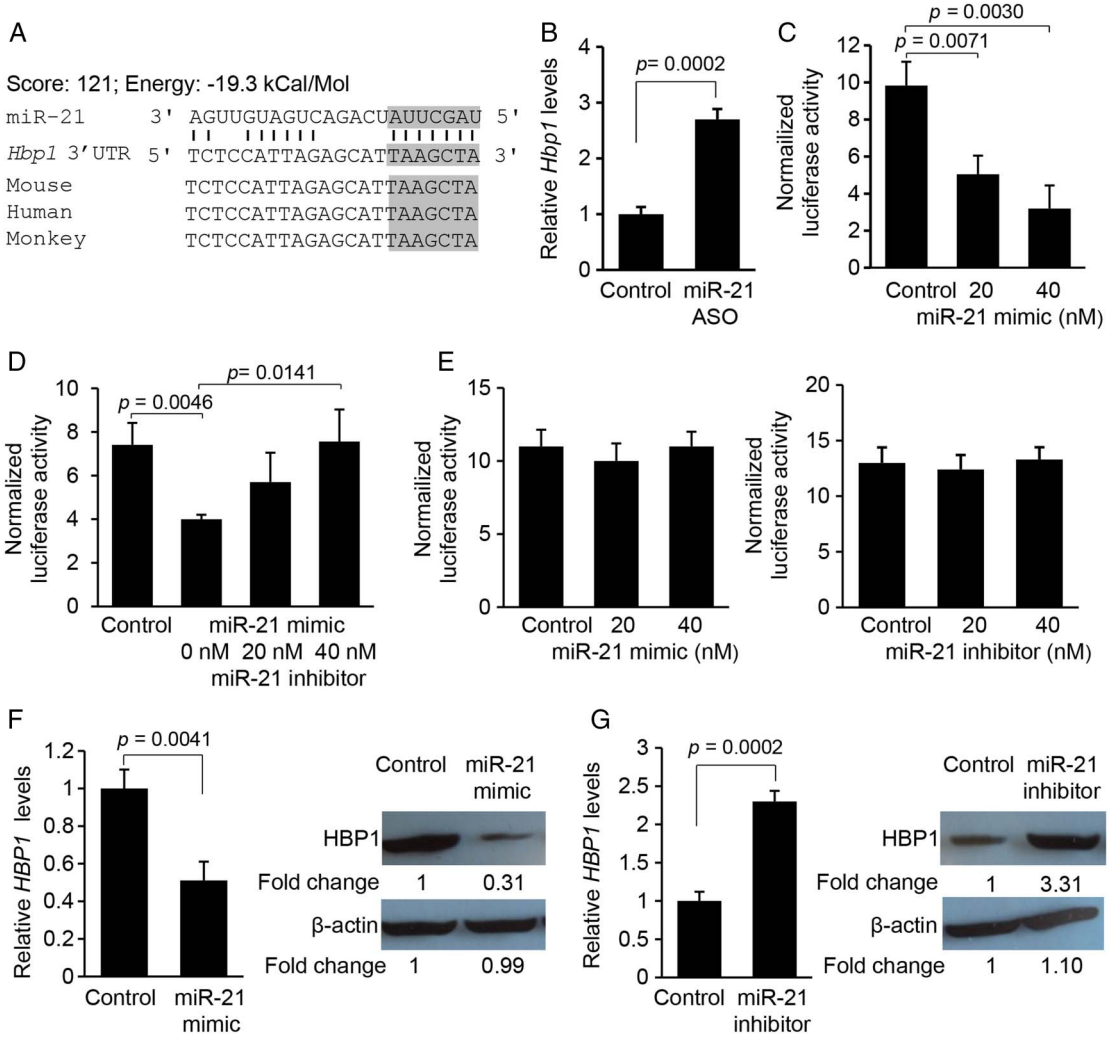

Figure 2 *Hbp1* is a direct target of miR-21. (A) Bioinformatic analysis showing that the seed sequence of miR-21 has a high level of complementarity to *Hbp1* 3′ UTR, prediction score and favourable binding energy. Complementary sequences to the seed region of miR-21 within the 3′ UTRs of *Hbp1* are conserved between human, mouse and monkey (grey highlight). (B) miR-21 knockdown in high fat diet (HFD)-treated mice led to increased *Hbp1* mRNA levels in liver. C57Bl/6 wildtype mice were kept on normal chow until 8 weeks of age and then maintained on HFD until 16 weeks of age. At 12 weeks of age, the mice were given miR-21-anti-sense oligonucleotide (ASO) (25 mg/kg, tail vein injection) until 16 weeks of age. C57Bl/6 mice maintained on HFD and treated with miR-21-MM-ASO served as controls. The expression levels of *Hbp1* were determined by qRT-PCR. Data are presented as means±SD (p=0.0002, Mann–Whitney test). (C) miR-21 mimic transfection into Hepa1,6 cells caused dose-dependent inhibition of the activity of a luciferase reporter gene linked to the 3′ UTR of mouse *Hbp1*. Data are presented as mean±SD. In this multiple-groups experiment, we only performed comparison between two groups among them and Student's t test was used for statistical analysis. (D) Conversely, transfection with a miR-21 inhibitor antagonised the binding of miR-21 mimics to the 3′ UTR of mouse *Hbp1*, which was reflected by increased luciferase activity. Data are presented as mean±SD. Student's t test was used for statistical analysis. (E) Mutated binding motif for miR-21 within *Hbp1* 3′UTR impaired miR-21 binding, which was reflected by (i) negligible change of luciferase activity after miR-21 mimics treatment; and (ii) miR-21 inhibitor treatment had no effect on luciferase activity. Data are presented as mean±SD (p≥0.1, Student's t test). (F) Transfection of miR-21 mimics into HepG2 cells inhibited expression levels of endogenous *HBP1* as revealed by qRT-PCR and western blot. Data are presented as mean±SD (p=0.0041, Student's t test). (G) miR-21 knockdown by transfecting miR-21 inhibitor into HepG2 cells caused an increase in endogenous *HBP1* at the protein and mRNA levels. Data are presented as mean±SD (p=0.0002, Student's t test).

We next determined its expression in the livers of dietary obese mice treated with miR-21-ASO. It was not surprising that *Hbp1* expression increased more than twofold in the livers of miR-21-ASO-treated mice compared with those treated with miR-21-MM-ASO (figure 2B). Taken together, hepatic expression of miR-21 was increased in dietary obese mice and livers of human patients with NAFLD/NASH, and *Hbp1*, as a potential target of miR-21, showed reduced expression in livers of obese mice and human patients with NAFLD (see online supplementary table S3 and figure S1D). Our findings suggested that the crosstalk between miR-21 and *Hbp1* might play an important role in hepatic lipid accumulation.

Hbp1 is a direct target of miR-21

To establish that miR-21 directly recognises the predicted target site within the 3′ UTR of *Hbp1*, the 3′ UTR of mouse *Hbp1* mRNA was cloned into a luciferase reporter vector (pMiR-Report) to generate pMiR-*Hbp1*. Mouse Hepa1,6 cells were transfected with pMiR-*Hbp1* and chemically synthesised miR-21 mimic or miR-21 inhibitor. We found that miR-21 mimics significantly downregulated luciferase activity in a dose-dependent fashion (figure 2C). Consistently, miR-21 inhibitor antagonised the inhibitory effect of miR-21 mimics on luciferase activity (figure 2D). Furthermore, we mutated the binding motif for miR-21 within the pMiR-*Hbp1* 3′ UTR and found that both

mimics and inhibitors of miR-21 had no effect on luciferase activity (figure 2E), indicating a potentially direct interaction between miR-21 and *Hbp1* mRNA. To further validate that *Hbp1* is a target of miR-21, we increased intracellular levels of miR-21 in HepG2 cells in the absence of fatty acid. qRT-PCR and western blot revealed that miR-21 significantly inhibited expression of *HBP1* (figure 2F). In contrast, miR-21 knockdown led to an increase in mRNA and protein levels of *HBP1* in HepG2 cells (figure 2G). Together, these results confirmed that *Hbp1* is a direct target of miR-21.

HBP1 inhibits expression of *SREBP1C*, *CCND1* and *CCNB1* by activating *p53*

HBP1 is a well-described transcriptional repressor that modulates expression of genes involved in cell cycle progression.[23] Therefore, we overexpressed *HBP1* in HepG2 cells and determined the expression levels of genes involved in cell cycle using Human Cell Cycle RT^2 Profiler PCR Assay. Interestingly, we observed that *p53* was the most upregulated after overexpression of *HBP1* (figure 3A). p53 functions as a tumour suppressor and potent inhibitor of lipogenesis by inhibiting transcription of *SREBP1C*,[24–26] leading to our hypothesis that miR-21 plays roles in both lipogenesis and carcinogenesis by interacting with the HBP1-p53 pathway.

Overexpression of *HBP1* led to increased mRNA levels of *p53*, implying that *HBP1* might activate transcription of *p53* by binding to its promoter. Therefore, we cloned the *p53* promoter into a luciferase reporter vector (pGL3-Basic) and generated pGL3-p53. Hepa1,6 cells were transfected with pGL3-p53 and *HBP1* expression vector. As expected, overexpression of *HBP1* induced luciferase activity (figure 3B), and *HBP1* knockdown led to decreased luciferase activity (figure 3C). Furthermore, *HBP1* knockdown impaired expression of endogenous *p53* (figure 3D), suggesting that *HBP1* was able to activate transcription of *p53*. HBP1 can function as a transcriptional activator by binding to a specific binding motif (GGGATGGG).[22] However, we did not identify this binding motif within the promoter of *p53*, signifying that HBP1 might activate transcription of *p53* by interacting with other transcription factors that have binding sites within the *p53* promoter.

Srebp1c is a transcription factor that activates genes encoding enzymes required for lipid synthesis.[27 28] Considering the role that *p53* plays in inhibiting lipogenesis by modulating *Srebp1c*,[26] we cloned the mouse *Srepb1c* promoter into pGL3-basic vector (pGL3-*Srebp1c*). As expected, co-transfection of *p53* expression vector pGL3-*Srebp1c* and into Hepa1,6 cells significantly reduced luciferase activity in a dose-dependent fashion (see online supplementary figure S2A), and in contrast, *p53* knockdown induced luciferase activity (see online supplementary figure S2B). Furthermore, we observed that overexpression of *p53* led to a decrease in endogenous mRNA levels of *SREBP1C* and its targeted lipogenic genes *SCD1* (stearoyl-CoA desaturase-1), *GPAT* (glycerol 3-phosphate acyltransferase), and *FASN* (fatty acid synthase),[29] and genes controlling cell cycle progression including *CCNB1* and *CCND1* in HepG2 cells (figure 3E).[30] *p53* knockdown led to the opposite effect (figure 3F), underscoring the central role of *p53* in modulating the expression of genes involved in lipogenesis and cell cycle progression.

To further determine whether *HBP1* prevents transcription of genes associated with lipogenesis and G1/S transition via *p53-SREBP1C* pathway, we overexpressed *HBP1* in HepG2 cells and determined expression levels of *p53*, *SREBP1C*, the lipogenic genes and *CCNB1* and *CCND1*. As confirmed by qRT-PCR, *HBP1* overexpression led to increased *p53*, which subsequently prevented expression of *SREBP1C* and *SCD1*, *FASN* and *GPAT*, as well as *CCNB1* and *CCND1* (figure 3G). In summary, our findings suggested that HBP1 is able to simultaneously inhibit expression of *CCNB1*, *CCND1* and *SREBP1C* by modulating *p53*.

miR-21 prevents expression of *p53* but promotes transcription of *SREBP1C* by modulating *HBP1* expression

We have shown that *HBP1* is a target of miR-21, and HBP1 can activate transcription of *p53*. Meanwhile, p53 is a transcriptional repressor of *Srebp1c*.[25 31] Thus, we hypothesised that miR-21 can simultaneously regulate expression of genes involved in lipogenesis and the G1/S transition by modulating the *HBP1-p53-SREBP1C* pathway. Indeed, overexpression of miR-21 in HepG2 cells inhibited expression of *HBP1*, which subsequently led to a reduction in *p53* and an increase in mRNA levels of *CCND1*, *CCNB1* and *SREBP1C*, as well as its target genes including *SCD1*, *FASN* and *GPAT* (figure 3H), while miR-21 knockdown led to an opposite effect (figure 3I). Our findings indicated that miR-21 is able to modulate expression of genes controlling lipogenesis and cell cycle progression via the p53-SREBP1C pathway.

miR-21 modulates lipid accumulation in HepG2 cells by interacting with the *HBP1-p53* pathway

We then determined whether overexpression of miR-21 can promote lipogenesis. As expected, miR-21 overexpression prevented expression of *HBP1* and *p53* (figure 4A), which subsequently promoted lipid accumulation in HepG2 cells (figure 4B, C).

To determine loss of function for miR-21 in lipid accumulation, we transfected miR-21 inhibitor into oleate-treated HepG2 cells to knock down upregulated miR-21. Antagonising miR-21 led to a significant increase in *HBP1* and *p53* (figure 4D), which subsequently prevented lipid accumulation (figure 4E, F). These data demonstrated that miR-21 was sufficient for the downregulation of *HBP1* and *p53*, which subsequently induced lipid accumulation. To further investigate the role of the interaction between miR-21 and *HBP1* in hepatic lipid accumulation, we mutated the binding motif for miR-21 within the 3′ UTR of *Hbp1* in the pMiR-*Hbp1* (referred to as pMiR-*Hbp1*Mu) and introduced the pMiR-*Hbp1* or pMiR-*Hbp1*Mu into oleate-treated HepG2 cells. Since oleate treatment increases miR-21 expression in HepG2 cells, it was expected that it would lead to a decrease of luciferase activity in HepG2 cells transfected with pMiR-*Hbp1* compared with pMiR-*Hbp1*Mu. In fact, oleate treatment of HepG2 cells transfected with pMiR-*Hbp1* resulted in robust repression of luciferase activity compared with pMiR-*Hbp1*-Mu (figure 4G). Together, our results indicated that *HBP1* is a direct target of miR-21 during lipid accumulation in HepG2 cells and the crosstalk of miR-21 with *HBP1* and *p53* plays an important role in hepatic lipid accumulation.

Inhibitory effect of miR-21-ASO on hepatic lipid accumulation is mediated by *HBP1*

To confirm that miR-21 promotes lipogenesis via *HBP1*, we initially antagonised miR-21 by transfecting miR-21-ASO into HepG2 cells to induce expression of *HBP1*, and then knocked down the induced *HBP1* using *HBP1*-siRNA. The results showed that miR-21 knockdown increased *p53* and *HBP1* and reduced lipid content in HepG2 cells, but additional treatment of *HBP1*-siRNA offset the effect of miR-21-ASO (figure 5A–C), which suggested that *HBP1*, in part, mediated the inhibitory effect of miR-21 inhibitor on lipid accumulation. To study the

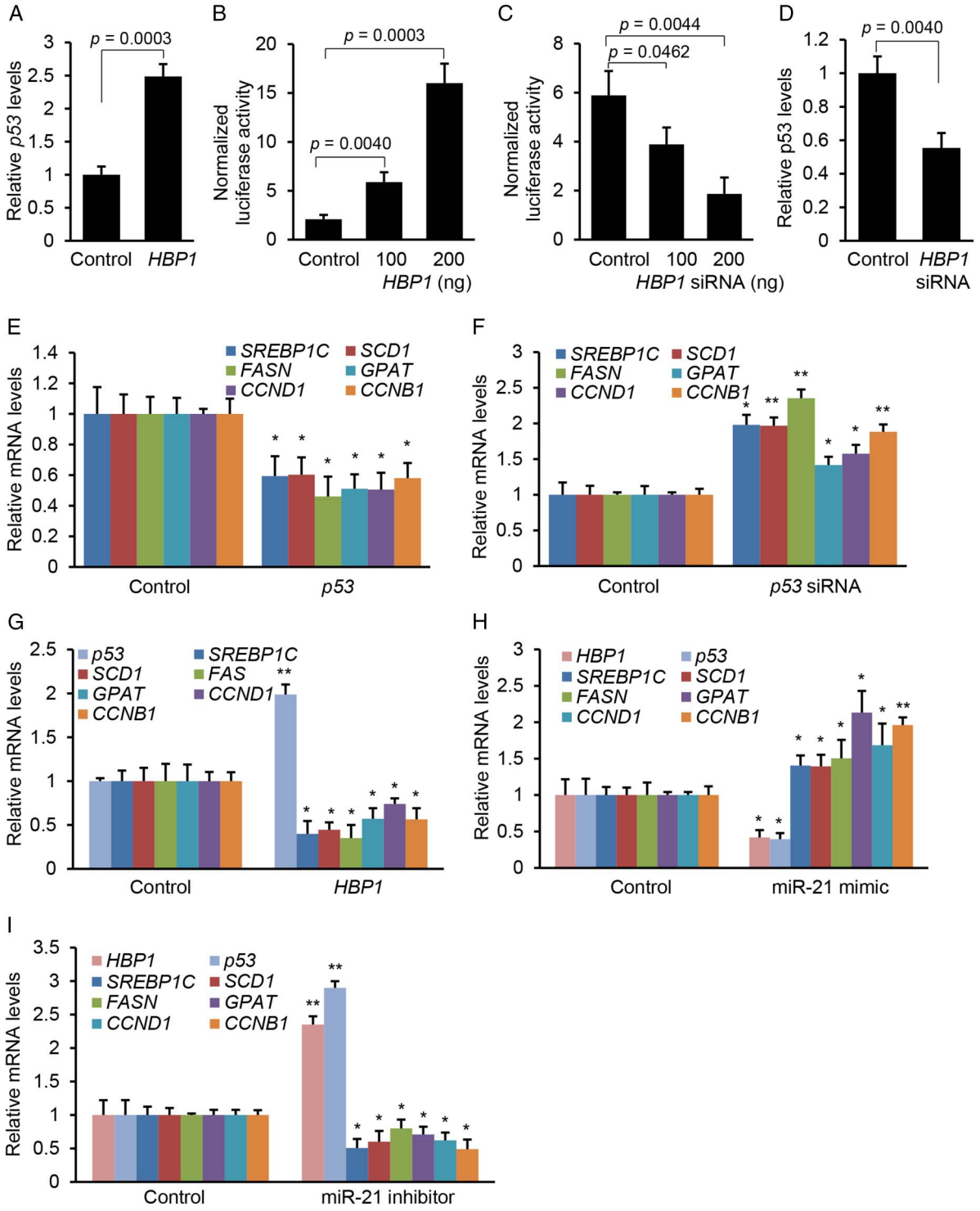

Figure 3 HBP1 is a transcriptional activator of *p53*. (A) Overexpression of *HBP1* increased mRNA levels of *p53* in human HepG2 cells. Data are presented as means±SD (p=0.0003, Student's t test). (B) Overexpression of *HBP1* caused dose-dependent increase of the activity of a luciferase reporter gene linked to the *p53* promoter. Data are presented as mean±SD. Student's t test was used for statistical analysis. (C) *HBP1* knockdown via its siRNA decreased luciferase activity driven by *p53* promoter. Data are presented as means±SD. Student's t test was used for statistical analysis. (D) *HBP1* knockdown via its siRNA resulted in decreased mRNA levels of *p53*. Data are presented as mean±SD (*p=0.0040, Student's t test). (E) Overexpression of *p53* led to deceased *SREBP1C*, lipogenic genes *SCD1*, *FASN* and *GPAT* as well as *CCND1* and *CCNB1* in HepG2 cells. Data are presented as mean±SD (*p<0.05; **p<0.001; Student's t test). (F) Knockdown of *p53* via its siRNA increased mRNA levels of *SREBP1C*, *FASN*, *SCD1*, *GPAT*, *CCND1* and *CCNB1* in HepG2 cells. Data are presented as mean±SD (*p<0.05; **p<0.001; Student's t test). (G) Overexpression of *HBP1* reduced expression of *p53*, which subsequently led to decreased expression of genes involved in lipogenesis and G1/S transition. Data are presented as mean±SD (*p<0.05; **p<0.001; Student's t test). (H) Overexpression of miR-21 inhibited *HBP1* and *p53*, which subsequently promoted expression of the lipogenic genes including *SCD1*, *FASN* and *GPAT* and the genes controlling cell cycle progression including *CCNB1* and *CCND1*. Data are presented as mean±SD (*p<0.05; **p<0.001; Student's t test). (I) miR-21 knockdown via its inhibitor led to increased *HBP1* and *p53* and decreased expression of the lipogenic and cell cycle-related genes. Data are presented as mean±SD (*p<0.05; **p<0.001; Student's t test).

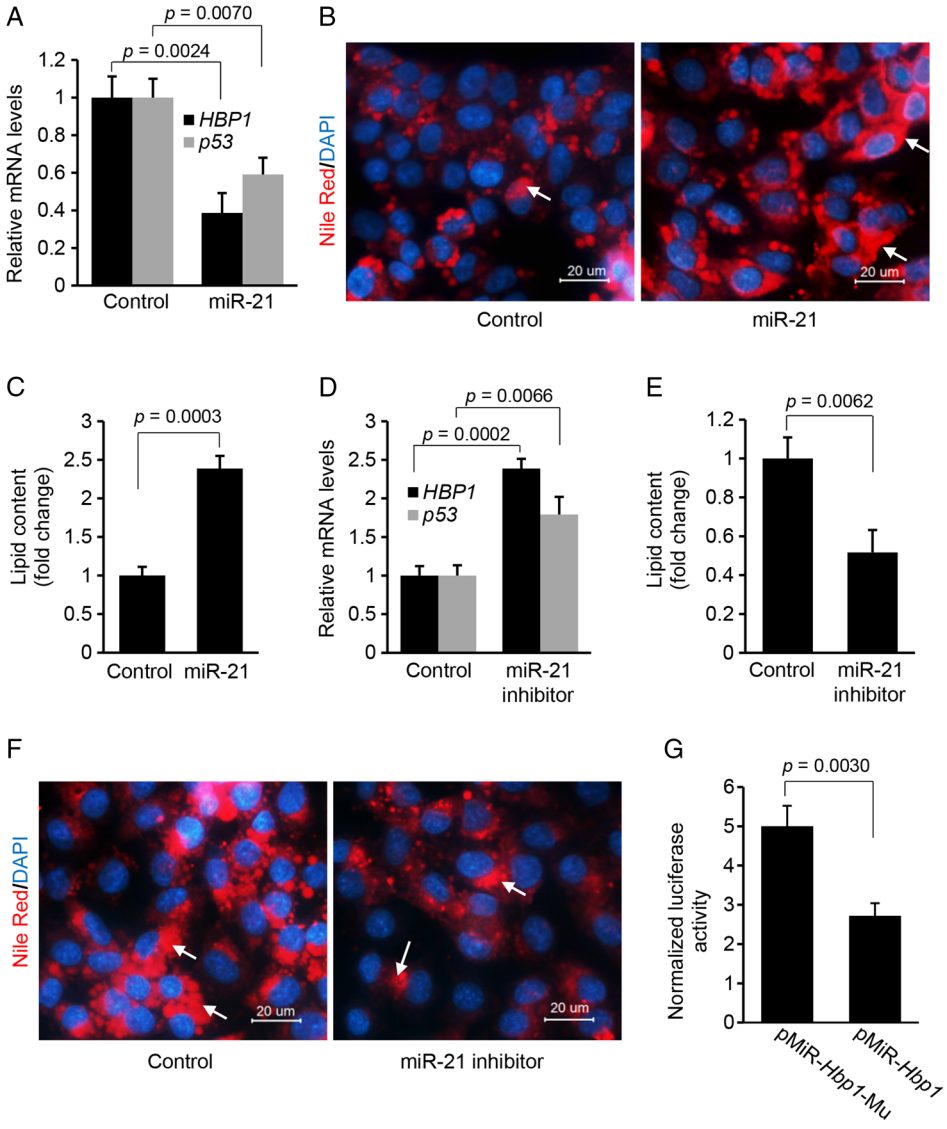

Figure 4 MiR-21 modulates lipid accumulation in HepG2 cells by interacting with the *HBP1-p53* pathway. (A) Overexpression of miR-21 inhibited expression of *HBP1* and *p53*, which (B and C) subsequently promoted lipid accumulation in HepG2 cells in the presence of 0.25 mM oleate. Data are presented as mean ±SD. Student's t test was used for statistical analysis. Lipid droplets were labelled with arrows. (D) miR-21 inhibitor transfection into HepG2 cells cultured with the medium containing 0.5 mM oleate led to an increase in *HBP1* and *p53*, which (E and F) antagonised the effect of upregulated miR-21 on lipid accumulation. Lipid droplets were labelled with arrows. Data are presented as mean±SD. Student's t test was used for statistical analysis. (G) Oleate treatment led to a decrease in luciferase activity of pMiR-*Hbp*1 as compared with pMiR-*Hbp1*Mu. Data are presented as mean±SD (p=0.0030, Student's t test).

role of the crosstalk between *p53* and miR-21 in lipogenesis, we transfected oleated-incubated HepG2 cells with miR-21 mimics or a combination of miR-21 mimics and *p53* expression vector. Nile-Red staining and qRT-PCR revealed that miR-21 mimics promoted lipid accumulation in HepG2 cells and the additional *p53* overexpression rescued the effect of miR-21 (see online supplementary figure S3A, B). We further determined whether *p53* deletion could offset the inhibitory effect(s) of miR-21-ASO on lipogenesis. The results showed that miR-21 knockdown led to decreased lipid content and increased *p53*, and additional treatment with *p53* siRNA offset the effects of miR-21-ASO (see online supplementary figure S3C-E). Taken together, our results indicated that miR-21-induced lipid accumulation is, in part, mediated by *HBP1* and *p53*.

HBP1 mediates the inhibitory effect of miR-21 inhibitor on proliferation, G1/S transition and xenograft tumour from HepG2 cells

To determine whether *HBP1*, at least in part, mediates the effects of miR-21 on proliferation and G1/S transition, we adopted a similar strategy as described above. MTT and soft agar colony assays revealed that miR-21-ASO administration caused suppression of cellular proliferation in HepG2 cells, but additional treatment of *HBP1*-siRNA counteracted the effects of miR-21-ASO (figure 5D, E). Cell cycle phase distribution of HepG2 cells further showed that miR-21 knockdown led to a significant increase in G1 phase cells and G1/S arrest, but additional treatment of *HBP1*-siRNA antagonised this effect of miR-21-ASO (figure 5F). Consistent with our in vitro findings, miR-21 knockdown inhibited growth of xenograft tumours in nude mice, and *HBP1*-siRNA treatment counteracted the effect of miR-21-ASO (figure 5G).

As we proposed, *p53* is an important mediator of the miR-21-Hbp1-p53 axis. To determine whether *p53* mediates the inductive effect of miR-21 on proliferation, we treated HepG2 cells with miR-21 mimic or a combination of miR-21 and *p53* expression vector. MTT assay, soft agar colony formation assay and cell cycle analysis revealed that miR-21 promoted proliferation and cell cycle progression, and additional overexpression of *p53* offset the inductive effects of miR-21 (see online supplementary figure S4A–E). Furthermore, miR-21-ASO treatment led to reduced proliferation, delayed G1/S transition and repressed growth of xenograft tumour, and the additional treatment of *p53* siRNA rescued the inhibitory effects of miR-21-ASO (see online supplementary figure S4F–K). In summary, our findings indicated that *HBP1* mediates, at least in part, the inhibitory effects of miR-21-ASO on G1/S transition, proliferation and growth of xenograft tumour.

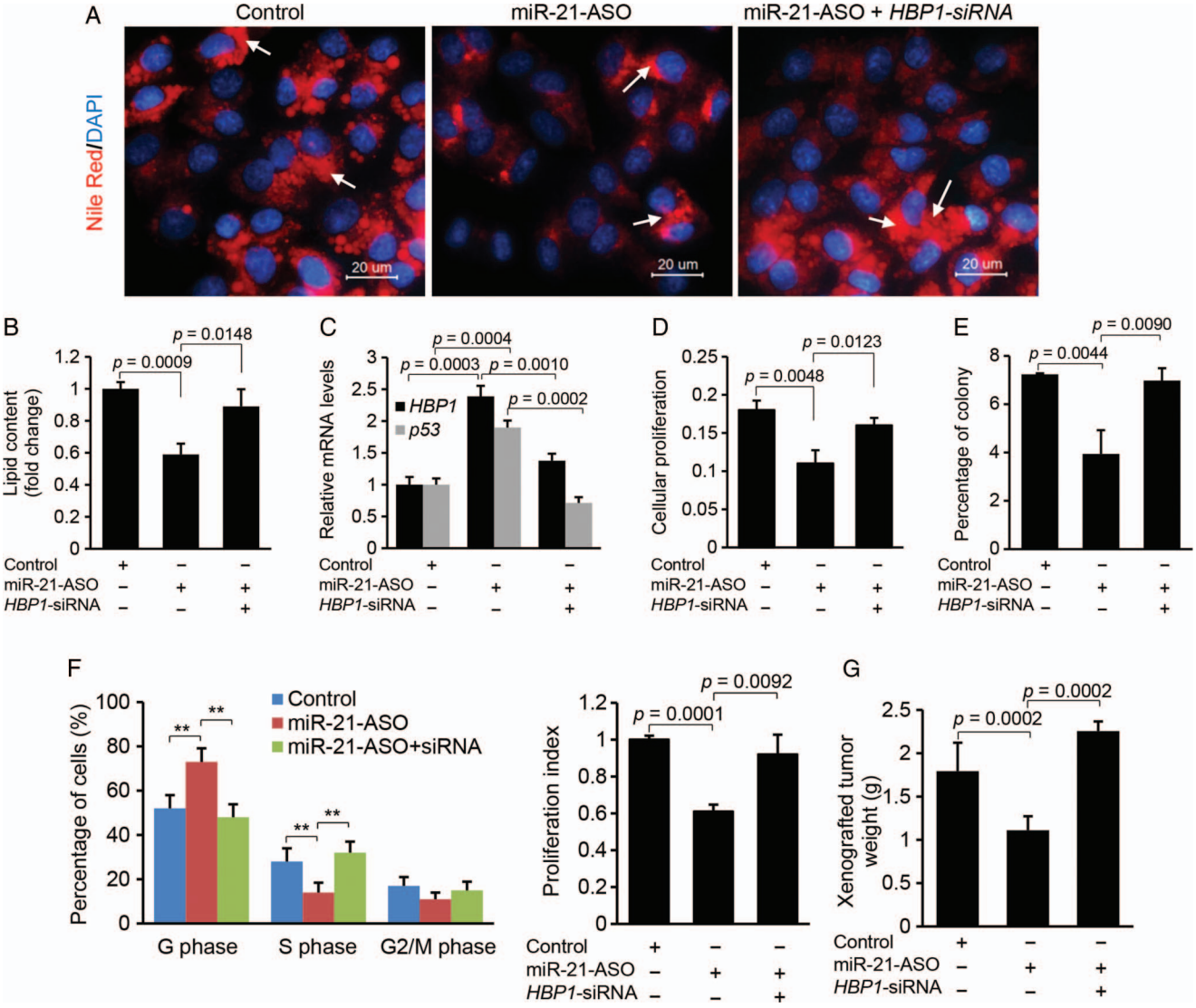

Figure 5 The inhibitory effects of miR-21-anti-sense oligonucleotide (ASO) on lipogenesis, G1/S transition and proliferation are mediated by *HBP1*. (A and B) miR-21 inhibitor transfection into HepG2 cells reduced lipid content, and additional treatment of *HBP1*-siRNA restored lipid levels. Lipid droplets were labelled with arrows. Data are presented as mean±SD. Student's t test was used for statistical analysis. (C) miR-21 inhibitor treatment induced expression of *HBP1* and *p53*, and additional knockdown of induced *HBP1* with its siRNA inhibited expression of *HBP1* and *p53*. Specifically, HepG2 cells were treated with oleate (0.5 mM) to induce miR-21, and then miR-21-ASO was transfected into HepG2 cells to knock down upregulated miR-21. Levels of miR-21, *HBP1* and *p53* were determined by qRT-PCR. Data are presented as mean±SD. Student's t test was used for statistical analysis. (D) MTT assay revealed that antagonising miR-21 via miR-21 inhibitor caused reduced cellular proliferation in HepG2 cells, and additional knockdown of *HBP1* by its siRNA rescued the effect of miR-21 inhibitor. Data are presented as mean±SD. Student's t test was used for statistical analysis. (E) Soft agar colony formation assay revealed that miR-21 knockdown inhibited the growth of HepG2 cells, and the additional treatment of *HBP1*-siRNA antagonised the effect of miR-21 inhibitor. Data are presented as mean±SD. Student's t test was used for statistical analysis. (F) miR-21-ASO treatment increased the number of cells in the G1 phase but decreased the number of cells in the S phase, and additional knockdown of upregulated *HBP1* by its siRNA antagonised the effect of miR-21 inhibitor. Quantification of the cell cycle phase distribution was analysed by flow cytometry. The proliferation index was reduced in the miR-21 inhibitor treated HepG2 cells and the additional treatment of *HBP*-siRNA offset the effect of miR-21 inhibitor. Data are presented as mean±SD (*p<0.05, **p<0.001, χ^2 test). (G) miR-21-ASO inhibited subcutaneous tumours from HepG2 cells in nude mice, and additional treatment of *HBP1*-siRNA counteracted the effect of miR-21-ASO. HepG2 cells treated with miR-21-MM-ASO, miR-21-ASO or a combination of miR-21-ASO and *HBP1*-siRNA were injected subcutaneously into different groups of nude mice. Data are presented as mean±SD. Student's t test was used for statistical analysis.

Antagonising miR-21 in dietary obese mice prevents hepatic lipid accumulation

Next, we assessed the functional contribution of increased *Hbp1* and *p53* expression to hepatic lipid accumulation by reducing miR-21 expression in dietary obese mice. C57Bl/6 mice, which had been on an HFD, were injected with either miR-21-ASO or miR-21-MM-ASO for 4 weeks. We observed that antagonising miR-21 significantly reduced levels of triglycerides in livers of HFD-treated animals (figure 6A, B), in contrast to plasma triglyceride levels (figure 6C). On the other hand, miR-21-ASO treatment had no effect on body and liver weight (see online supplementary table S6). As expected, we also observed a 91% reduction of hepatic miR-21 expression in mice that received miR-21-ASO compared with miR-21-MM-ASO and a twofold increase of *Hbp1* and *p53* (figure 6D). Four-week treatment of miR-21-ASO showed a strong inhibitory effect on

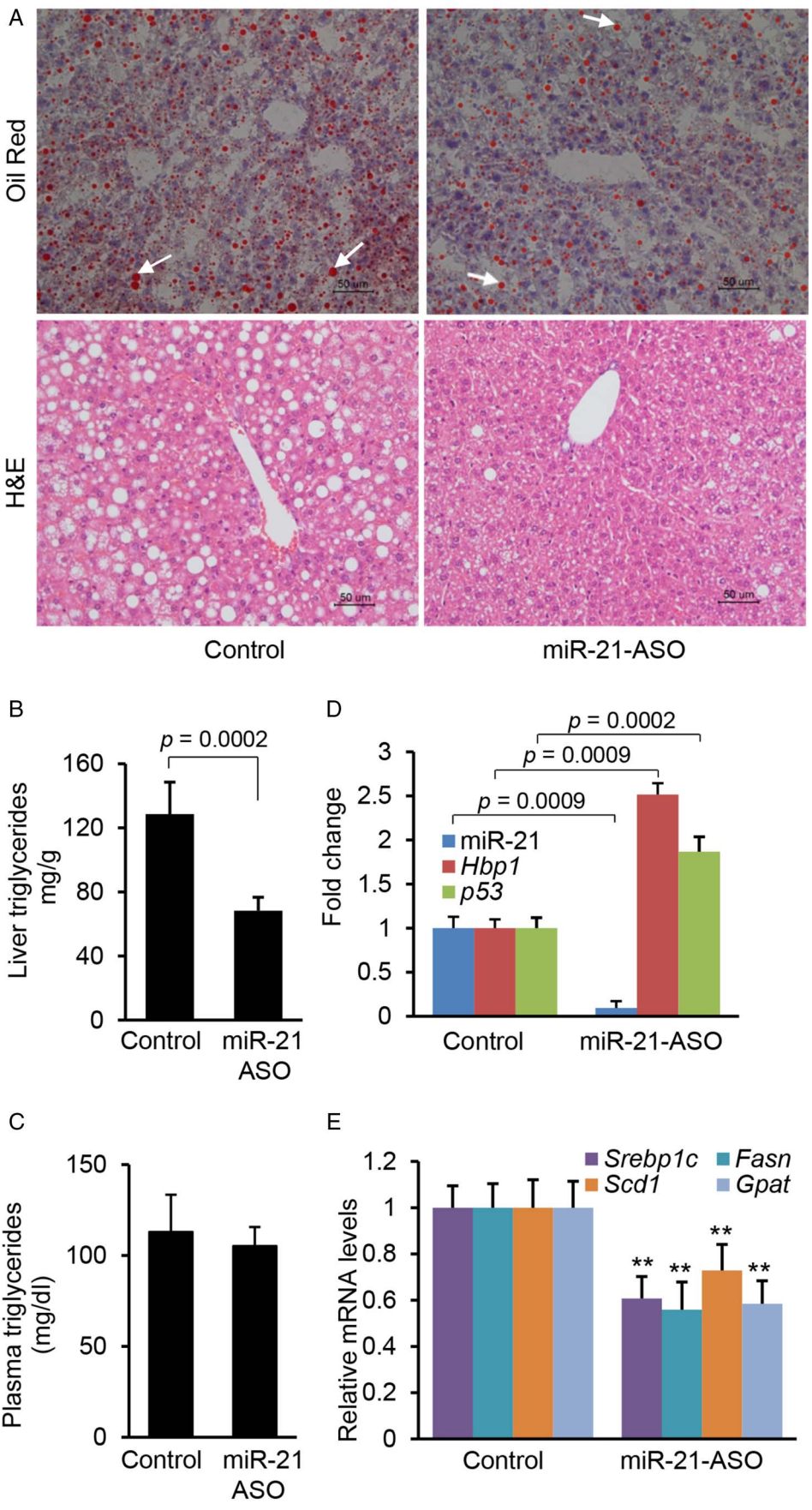

Figure 6 Antagonising miR-21 prevented hepatic lipid accumulation in high fat diet (HFD)-treated mice. (A and B) miR-21 knockdown inhibited lipid accumulation in livers of HFD-fed mice injected with miR-21-anti-sense oligonucleotide (ASO). Representative images are shown. Lipid droplets in livers are labelled with arrows. Cellular triglyceride content was measured by Oil Red staining and triglyceride content was measured with a triglyceride estimation kit. Data are presented as mean±SD ($p<0.0002$, Mann–Whitney test). (C) miR-21 knockdown had no effect on plasma triglyceride in HFD-treated mice. Data are presented as mean±SD ($p\geq0.1$, Mann–Whitney test). (D) miR-21-ASO injection into dietary obese mice resulted in downregulated miR-21 and increased *Hbp1* and *p53* expression. Data are presented as mean±SD. Mann–Whitney test was used for statistical analysis. (E) qRT-PCR revealed that HFD-treated mice with decreased levels of miR-21 also retained reduced expression of *Scd1*, *Fasn* and *Gpat* after miR-21-ASO injection. C57Bl/6 mice at 8 weeks of age were kept on HFD for an additional 8 weeks. At 12 weeks of age, mice received a dose of 25 mg/kg miR-21-ASO or miR-21-MM-ASO (0.9% NaCl) weekly for 4 weeks via tail vein injection. Data are presented as mean ±SD. Mann–Whitney test was used for statistical analysis.

hepatosteatosis, but there were no differences in liver and body weight. Therefore, we increased miR-21-ASO treatment time to 8 weeks, which resulted in decreases in both liver weight (see online supplementary table S7) and hepatic lipid content (see online supplementary figure S5B). However, no difference in body weight (see online supplementary table S7), serum free fatty acid and glycerol still was observed (see online supplementary figure S6A, B). In addition, we also observed that miR-21-ASO treatment had no effect on plasma liver enzymes (see online supplementary table S8). These findings indicated that the crosstalk of miR-21 with *Hbp1* and *p53* plays an important role in hepatosteatosis.

We further compared expression levels of *Srebp1c* and lipogenic genes in livers of miR-21-ASO and miR-21-MM-ASO treated mice. As expected, miR-21-ASO treatment led to a significant reduction in *Srebp1c* in the livers of HFD-treated mice (figure 6E). Reduction of *Srebp1c* due to miR-21 knockdown should impair expression of the lipogenic genes. Indeed, in the miR-21-ASO treated group, the mRNA of three enzymes including *Scd1*, *Fasn* and *Gpat* was downregulated at least 1.5 times those of controls (figure 6E).[29] Thus, the reduction of *Srebp1c* was associated with a dramatic reduction in the expression of the target enzymes responsible for lipogenesis, which prevented hepatic lipid accumulation. qRT-PCR also revealed that miR-21 knockdown had no effect on β-oxidation-related genes including *Cpt1α*, *Acc2* and *PGC1α* (see online supplementary figure S6C).[32 33]

In summary, our data have shown that HFD treatment led to increased miR-21, decreased *Hbp1* and *p53*, which subsequently promoted hepatic lipid accumulation and the potential for HCC, whereas antagonising miR-21 led to the opposite and more therapeutic effect. *Hbp1* is inhibited with increased miR-21 levels and its knockdown impaired transcription of *p53* by *Hbp1*, which led to reduced *p53*. The loss of *p53* then resulted in increased transcription of *Srebp1c*, *CCNB1* and *CCND1*, which promoted both lipogenesis and cell replication (figure 7). Our findings indicate the miR-21 plays an important role in linking NAFLD to HCC by interacting with the *Hbp1-p53-Srebp1c* pathway.

DISCUSSION

Our study addresses a potentially important role for miR-21 in the development of NAFLD and HCC and defines a novel mechanism by which miR-21 contributes to lipogenesis and carcinogenesis via the *Hbp1-p53-Srebp1c* pathway. The observation that antagonising miR-21 in dietary obese mice potentially improves these metabolic parameters clearly indicates a functional role for increased miR-21 expression in the development of NAFLD. In addition, we also observed that miR-21 knockdown prevented an in situ model of tumorigenesis by targeting *HBP1*. Increased miR-21 expression is not restricted to murine obesity models of NAFLD and HCC,[19 34] but is also detected in human patients with NASH and HCC.[6 34 35] Thus, miR-21-ASO may act as a unique potential therapeutic approach for the treatment of both disorders.

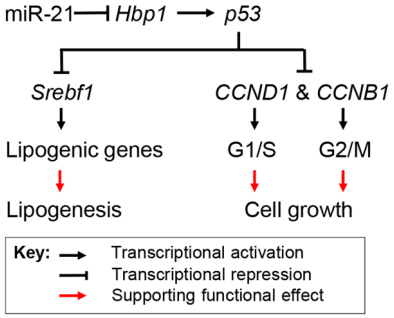

Figure 7 Proposed mechanism by which miR-21 links hepatic lipid accumulation and the development of cancer. Hbp1 is a transcriptional activator of *p53*, a suppressor of cell cycle progression and inhibitor of lipogenesis by inhibiting transcription of *Srebp1c*. By directly inhibiting *Hbp1* expression, miR-21 prevents expression of *p53*, which facilitates transcription of genes that are required for lipogenesis and the G1/S transition of cell cycle. As a result, increased miR-21 promotes both hepatic lipid accumulation and potentially carcinogenesis.

Despite its putative role in carcinogenesis,[36] the mechanism by which miR-21 regulates NAFLD is unknown. In this study, we observed that HFD administration resulted in increased miR-21 and its knockdown prevented hepatic lipid accumulation. In addition, we have functionally validated *Hbp1* as a bona fide target of miR-21, and Hbp1 is a transcriptional activator of *p53*. It is known that p53 acts as both a tumour suppressor and inhibitor of lipogenesis by inhibiting *Srebp1c*.[24 25 31] Our findings, combined with those of others, indicate that miR-21 plays critical roles in the pathogenesis of NAFLD and HCC. In addition, miR-21 deletion in *p53* knockout mice reduced the incidence of liver cancer;[37] and *p53* deletion alone promoted hepatosteatosis,[25] further supporting the unique role for miR-21 in linking NAFLD to HCC via the *Hbp1-p53-Srepb1c* pathway. miR-21 significantly inhibits expression of *PTEN*,[34] a negative regulator of NASH in mice,[38] suggesting that it might, in part, mediate the inhibitory effect of miR-21 on hepatosteatosis. In this study, we found that *Hbp1* is a direct target of miR-21 and confirmed that *Hbp1* modulates the inhibitory function of miR-21-ASO on hepatosteatosis and carcinogenesis simultaneously.

We have shown that miR-21 is highly expressed in hepatocytes (figure 1A). Meanwhile, miR-21 is increased but its target *Hbp1* is reduced in livers of HFD-treated mice and human individuals with NAFLD and HCC. All these features of miR-21 lead us to focus on its role in linking NAFLD to HCC. Although other miRNAs might contribute to the development of NAFLD and HCC, few other hepatocyte-specific miRNAs meet the above criteria like miR-21. These include increased expression in both NAFLD and HCC of human and mouse, reduced expression of their target genes in mouse models and human patients, and high expression in hepatocytes. We demonstrated that miR-21 knockdown led to upregulated *Hbp1* and *p53*, downregulated *Srebp1c* and decreased expression of hepatic *Scd1*, *Gpat* and *Fasn*. These findings are consistent with earlier reports that *p53* knockout promoted *Srebp1c* transcription and in turn increased expression of *Scd1*, *Gpat* and *Fasn*, and subsequently hepatic lipogenesis,[25 28] suggesting that miR-21-dependent *Hbp1-p53* pathway inhibition of *Srebp1c* transcription represents a candidate pathway to cause NAFLD.

There is evidence to suggest that inhibition of *p53* attenuates steatosis and liver injury,[39 40] which is inconsistent with our findings and those of others.[25 26 41] One possible explanation is that p53 is a negative regulator of hepatic lipid accumulation in the early stages of NAFLD, but *p53* is highly expressed at the advanced stages of NAFLD, which may contribute to the high level of apoptosis associated with NASH. In patients with liver steatosis without inflammation, *p53* expression was significantly lower than in steatohepatitis,[42] further suggesting that *p53* plays different roles in the various developmental stages of NAFLD. Although the mechanism(s) by which miR-21 controls lipogenesis and carcinogenesis in liver clearly requires further investigation, our study has identified an important role for the interaction of miR-21 with *Hbp1* in obesity-induced NAFLD and HCC.

Contributors HW and RN: acquisition of data. XC and CJS: analysis and interpretation of data. GS: obtaining funding, study supervision, study concept and design and drafting of the manuscript.

Funding Supported in part from grants received from the NIDDK R01 (1R01DK102601-01), Minnesota Medical Foundation, NIH Clinical and Translational Science Award at the University of Minnesota (UL1TR000114).

Competing interests None declared.

Ethics approval All procedures involving mice were approved by the Institutional Animal Care Committee at the University of Minnesota, University of California San Francisco, and the Agency for Science Technology and Research Singapore.

Provenance and peer review Not commissioned; externally peer reviewed.

REFERENCES

1 Yang JD, Roberts LR. Hepatocellular carcinoma: a global view. *Nat Rev Gastroenterol Hepatol* 2010;7:448–58.
2 Nair S, Mason A, Eason J, *et al*. Is obesity an independent risk factor for hepatocellular carcinoma in cirrhosis? *Hepatology* 2003;36:150–5.
3 Calle E, Kaaks R. Overweight, obesity and cancer: epidemiological evidence and proposed mechanisms. *Nat Rev Cancer* 2004;4:579–91.
4 Bartel D. MicroRNAs: genomics, biogenesis, mechanism, and function. *Cell* 2004;116:281–97.
5 Esquela-Kerscher A, Slack F. Oncomirs-microRNAs with a role in cancer. *Nat Rev Cancer* 2006;6:259–69.
6 Cheung O, Puri P, Eicken C, *et al*. Nonalcoholic steatohepatitis is associated with altered hepatic microRNA expression. *Hepatology* 2008;48:1810–20.
7 Gramantieri L, Fornari F, Callegari E, *et al*. MicroRNA involvement in hepatocellular carcinoma. *J Cell Mol Med* 2008;12:2189–204.
8 Esau C, Davis S, Murray SF, *et al*. miR-122 regulation of lipid metabolism revealed by in vivo antisense targeting. *Cell Metab* 2006;3:87–98.
9 Ladeiro Y, Couchy G, Balabaud C, *et al*. MicroRNA profiling in hepatocellular tumors is associated with clinical features and oncogene/tumor suppressor gene mutations. *Hepatology* 2008;47:1955–63.
10 Ng R, Wu H, Xiao H, *et al*. Inhibition of microRNA-24 expression in liver prevents hepatic lipid accumulation and hyperlipidemia. *Hepatology* 2014;60:554–64.
11 Ahrens M, Ammerpohl O, von Schönfels W, *et al*. DNA methylation analysis in nonalcoholic fatty liver disease suggests distinct disease-specific and remodeling signatures after bariatric surgery. *Cell Metab* 2013;18:296–302.
12 Friedman R, Farh K, Burge C, *et al*. Most mammalian mRNAs are conserved targets of microRNAs. *Genome Res* 2009;19:92–105.
13 Krek A, Grün D, Poy M, *et al*. Combinatorial microRNA target predictions. *Nat Genet* 2005;37:495–500.
14 Yang J-H, Li J-H, Shao P, *et al*. starBase: a database for exploring microRNA–mRNA interaction maps from Argonaute CLIP-Seq and Degradome-Seq data. *Nucleic Acids Res* 2011;39(Suppl 1):D202–9.
15 Harfe BD, McManus MT, Mansfield JH, *et al*. The RNaseIII enzyme Dicer is required for morphogenesis but not patterning of the vertebrate limb. *Proc Natl Acad Sci USA* 2005;102:10898–903.
16 Postic C, Magnuson MA. DNA excision in liver by an albumin-Cre transgene occurs progressively with age. *Genesis* 2000;26:149–50.
17 Mattis AN, Song G, Hitchner K, *et al*. A screen in mice uncovers repression of lipoprotein lipase by microRNA-29a as a mechanism for lipid distribution away from the liver. *Hepatology* 2014;61:142–51.
18 Nakai H, Fuess S, Storm TA, *et al*. Unrestricted hepatocyte transduction with adeno-associated virus serotype 8 vectors in mice. *J Virol* 2005;79:214–24.
19 Vickers KC, Shoucri BM, Levin MG, *et al*. MicroRNA-27b is a regulatory hub in lipid metabolism and is altered in dyslipidemia. *Hepatology* 2013;57:533–42.
20 Cui W, Chen SL, Hu K-Q. Quantification and mechanisms of oleic acid-induced steatosis in HepG2 cells. *Am J Transl Res* 2010;2:95–104.
21 Gomez-Lechon MJ, Donato MT, Martínez-Romero A, *et al*. A human hepatocellular in vitro model to investigate steatosis. *Chem Bio Interact* 2007;165:106–16.
22 Li H, Wang W, Liu X, *et al*. Transcriptional factor HBP1 targets p16INK4A, upregulating its expression and consequently is involved in Ras-induced premature senescence. *Oncogene* 2010;29:5083–94.
23 Tevosian SG, Shih HH, Mendelson KG, *et al*. HBP1: a HMG box transcriptional repressor that is targeted by the retinoblastoma family. *Genes Dev* 1997;11:383–96.
24 Levine AJ, Momand J, Finlay CA. The p53 tumour suppressor gene. *Nature* 1991;351:453–6.
25 Wang X, Zhao X, Gao X, *et al*. A new role of p53 in regulating lipid metabolism. *J Mol Cell Biol* 2013;5:147–50.
26 Yahagi N, Shimano H, Matsuzaka T, *et al*. p53 involvement in the pathogenesis of fatty liver disease. *J Biol Chem* 2004;279:20571–5.
27 Edwards PA, Tabor D, Kast HR, *et al*. Regulation of gene expression by SREBP and SCAP. *Biochim Biophys Acta* 2000;1529:103–13.
28 Horton JD, Goldstein JL, Brown MS. SREBPs: activators of the complete program of cholesterol and fatty acid synthesis in the liver. *J Clin Invest* 2002;109:1125–31.
29 Postic C, Girard J. The role of the lipogenic pathway in the development of hepatic steatosis. *Diabetes Metab* 2008;34:643–8.
30 Vermeulen K, Van Bockstaele DR, Berneman ZN. The cell cycle: a review of regulation, deregulation and therapeutic targets in cancer. *Cell Prolif* 2003;36:131–49.
31 Schupp M, Chen F, Briggs ER, *et al*. Metabolite and transcriptome analysis during fasting suggest a role for the p53-Ddit4 axis in major metabolic tissues. *BMC Genomics* 2013;14:758.
32 Kawano Y, Cohen DE. Mechanisms of hepatic triglyceride accumulation in non-alcoholic fatty liver disease. *J Gastroenterol* 2013;48:434–41.
33 Bartlett K, Eaton S. Mitochondrial β-oxidation. *Eur J Biochem* 2004;271:462–9.
34 Meng F, Henson R, Wehbe-Janek H, *et al*. MicroRNA-21 regulates expression of the PTEN tumor suppressor gene in human hepatocellular cancer. *Gastroenterology* 2007;133:647–58.
35 Becker P, Niesler B, Tschopp O, *et al*. MicroRNAs as mediators in the pathogenesis of non-alcoholic fatty liver disease and steatohepatitis. *Z Gastroenterol* 2014;52:1–27.
36 Krichevsky AM, Gabriely G. miR-21: a small multi-faceted RNA. *J Cell Mol Med* 2009;13:39–53.
37 Ma X, Choudhury SN, Hua X, *et al*. Interaction of the oncogenic miR-21 microRNA and the p53 tumor suppressor pathway. *Carcinogenesis* 2013;34:1216–23.
38 Watanabe S, Horie Y, Suzuki A. Hepatocyte-specific Pten-deficient mice as a novel model for nonalcoholic steatohepatitis and hepatocellular carcinoma. *Hepatol Res* 2005;33:161–6.
39 Castro RE, Ferreira D, Afonso MB, *et al*. miR-34a/SIRT1/p53 is suppressed by ursodeoxycholic acid in the rat liver and activated by disease severity in human non-alcoholic fatty liver disease. *J Hepatol* 2013;58:119–25.
40 Derdak Z, Villegas KA, Harb R, *et al*. Inhibition of p53 attenuates steatosis and liver injury in a mouse model of non-alcoholic fatty liver disease. *J Hepatol* 2013;58:785–91.
41 Jiang P, Du W, Wang X, *et al*. p53 regulates biosynthesis through direct inactivation of glucose-6-phosphate dehydrogenase. *Nat Cell Biol* 2011;13:310–16.
42 Panasiuk A, Dzieciol J, Panasiuk B, *et al*. Expression of p53, Bax and Bcl-2 proteins in hepatocytes in non-alcoholic fatty liver disease. *World J Gastroenterol* 2006;12:6198.

Supplementary Materials and Methods

Hepatocyte-specific miRNA Profiling

To identify miRNAs that were highly expressed in hepatocytes, we profiled global miRNAs in hepatocytes by comparing miRNA expression of livers between *Dicer1*$^{fl/fl}$ (n=2) and *Dicer1*$^{\Delta hep}$ mice (n=2) using Taqman Array MicroRNA Card (Applied Biosystems). These arrays were designed to investigate all miRNAs discovered in human, mouse and rat. Specifically, we isolated total RNA using the miRNeasy kit (Qiagen) from livers of *Dicer1*$^{fl/fl}$ and *Dicer1*$^{\Delta hep}$ mice[1 2], and the quality of total RNAs were determined using Bioanalyzer 2100. A total of 500 ng of RNA was used for miRNA-specific cDNA synthesis using Megaplex RT Primers and MicroRNA Reverse Transcription Kit (all Applied Biosystems). Taqman MicroRNA Array was run according to the manufacturer's protocol. Data analysis was performed using Viia 7 (Applied Biosystems) and Microsoft Access and the fold change was calculated using $2^{-\Delta\Delta Ct}$ method.[3] Internal control was U6 nuclear small RNA and U6 was measured five times in each sample. miR-21 expression was further confirmed between *Dicer1* knockout and wild-type mice using Taqman microRNA Assay from Invitrogen.

Fatty Acid Treatment of HepG2 Cells

HepG2 cells were seeded in a 4-well chamber slides using DMEM medium with 10% FBS and allowed to adhere overnight. To determine the inductive effect of miR-21 on lipogenesis, HepG2 cells were then treated with DMEM supplemented with 1% fatty acid free BSA and oleate (0.25 mM). Simultaneously, HepG2 cells cultured in the DMEM containing 0.25 mM oleate were transfected with miR-21 mimic (40 nM) or scrambled control (both Dharmacon) using Lipofectamine 2000. After 24 hours of transfection, Nile-Red Staining was used to

determine the intracellular lipid content in HepG2 cells. To investigate the inhibitory effect of miR-21 inhibitor on lipogenesis, HepG2 cells were then treated with DMEM supplemented with 1% fatty acid free BSA and oleate (0.5 mM). Simultaneously, HepG 2 cells cultured with the DMEM containing 0.5 mM oleate were transfected with miR-21-ASO (40 nM) or miR-21-MM-ASO (control) (Both Exiqon). Lipid accumulation was determined by Nile-Red Staining followed by microfluorimeter detection or imaging.

p53 expression vector (Plasmid #: 12091) and *p53* and *Hbp1* siRNA expression vectors were purchased from Addgene and Origene, respectively; and *HBP1* expression vector (pPM-hHBP1-His vector) was purchased from Applied Biological Materials (ABM) Inc. To determine whether the inhibitory effect of miR-21-ASO on lipogenesis is mediated by *HBP1*, HepG2 cells cultured in the DMEM containing 0.5 mM oleate were transfected with miR-21-ASO (40 nM in 4-well chamber slides), or miR-21-ASO combined with *HBP1* siRNA expression vector (200 ng/well in 4-well chamber slides). To determine whether *p53* is able to impair the ability of miR-21 mimic to induce lipogenesis, HepG2 cells cultured in the DMEM containing 0.25 mM oleate were transfected with miR-21 mimic (40 nM) or a combination of miR-21 mimic and *p53* expression vector (200 ng/ well in 4-well chamber slides). To further determine the role of the interaction between miR-21 and *p53*, HepG2 cells cultured in the DMEM containing 0.5 mM oleate were transfected with miR-21-ASO (40 nM) or a combination of miR-21-ASO and *p53* siRNA (100 ng). Lipofectamine 2000 was used for miR-21 mimic and miR-21-ASO transfection. The cells were cultured for an additional 24 hours, after which lipid accumulation was determined by Nile Red Staining (Sigma-Aldrich).

Lipid Accumulation Assay

The lipid content in HepG2 cells was determined using Nile Red, a vital lipophilic dye (9-diethylamino-5H-benzo [alpha] phenoxazine-5-one) from Sigma-Aldrich, which has been shown to selectively stain intracellular lipid droplets. Monolayers were washed with PBS and fixed with 4% paraformaldehyde at room temperature for 10 minutes. After washing, the cells were incubated for 20 minutes with Nile Red solution at a final concentration of 1mg/L in PBS at 37°C. After removal of chamber, the slides were mounted with Prolong® Gold anti-fade reagent with DAPI (Invitrogen) for visualization under fluorescence microscope.

Reporter Vector Construction and Luciferase Assay

To generate the luciferase reporter vectors, *Hbp1* 3' UTR was amplified by PCR from mouse cDNA, and inserted into the pMiR-Reporter vector (Ambion), referred as to pMiR-*Hbp1*. Two bases of the binding site for miR-21 within the 3'UTR of *Hbp1* were mutated using QuikChange II Site-Directed Mutagenesis Kit (Agilent Technologies) per the manufacture's instruction, and referred as to pMiR-*Hbp1-Mu*. Twenty-four hours before transfection, 5×10^4 Hepa1,6 cells were plated per well in a 24-well plate. Then, 200 ng of pMiR-*Hbp1* and miR-21 mimic or miR-21 inhibitor (20 nM or 40 nM) as well as 30 ng of β-*gal* plasmid pSV-β-Galactosidase Control Vector (Promega) were transfected using Lipofectamine 2000 (Invitrogen). Scrambled control (Dharmacon) or miR-21-MM-ASO (Exiqon) was used as the control for miR-21 mimic or miR-21-ASO, respectively.

p53 promoter (1.5 kb) was amplified from mouse genomic DNA and was cloned into pGL3-basic vector (Promega), referred as to pGL3-*p53*. 24 hours before transfection, 5×10^4 cells Hepa 1,6 were plated per well in a 24-well plate. Then, 200 ng of pGL3-*p53* with 100 ng or 200 ng *HBP1* expression vector (pPM-hHBP1-His vector) or mice *HBP1* siRNA expression vector (Origene) as well as 30 ng of β-*gal* plasmid pSV-β-Galactosidase Control Vector (Promega)

were transfected into Hepa1, 6 cells using Lipofectamine 2000 (Invitrogen). After 24 hours of transfection, luciferase and β-galactosidase assays were done using the Luciferase Assay System and Beta-Glo® Assay System (Promega). Luciferase activities were normalized to galactosidase activities; wells were transfected in triplicate; and each well was assayed in triplicate.

Srebp1c promoters (1.5 kb) were amplified from mouse genomic DNA and was cloned into pGL3-basic vector, referred as to pGL3-*Srebp1c.* 24 hours before transfection, 5×10^4 Hepa 1,6 cells were plated per well in a 24-well plate. Then, 200 ng of pGL3-*Srebp1c* with 100 ng or 200 ng *p53* expression vector or *p53* siRNA expression vector (100 ng) and 30 ng of β-*gal* plasmid pSV-β-Galactosidase Control Vector (Promega) were transfected into Hepa1,6 cells using Lipofectamine 2000 (Invitrogen). After 24 hours, luciferase and β-galactosidase assays were performed using the Luciferase Assay System and Beta-Glo® Assay System (Promega). Luciferase activities were normalized to galactosidase activities; wells were transfected in triplicate; and each well was assayed in triplicate.

miRNA Transfection and Gene Expression

5×10^4 of HepG2 cells were seeded in a 24-well plate and allowed to adhere overnight. To determine the effects of miR-21 overexpression and knockdown on gene expression, HepG2 cells cultured in the DMEM with 10% FBS were transfected with miR-21 mimic (40 nM) or inhibitor (40 nM) using Lipofectamine 2000. The equal concentration of scrambled control or miR-21-MM-ASO was used as control for miR-21 mimic or miR-21-ASO, respectively. 24 hours after transfection, cells were washed using cold PBS and the total RNA were isolated for gene expression analysis.

5×10^4 of HepG2 cells were seeded in a 24-well plate and allowed to adhere overnight. To overexpress *HBP1* or *p53,* 200 ng of pPM-hHBP1-His vector (Applied Biological Materials

(ABM) Inc.,) or *p53* expression vector (Addgene) was transfected into HepG2 cells using Lipofectamine 2000. The control HepG2 cells received empty pcDNA™3.1 vector (Life Technologies). 48 hours after transfection, cells were harvested for RNA isolation and gene expression analysis. To knock down *p53* or *HBP1*, human *p53* siRNA expression vector (100 ng) or *HBP1* siRNA expression vector (100 ng) was introduced into HepG2 cells using Lipofectamine 2000. 48 hours after transfection, the HepG2 cells were collected for RNA isolation and gene expression analysis.

To study whether *HBP1* mediates the inhibitory effect of miR-21-ASO on lipogenesis, 5×10^4 of HepG2 cells were seeded in a 24-well plate and allowed to adhere overnight. Then, the cells cultured in the DMEM containing 0.5 mM oleate were transfected with miR-21-ASO (40 nM), or a combination of miR-21-ASO with *HBP1* siRNA expression vector (200 ng/well). After 48 h, the HepG2 cells were collected for lipid content determination and gene expression analysis. Lipid content in HepG2 cells were determined using Nile-Read staining and gene expression was measured using qRT-PCR.

Histological analysis

Liver samples were embedded in Tissue-Tek OCT embedding compound, and frozen on dry ice. 8 µm-thick sections were cut with a Leica CM3050 S cryostat, air-dried, and fixed in 10% formalin. After washing, sections were stained with an Oil-Red-O (Sigma-Aldrich)/60% isopropanol solution (Fisher Scientific). Briefly, sections were rinsed with 60% isopropanol and stained for 20 min with prepared Oil Red O solution (0.5% in isopropanol followed by dilution to 60% with distilled water and filtered). After rinses in 60% isopropanol and distilled water, slides were counterstained with hematoxylin for 4 min, rinsed with water, and mounted. Hematoxylin and Eosin Staining kit (Scytek laboratories, Inc.) was used in paraformaldehyde-

fixed, paraffin-embedded sections of liver according to manufacturer's protocol. Images were taken with Zeiss Axioplan 2 Upright Microscope.

RNA Isolation and Quantitative Reverse Transcription-PCR (qRT-PCR)

Total RNA was isolated with miRNeasy Mini Kit (Qiagen). To assess gene expression, 1 μg RNA was used for cDNA synthesis with Superscript III reverse transcription reagent (Invitrogen). PCR amplification was performed at 50°C for 2 minutes and 95°C for 10 minutes, followed by 40 cycles at 95°C for 15 seconds and 60°C for 1 minute in a 7900 real time-PCR system with SYBR green (Applied Biosystems). For each sample, we analyzed β-actin, GAPDH or 18S rRNA expression to normalize target gene expression. Primers for qRT-PCR were designed with Primer Express software (Applied Biosystems). Primers used for quantitative RT-PCR were listed in Supplementary Table 4.

To determine levels of miRNA expression, 10 ng RNA were used for miRNA-specific cDNA synthesis with the TaqMan MicroRNA Reverse Transcription Kit and Taqman MicroRNA Assays (all Applied Biosystems). PCR amplification was performed at 95°C for 10 minutes, followed by 40 cycles at 95°C for 15 seconds and 60°C for 1 minute in a 7900 real time-PCR system (Applied Biosystems). The small RNA Sno202 and RNU6 were used to normalize target miRNA expression. Relative changes in gene and miRNA expression were determined using the $2^{-\Delta\Delta Ct}$ method.[3]

MTT* (3-(4,5-dimethylthiazol-2-yl)-2,5-diphenyltetrazoliumbromide) *Assay

Cell proliferation was determined using a MTT cell proliferation kit (Cell Biolabs, Inc.). 5×10^3 of HepG2 cells were seeded in each 96-well plate and allowed to adhere overnight. The cells were then transfected with scrambled control (40 nM), miR-21-ASO (40 nM), or miR-21

mimics (40 nM). After 48 hours culture, cells were used for MTT assay per the manufacturer's instruction (Cell Biolabs, Inc). To determine whether *HBP1* or *p53* mediates the inhibitory effect of miR-21-ASO on cell proliferation, we transfected HepG2 cells with miR-21-ASO (40 nM) or a combination of miR-21-ASO and *HBP1*siRNA expression vector (100 ng) or *p53* siRNA expression vector (100 ng). After 48 hours culture, cells were used for MTT assay per the manufacturer's instruction (Cell Biolabs, Inc). To determine whether *p53* overexpression was able to antagonize the effect of miR-21 on proliferation, we transfected miR-21 mimics (20 nM) or a combination of miR-21 mimics (20 nM) and *p53* expression vector (100 ng) in a 24-well plate. After 48 hours of transfection, cells were used for MTT assay per the manufacturer's instruction (Cell Biolabs, Inc). HepG2 cells were transfected with lipofectamine 2000.

Soft Agar Colony Formation Assay

HepG2 cells (0.5×10^6) in 35-mm plastic dishes were transfected with miR-21 mimics (40 nM) or inhibitors (40 nM). Two days after transfection, transfected cells were suspended with 8 ml of 0.4% top agar (Sigma-Aldrich) and 2×DMEM supplemented with 20% fetal bovine serum before being poured onto 6-cm tissue culture dishes coated with 3.5 ml of 0.7% bottom agar. Fourteen days later, three areas per plate were chosen randomly, the number of visible colonies was counted. To determine whether *HBP1* and *p53* mediate the inhibitory effects of miR-21-ASO on HepG2 cells colony formation, HepG2 cells were transfected with miR-21-ASO (40 nM) or a combination of miR-21-ASO (40 nM) and *p53* siRNA expression vector (100 ng) or *HBP1* siRNA expression vector (1 μg). After transfection for 48 hours, cells were suspended with 8 ml of 0.4% top agar (Sigma-Aldrich) and 2×DMEM supplemented with 20% fetal bovine serum before being poured onto 6-cm tissue culture dishes coated with 3.5 ml of 0.7% bottom agar.

Fourteen days later, three areas per plate were chosen randomly, the number of visible colonies was counted.

Xenograft Tumor Assay

HepG2 cells were placed in a 6-well plate 24 hours prior to transfection. HepG2 cells were transfected miR-21-ASO (40 nM), miR-21-MM-ASO (40 nM) or a combination of miR-21-ASO and *HBP1* siRNA expression vector (1 μg) or *p53* siRNA expression vector (400 ng). After 24 hours, 5×10^5cells in 0.1 ml PBS were injected subcutaneously into the right flank of athymic nude mice (n=9) to establish a model of tumor-bearing mice. Tumor growth was observed every 3 days by measuring its diameter with Vernier calipers. Tumor weight was calculated by gram. Tumor volume (cm^3) = $d^2 \times D/2$, where d is the shortest and D is the longest diameter, respectively. Mice were sacrificed when the tumor size reached 1.5 cm in diameter. All protocols complied with, and all animals received humane care according to, the criteria outlined in the NIH "Guide for the Care and Use of Laboratory Animals."

Cell Cycle Analysis

HepG2 cells were plated in a 6-well plate 24 hours before transfection. After 48 hours of transfection with miR-21 mimic (40 nM) or inhibitor (40 nM), the cells were detached from the plates by trypsin incubation, rinsed with PBS and fixed in 70% (v/v) ethanol. They were then re-suspended in PBS and incubated with RNase (100 μg/ml) and propidium iodide (60 μg/ml) (Sigma-Aldrich). Cells were analyzed using the FACSCalibur System (BD Biosciences), and the cell cycle phase was analyzed by using CellQuest software. The proliferation index (PI) was calculated as follows: PI = (S+G2/M)/G1. S, G2/M and G1 refer to the percentage of cells in S phase, G2/M phase and G1 phase, respectively. PI=(S+G2/M)/G1. To determine whether *p53* or *HBP1* mediates the inhibitory effect of miR-21-ASO on cell cycle progression, HepG2 cells

were transfected with miR-21-ASO (40 nM) or a combination of miR-21-ASO (40 nM) and *HBP1* siRNA expression vector (1 µg) or *p53* siRNA expression vector (100 ng). After 48 hours of transfection, the HepG2 cells were treated as above for cell cycle analysis.

Human Cell Cycle RT² Profiler™ PCR Array

We determined the effect of *HBP1* on expression of genes controlling cell cycle using Human Cell Cycle RT² *Profiler*™ PCR Array (Qiagen). The Human Cell Cycle RT² *Profiler*™ PCR Array profiles the expression of 84 genes key to cell cycle regulation. Briefly, HepG2 cells were plated in a 6 well plate 24 hours prior to transfection. HepG2 cells were transfected with 1 µg of pPM-hHBP1-His vector (Applied Biological Materials (ABM) Inc.,) using Lipofectamine 2000. The control HepG2 cells were treated with empty pcDNA™3.1 vector (Life Technologies). 48 hours after transfection, cells were harvested for RNA extract. A total of 2 µg RNA was used to perform the reverse transcription using SuperScript® III Reverse Transcriptase (Invitrogen). Cell Cycle RT² *Profiler*™ PCR Array was run according to the manufacturer's protocol. Data analysis was performed using $2^{-\Delta\Delta Ct}$ method.[3] Internal control is β-actin. *p53* expression was further confirmed between *HBP1* expressed vector treated cells and pcDNA3.1 vector treated cells using qRT-PCR.

Plasma Lipid Analysis

Blood was collected into tubes, containing 4 mM of EDTA, from cardiac puncture of C57Bl/6 mice after 4 or 8 weeks of HFD treatment. Plasma was separated by centrifugation (3000 x RPM for 20 min at 4 °C and triglyceride (mg/dl, Roche Diagnostics) was quantified enzymatically. Serum chemistry was carried out by the Pathology Laboratory of the University of Minnesota.

Hepatic Lipid Analysis

Mouse liver (100 mg) was placed in 1 ml chloroform/methanol (2:1) mixture and incubated on mice for 10 minutes before homogenization. Lipids were extracted from liver homogenates through room temperature orbital shaking (2 hours) followed by centrifugation (5000 RPM for 5 minutes). Supernatants were collected and washed with 0.4 ml chloroform/methanol (2:1) mixture by centrifugation at 5000 RPM for 20 minutes (room temperature). New supernatants were washed with 0.2 volume of 0.9% NaCl. After centrifuging for 5 minutes at 5000 RPM, supernatants were removed and lower-phase was dried at 42°C. Dried lipids were re-suspended in 2% Triton X-100. Liver triglycerides were quantified via a colorimetric assay using a triglyceride assay kit from Roche Diagnostics according to the manufacturer's protocols.

Western Blot Analysis

Western blot was performed following standard procedures. HBP1 primary antibodies were purchased from Abcam; and binding was visualized using SuperSignal west femto maximum sensitivity substrate (Cat # 34095, Thermo Fisher Scientific Inc.).

References

1. Harfe BD, McManus MT, Mansfield JH, Hornstein E, Tabin CJ. The RNaseIII enzyme Dicer is required for morphogenesis but not patterning of the vertebrate limb. *Proc Natl Acad Sci U S A* 2005;102(31):10898-903.
2. Mattis AN, Song G, Hitchner K, Kim RY, Lee AY, Sharma AD, et al. A screen in mice uncovers repression of lipoprotein lipase by microRNA-29a as a mechanism for lipid distribution away from the liver. *Hepatology* 2015; 61(1):141-52.
3. Schmittgen TD, Livak KJ. Analyzing real-time PCR data by the comparative C(T) method. *Nature Protoc* 2008;3(6):1101-8.

Supplementary Figures:

Figure 1. HFD treatment increases both hepatic and plasma triglycerides. (A) Oil-Red staining showing that HFD treatment led to increased hepatic lipid accumulation in mice. Lipid droplets in livers were labeled with arrows. (B,C) HFD treatment led to high levels of hepatic and plasma triglycerides. Lipids were extracted from the livers of mice treated with standard diet (n=6) or HFD (n=6) and triglycerides measured using a colorimetric assay. Representative histological images are shown. Data are expressed as mean ± SD. Mann-Whitney was used for statistical analysis. (D) HFD treatment led to reduced expression of *Hbp1* in livers of dietary obese mice. Data are expressed as mean ± SD. Mann-Whitney was used for statistical analysis.

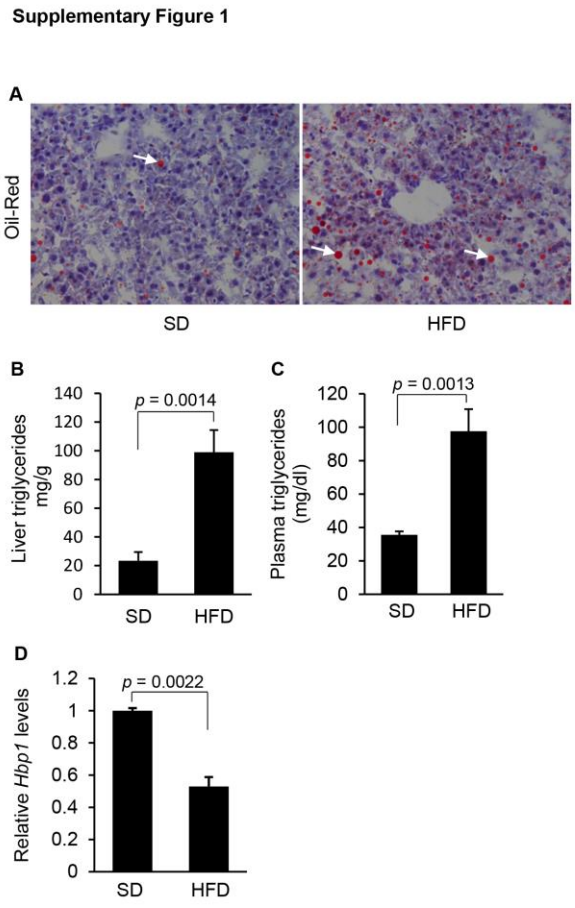

Figure 2. (A) Overexpression of *p53* caused dose-dependent inhibition of the activity of a luciferase reporter gene linked to the *Srebp1c* promoter. (B) *p53* knockdown via its siRNA released the inhibitory effect of *p53* on *Srebp1c* transcription, which was reflected by increased luciferase activity. Data are expressed as mean ± SD. In this multiple-groups experiment, we only performed comparison between two groups and Student T test was used for statistical analysis.

Supplementary Figure 2

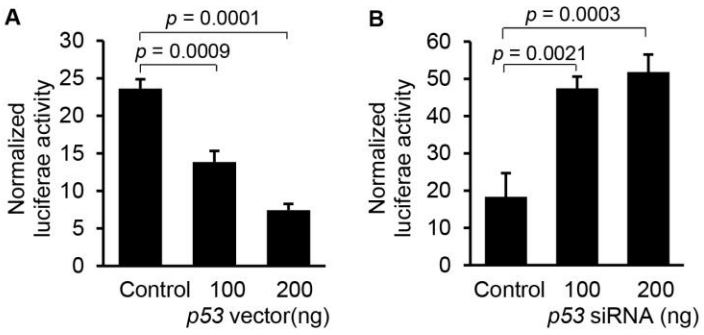

Figure 3. miR-21 modulates lipid accumulation in HepG2 cells by interacting with *p53*. (A, B) Transfection of miR-21 mimic into HepG2 cells incubated with oleate led to increased intracellular lipid content, and additional overexpression of *p53* offset the effect of miR-21. Lipid droplets in human hepatocytes were labeled with arrows. Data are expressed as mean ± SD. Student T test was used for statistical analysis. (C,D) miR-21 inhibitor transfection into HepG2 cells cultured with the medium containing 0.5 mM oleate led to a decrease in intracellular lipid content, and additional treatment of *p53* siRNA antagonized the effect of miR-21 inhibitor on lipid accumulation. Lipid droplets in human hepatocytes were labeled with arrows. Data are expressed as mean ± SD. Student T test was used for statistical analysis. (E) Mechanically, miR-21inhibitor treatment induced expression of *p53* and additional transfection of *p53* siRNA into HepG2 cells knocked down induced *p53*. Briefly, HepG2 cells were cultured with DMEM containing 0.5 mM oleate. 24 hours after miR-21 inhibitor transfection, *p53* siRNA was further introduced into HepG2 cells in attempt to knock down *p53* induced by miR-21 inhibitor. Data are expressed as mean ± SD. Student T test was used for statistical analysis.

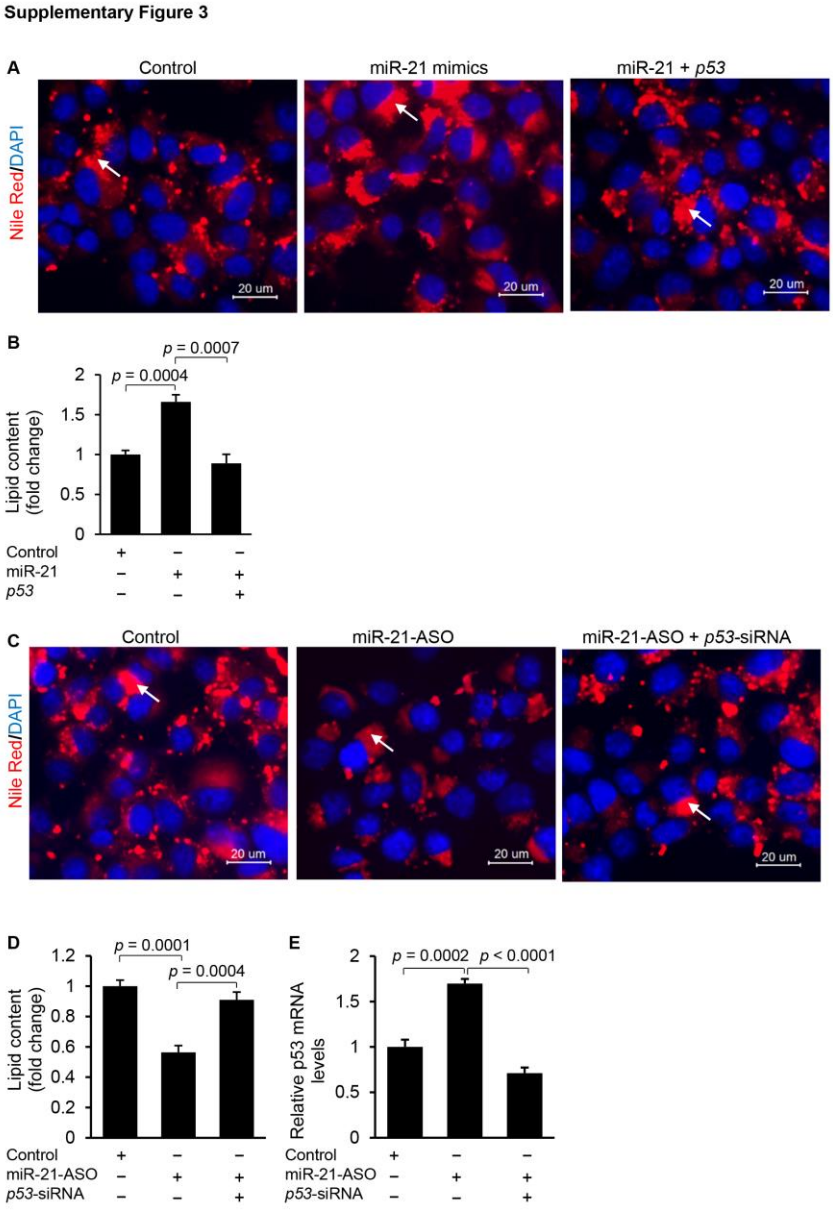

Figure 4. The inhibitory effects of miR-21-ASO on cell cycle progression and proliferation are mediated by *p53*. (A) miR-21 mimic transfection into HepG2 cells inhibited expression of *p53*, and treatment of *p53* expression vector significantly increased expression of *p53*. Data are presented as mean ± SD. Student T test was used for statistical analysis. (B) MTT assay revealed that miR-21 overexpression induced proliferation, and overexpression of *p53* counteracted the inductive effect of miR-21 on proliferation. Data are presented as mean ± SD. Student T test was used for statistical analysis. (C) Soft agar colony formation assay revealed that miR-21 overexpression promoted the colony formation of HepG2 cells, and further overexpression of *p53* antagonized the effect of miR-21. Data are presented as mean ± SD. Student T test was used for statistical analysis. (D,E) miR-21 mimic treatment led to a decrease in the number of cells in the G1 phase but an increase in the number of cells in S phase, and additional overexpression of *p53* antagonized the effect of miR-21. Quantification of the cell cycle phase distribution was analyzed by flow cytometry. The proliferation index was increased in the miR-21 mimic-treated HepG2 cells and overexpression of *p53* offset the effect of miR-21. Data are presented as mean ± SD (*$p < 0.05$, **$p < 0.001$, Chi-Square Test). (F) miR-21 inhibitor transfection into HepG2 cells induced expression of *p53*, and additional knockdown of induced *p53* with its siRNA inhibited expression of *p53*. Specifically, HepG2 cells were treated with oleate (0.5 mM) to induce miR-21, and then miR-21-ASO was transfected into HepG2 cells to knock down upregulated miR-21. Levels of *p53* were determined by qRT-PCR. Data are presented as mean ± SD. Student T test was used for statistical analysis. (G) MTT assay revealed that antagonizing miR-21 via miR-21 inhibitor led to reduced cellular proliferation in HepG2 cells, and additional knockdown of *p53* by its siRNA rescued the effect of miR-21 inhibitor. Data are presented as mean ± SD. Student T test was used for statistical analysis. (H) Soft agar colony formation assay revealed that miR-21 knockdown inhibited the growth of HepG2 cells, and the additional treatment of *p53*-siRNA antagonized the effect of miR-21 inhibitor. Data are presented as mean ± SD. Student T test was used for statistical analysis. (I,J) miR-21 inhibitor treatment prevented cell cycle progression, and additional knockdown of *p53* rescued the effect of miR-21 inhibitor. miR-21 knockdown increased the number of cells in the G1 phase but decreased the number of cells in S phase, and additional knockdown of up-regulated *p53* by its siRNA antagonized the effect of miR-21 inhibitor. Quantification of the cell cycle phase distribution was analyzed by flow cytometry. The proliferation index was reduced in the miR-21 inhibitor treated HepG2 cells and the additional treatment of *p53*-siRNA offset the effect of miR-21 inhibitor. Data are presented as mean ± SD (**$p < 0.001$, Chi-Square Test). (K) miR-21-ASO inhibited growth of subcutaneous tumors from HepG2 cells in nude mice, and additional treatment of *p53*-siRNA counteracted the effect of miR-21-ASO. HepG2 cells treated with scramble control, miR-21-ASO or a combination of miR-21-ASO and *p53*-siRNA were injected subcutaneously into nude mice. Data represent mean ± SD. Mann-Whitney was used for statistical analysis of tumor weight.

Supplementary Figure 4

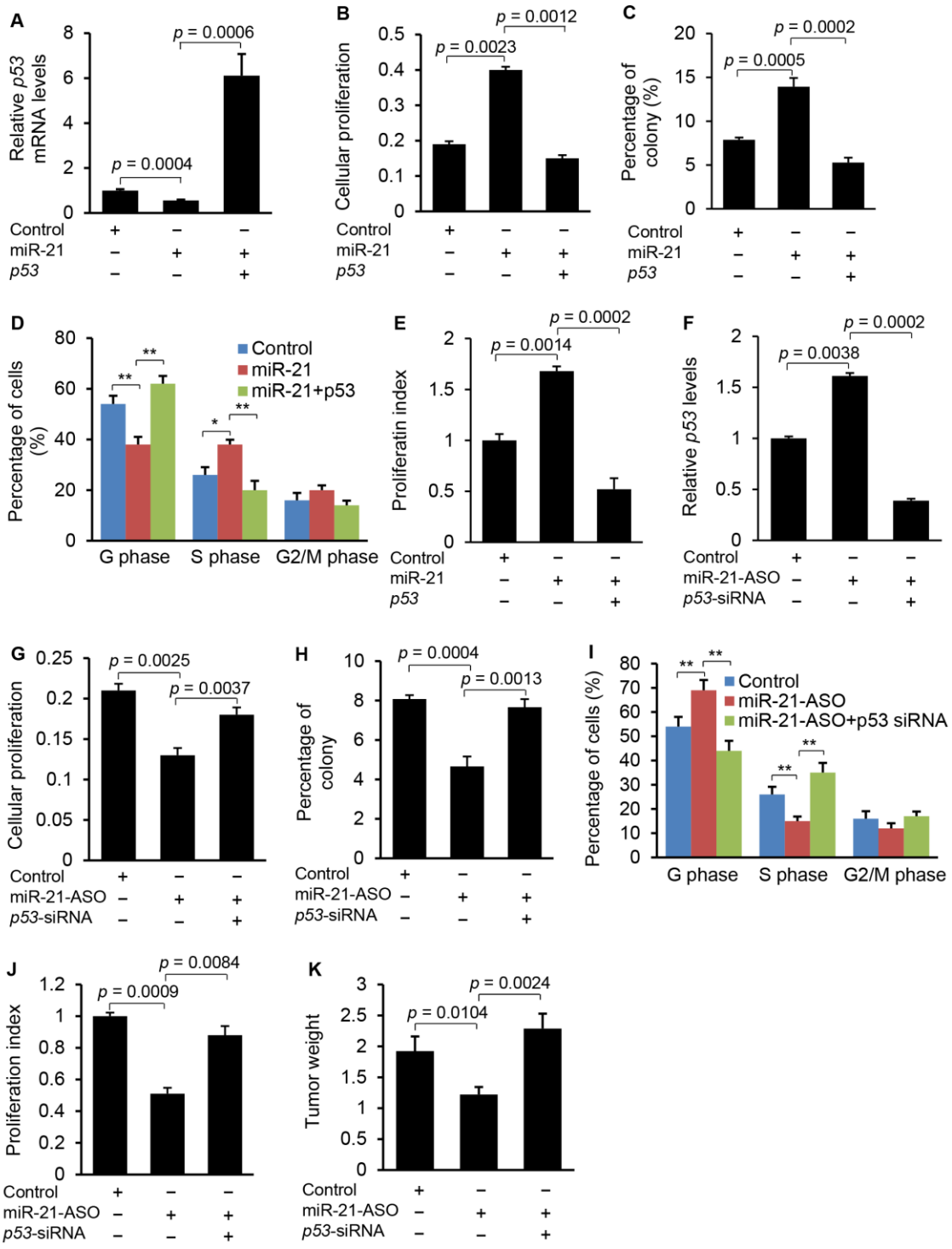

Figure 5. Knocking down miR-21 prevented hepatic lipid accumulation in HFD-treated mice. (A,B) miR-21 knockdown inhibited lipid accumulation in livers of HFD-fed mice injected with miR-21-ASO. Representative images (Oil-Red) are shown. Lipid droplets in livers were labeled with arrows. Cellular triglyceride content was measured by Oil Red staining and triglyceride (TG) content (per mg protein) was measured with a triglyceride estimation kit. Briefly, 8-week old mice were kept on HFD until 20 weeks of age. At 12 weeks of age, mice were divided into two groups: one group (n=8) received miR-21-MM-ASO and the other group received miR-21-ASO for another eight weeks. (C) miR-21-ASO injection into dietary obese mice resulted in down-regulated miR-21 and increased *Hbp1* and *p53* expression. Data represent mean ± SD. Mann-Whitney was used for statistical analysis. **p* < 0.05.

Supplementary Figure 5

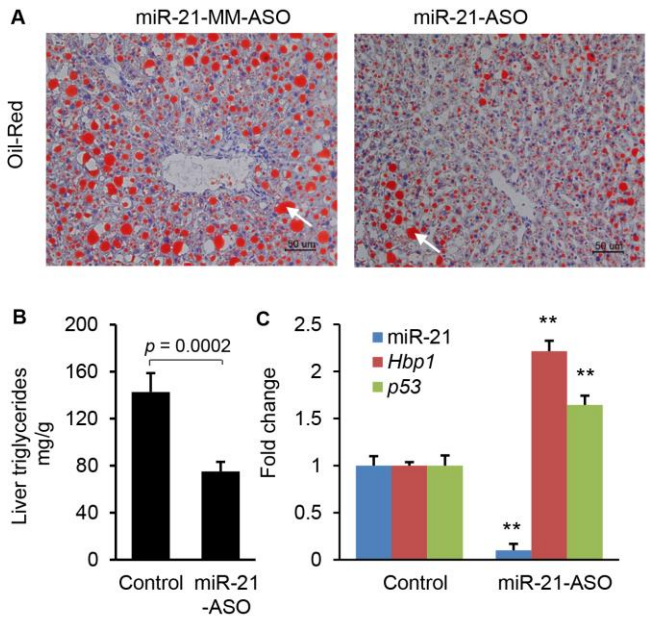

Figure 6. miR-21 knockdown had no effect on serum free fatty acid and glycerol as well as the expression of the genes encoding enzymes for fatty acid oxidation. (A,B) miR-21-ASO treatment had no effect on levels of serum free fatty acid and glycerol in dietary obese mice. (C) qRT-PCR revealed that miR-21 knockdown did not change the expression of β-oxidation-related genes including *Cpt1α*, *Acc2* and *PGC1α*.

Supplementary Figure 6

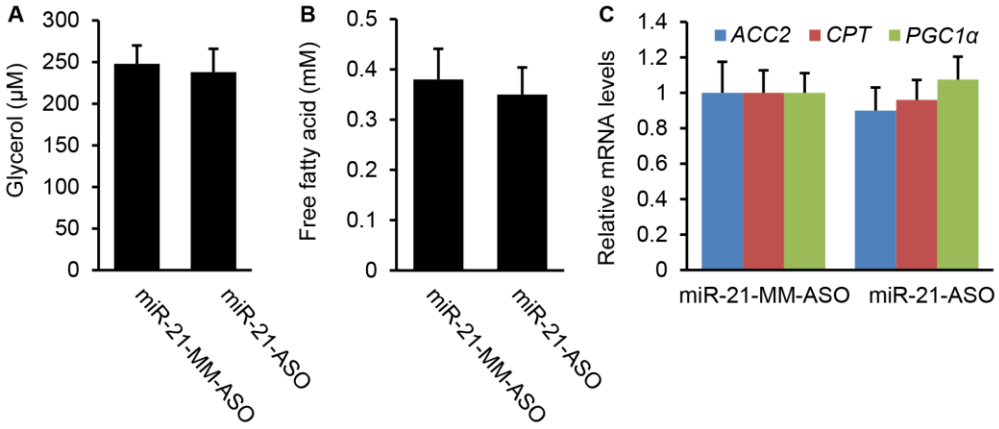

Supplementary Table 1. 1219 down-regulated probes in livers of human patients with NAFLD/NASH.

Probe ID	p-value	Log (Fold Change)	Gene Symbol	Gene Description
7916225	0.00002042	-0.79297091	RPS13	ribosomal protein S13
8095744	0.00003301	-0.92809751	AREG	amphiregulin
8016739	0.00003413	-0.76219365	TOB1	transducer of ERBB2, 1
8121850	0.00007819	-0.96944624	HEY2	hairy/enhancer-of-split related with YRPW motif 2
8166219	0.00013805	-0.52888646	SYAP1	synapse associated protein 1
7907970	0.00017988	-0.63720968		
7924058	0.00019095	-0.62327473	IRF6	interferon regulatory factor 6
8152642	0.00019118	-0.58996711	FAM83A-AS1	FAM83A antisense RNA 1
7892578	0.00020598	-0.86107507		
8167356	0.00021234	-0.5746145	GLOD5	glyoxalase domain containing 5
8122732	0.00021362	-0.69869308		
8115831	0.00024035	-1.39904664	DUSP1	dual specificity phosphatase 1
8174361	0.00024065	-1.10270028	TSC22D3	TSC22 domain family, member 3
7910901	0.00025567	-0.57259484	LOC100130331	POTE ankyrin domain family, member F pseudogene
7980096	0.00026905	-1.06351259		
8104136	0.00031457	-0.57617112	HMX1	H6 family homeobox 1
7899018	0.00034108	-0.58214279	TMEM57	transmembrane protein 57
8154381	0.00040117	-0.89537625	LURAP1L	leucine rich adaptor protein 1-like
8044574	0.00042422	-1.31166294	IL1RN	interleukin 1 receptor antagonist
7893573	0.00042537	-0.8413454		
7894916	0.00043289	-0.74484068		
7966631	0.00044308	-0.52391017	LHX5	LIM homeobox 5
8180222	0.00045126	-0.73639191	CFHR4	complement factor H-related 4
7908499	0.00045842	-1.02950046	CFHR5	complement factor H-related 5
8132013	0.00050245	-0.41798903	CHN2	chimerin 2
8144982	0.00055067	-0.47603714	NPM2	nucleophosmin/nucleoplasmin 2
8081036	0.00056767	-0.86673648	CADM2	cell adhesion molecule 2
8123800	0.00058719	-0.53901395		
8098782	0.00065132	-0.52548035	CPLX1	complexin 1
7946504	0.00068011	-0.45301645	TMEM41B	transmembrane protein 41B
8121794	0.00076598	-0.74999714	SMPDL3A	sphingomyelin phosphodiesterase, acid-like 3A
8149809	0.00077964	-0.42161283		
8069574	0.00083873	-0.6975465	C21orf91	chromosome 21 open reading frame 91
8040898	0.00084825	-0.60386321	TRIM54	tripartite motif containing 54
7989611	0.00088558	-0.64984027	FAM96A	family with sequence similarity 96, member A
8024485	0.00088896	-1.31050838	GADD45B	growth arrest and DNA-damage-inducible, beta
8180275	0.00089652	-0.73017018	PCDHA1	protocadherin alpha 1
7893001	0.00091425	-0.61391617		
8167625	0.00097516	-0.43744251	CCNB3	cyclin B3
8122317	0.00098027	-0.40045385	HEBP2	heme binding protein 2
8094938	0.00099488	-0.78036905	NIPAL1	NIPA-like domain containing 1
7961371	0.00103814	-0.61238977	DUSP16	dual specificity phosphatase 16
8111136	0.00106935	-1.05109382	FAM134B	family with sequence similarity 134, member B
8034698	0.00110117	-1.02876002	MIR23A	microRNA 23a
8140386	0.0011019	-0.4358513	STYXL1	serine/threonine/tyrosine interacting-like 1
8137526	0.00110482	-0.82985909	INSIG1	insulin induced gene 1
8174675	0.00120137	-0.53338897	SLC25A5-AS1///SLC25A5	SLC25A5 antisense RNA 1///solute carrier family 25 (mitochondrial carrier; adenine nucleotide translocator), member 5
8024038	0.00133153	-0.42402897	AZU1	azurocidin 1
7894268	0.00137202	-0.80404844		
8039340	0.00151127	-0.45677351	TNNT1	troponin T type 1 (skeletal, slow)
8086330	0.00153113	-1.84839709	CSRNP1	cysteine-serine-rich nuclear protein 1
8152215	0.00158019	-0.5133994	KLF10///KLF10	Kruppel-like factor 10///Kruppel-like factor 10
7928218	0.0015906	-0.79662233	CDH23	cadherin-related 23
7947199	0.00161768	-0.46886289	LGR4	leucine-rich repeat containing G protein-coupled receptor 4
7906863	0.00162373	-0.44543897	UAP1	UDP-N-acteylglucosamine pyrophosphorylase 1
8052934	0.00163613	-0.47586977	MCEE	methylmalonyl CoA epimerase
8040362	0.00168743	-0.69510683		

7967789	0.00174682	-0.64920848	PXMP2	peroxisomal membrane protein 2, 22kDa
7895162	0.00178057	-0.46039958		
8083569	0.00178308	-0.79711107	TIPARP	TCDD-inducible poly(ADP-ribose) polymerase
7892628	0.00181803	-0.72775738		
7892797	0.00181805	-0.43085863		
7895866	0.00183265	-0.96302911		
8033956	0.00183473	-0.41030632	S1PR2	sphingosine-1-phosphate receptor 2
7969177	0.00185368	-0.43959976	ST13P4	suppression of tumorigenicity 13 (colon carcinoma) (Hsp70 interacting protein) pseudogene 4
8025828	0.00185487	-1.15153203	LDLR	low density lipoprotein receptor
7959827	0.00187837	-0.35015972	TMEM132C	transmembrane protein 132C
7985898	0.00194622	-0.37701062	WDR93	WD repeat domain 93
7962537	0.00195513	-0.98323651	SLC38A2	solute carrier family 38, member 2
8158554	0.00197004	-0.37942865	PRRX2	paired related homeobox 2
8096077	0.00202598	-1.01498157		
8096661	0.00206275	-0.4885318		
8032273	0.00210311	-0.48392927		
8126946	0.00212526	-0.42875452		
8028652	0.00216135	-1.21798455	ZFP36	ZFP36 ring finger protein
8173106	0.00219743	-0.4609312	ITIH6	inter-alpha-trypsin inhibitor heavy chain family, member 6
8067955	0.00220035	-0.4353128	CXADR	coxsackie virus and adenovirus receptor
7927814	0.0022399	-0.47780987	SIRT1	sirtuin 1
8036902	0.00227133	-0.56879519	SERTAD1	SERTA domain containing 1
8034286	0.00228385	-0.43253	ECSIT	ECSIT signalling integrator
8169352	0.00229803	-0.58505298	NXT2	nuclear transport factor 2-like export factor 2
8138741	0.00229978	-0.45670343	HOXA6	homeobox A6
7922162	0.00231424	-0.8041639	SLC19A2	solute carrier family 19 (thiamine transporter), member 2
7997257	0.00233541	-0.55018592	ZFP1	ZFP1 zinc finger protein
7943218	0.00239565	-0.4273094	PANX1	pannexin 1
8101648	0.00240798	-0.6334724	HSD17B11	hydroxysteroid (17-beta) dehydrogenase 11
7938368	0.00241197	-0.58274175		
7928630	0.00241664	-0.37087115	EIF5AL1///EIF5A	eukaryotic translation initiation factor 5A-like 1///eukaryotic translation initiation factor 5A
7925128	0.00242339	-0.62687995		
7925813	0.0024389	-0.56368497	PRR26	proline rich 26
7987099	0.00248494	-0.44641745	OTUD7A	OTU domain containing 7A
7974870	0.00248683	-0.52323329	SNAPC1	small nuclear RNA activating complex, polypeptide 1, 43kDa
8095341	0.00258274	-0.51313788		
7905324	0.00259819	-0.50365441	C1orf56///C1orf56	chromosome 1 open reading frame 56///chromosome 1 open reading frame 56
7958000	0.00260001	-0.41980653	CHPT1	choline phosphotransferase 1
8040473	0.00260512	-0.71029488	RHOB	ras homolog family member B
8027345	0.00260822	-0.44951545	ZNF492	zinc finger protein 492
7894489	0.00262948	-0.43569551		
8126474	0.00269744	-0.3809945	PPP2R5D///MEA1	protein phosphatase 2, regulatory subunit B', delta///male-enhanced antigen 1
7940971	0.00269815	-0.476535	KCNK4///TEX40	potassium channel, subfamily K, member 4///testis expressed 40
8156309	0.00280094	-1.91857805	GADD45G	growth arrest and DNA-damage-inducible, gamma
8052123	0.00282848	-0.49124312		
8114185	0.0028402	-0.36110419	CDKN2AIPNL	CDKN2A interacting protein N-terminal like
8025515	0.00287786	-0.44084668	RDH8	retinol dehydrogenase 8 (all-trans)
8167862	0.00289701	-0.48092759	PAGE2B	P antigen family, member 2B
8055287	0.00289919	-0.43796413	MZT2A	mitotic spindle organizing protein 2A
8043743	0.00292461	-0.67967357		
8174026	0.00293023	-0.55828121	YWHAQP8	YWHAQ pseudogene 8
8152355	0.00296149	-0.77105697	SYBU	syntabulin (syntaxin-interacting)
8042107	0.00297762	-0.50763377	EIF3F	eukaryotic translation initiation factor 3, subunit F
8103524	0.00304423	-0.32197155	TMEM192	transmembrane protein 192
8044927	0.00306715	-0.73908427	INHBB	inhibin, beta B
7893298	0.00307572	-1.04787723		
7902282	0.00307667	-0.38643169	HHLA3	HERV-H LTR-associating 3
7955896	0.00308094	-0.46793182	COPZ1	coatomer protein complex, subunit zeta 1
8018482	0.00308408	-0.46854697	WBP2	WW domain binding protein 2
7987381	0.00308548	-0.37073497	CSNK1A1P1	casein kinase 1, alpha 1 pseudogene 1
8097655	0.00312283	-0.56275697		

7933084	0.00319926	-0.90824229	NAMPT	nicotinamide phosphoribosyltransferase
7899932	0.00321168	-0.39531876	GJB3	gap junction protein, beta 3, 31kDa
7984008	0.00322888	-0.60391894		
7938348	0.00323796	-0.71731105	WEE1	WEE1 homolog (S. pombe)
8109663	0.00327684	-0.37097365	GABRA1	gamma-aminobutyric acid (GABA) A receptor, alpha 1
8037535	0.00334481	-0.5266372		
7931348	0.00338259	-0.41154445	FOXI2	forkhead box I2
8057599	0.00339997	-0.49814204	TFPI	tissue factor pathway inhibitor (lipoprotein-associated coagulation inhibitor)
7972062	0.00341863	-0.53169338	FBXL3	F-box and leucine-rich repeat protein 3
7922523	0.00341999	-0.72352437		
8084035	0.00342392	-0.3806076	ZNF639	zinc finger protein 639
8002556	0.00343743	-0.41156863	TAT	tyrosine aminotransferase
8077944	0.00356907	-0.44030569	CAND2	cullin-associated and neddylation-dissociated 2 (putative)
8048319	0.00358257	-1.34572837	VIL1	villin 1
8030999	0.00360323	-0.73399042	ZNF331	zinc finger protein 331
7893809	0.00363236	-0.48877502		
7939492	0.00363515	-0.59049103	C11orf96	chromosome 11 open reading frame 96
8086028	0.00372278	-0.36696877	GLB1	galactosidase, beta 1
8129562	0.00374956	-1.10524489	CTGF	connective tissue growth factor
7907655	0.00380461	-0.59433884		
8029507	0.00381324	-0.46886473	PVRL2	poliovirus receptor-related 2 (herpesvirus entry mediator B)
8113616	0.00390139	-0.44379853	FEM1C	fem-1 homolog c (C. elegans)
8134091	0.00397943	-0.39306923	CLDN12	claudin 12
8030299	0.00400619	-0.38283339	CCDC155	coiled-coil domain containing 155
8165907	0.00401462	-0.42457406		
8127629	0.00412227	-0.43334274	COX7A2	cytochrome c oxidase subunit VIIa polypeptide 2 (liver)
7937330	0.00412576	-0.72633257	IFITM2	interferon induced transmembrane protein 2
8161884	0.00413807	-0.3905697	PRUNE2	prune homolog 2 (Drosophila)
8040103	0.00418069	-0.50310353	ID2	inhibitor of DNA binding 2, dominant negative helix-loop-helix protein
7933723	0.00418145	-0.48001218	IPMK	inositol polyphosphate multikinase
7977340	0.00421513	-0.61037656	BTBD6	BTB (POZ) domain containing 6
8070665	0.00422801	-2.17844415	SIK1	salt-inducible kinase 1
8150592	0.00424845	-0.92584694	CEBPD	CCAAT/enhancer binding protein (C/EBP), delta
7931553	0.00425034	-0.44916502	UTF1	undifferentiated embryonic cell transcription factor 1
7906819	0.00426254	-0.42172089	ATF6	activating transcription factor 6
8028563	0.0043084	-0.36296876	SARS2///MRPS12	seryl-tRNA synthetase 2, mitochondrial///mitochondrial ribosomal protein S12
7968272	0.00434427	-0.40411607		
8124848	0.00435247	-1.24562714	IER3	immediate early response 3
7955589	0.00438037	-1.83708367	NR4A1	nuclear receptor subfamily 4, group A, member 1
8075332	0.00440358	-0.34419627	TBC1D10A	TBC1 domain family, member 10A
7926531	0.00440758	-0.78966531	ARL5B	ADP-ribosylation factor-like 5B
8172028	0.00443478	-0.56427871		
7963061	0.00445042	-0.39782438	C1QL4	complement component 1, q subcomponent-like 4
8076734	0.00446229	-0.32904051	WNT7B	wingless-type MMTV integration site family, member 7B
7997245	0.00447818	-0.57646424		
8022912	0.0044798	-0.42757287	MIR187	microRNA 187
7928823	0.00450568	-0.46092822	OPN4	opsin 4
7896542	0.00452104	-0.44880106		
8029489	0.00457471	-0.58404465	BCAM	basal cell adhesion molecule (Lutheran blood group)
8041561	0.0045827	-0.69651727	MORN2	MORN repeat containing 2
8056102	0.00458612	-0.47832061	LY75-CD302///CD302///CD302	LY75-CD302 readthrough///CD302 molecule///CD302 molecule
8172654	0.00460281	-0.4908284	USP27X-AS1	USP27X antisense RNA 1 (head to head)
8089011	0.00460815	-0.58678728	PROS1	protein S (alpha)
8032051	0.00462119	-0.48997936	ODF3L2	outer dense fiber of sperm tails 3-like 2
8026341	0.00462468	-0.39211721	MIR639///TECR	microRNA 639///trans-2,3-enoyl-CoA reductase
7979906	0.00462887	-0.33595199	COX16	COX16 cytochrome c oxidase assembly homolog (S. cerevisiae)
8067585	0.00463215	-0.48589407	BHLHE23	basic helix-loop-helix family, member e23
8169080	0.00464251	-0.46899293	H2BFM	H2B histone family, member M
8055952	0.00467622	-2.38162242	NR4A2	nuclear receptor subfamily 4, group A, member 2
8145440	0.00468513	-0.4207451	PPP2R2A	protein phosphatase 2, regulatory subunit B, alpha

7997281	0.00474822	-0.31522401	LOC100288358///TERF2IP	uncharacterized LOC100288358///telomeric repeat binding factor 2, interacting p
7921473	0.00475568	-0.40804966	CCDC19	coiled-coil domain containing 19
8001658	0.00475659	-0.49442371	C16orf80	chromosome 16 open reading frame 80
7984011	0.00479953	-0.4501947	FOXB1	forkhead box B1
7966321	0.00481561	-0.48311361	GPN3	GPN-loop GTPase 3
8081548	0.00491062	-0.34885596	PVRL3	poliovirus receptor-related 3
7961702	0.00493373	-0.51273359	KCNJ8	potassium inwardly-rectifying channel, subfamily J, member 8
7902290	0.00497914	-0.85723533	CTH	cystathionase (cystathionine gamma-lyase)
7893126	0.00499271	-0.50921745		
7895999	0.00508128	-0.80143545		
8038477	0.00513034	-0.39106372	AKT1S1	AKT1 substrate 1 (proline-rich)
7992447	0.00515645	-0.46435071	SYNGR3	synaptogyrin 3
7988033	0.00515705	-0.34336504	EPB42	erythrocyte membrane protein band 4.2
8042211	0.00518106	-0.40948862	B3GNT2	UDP-GlcNAc:betaGal beta-1,3-N-acetylglucosaminyltransferase 2
8175775	0.00525884	-0.36505992	MAGEA1	melanoma antigen family A, 1 (directs expression of antigen MZ2-E)
8113220	0.00528051	-0.4084689	ELL2	elongation factor, RNA polymerase II, 2
8041048	0.00528818	-0.76435982	FOSL2	FOS-like antigen 2
8027390	0.0053856	-0.57256643	POP4	processing of precursor 4, ribonuclease P/MRP subunit (S. cerevisiae)
7910638	0.00539462	-0.32394432		
7971905	0.00541491	-0.99462736	PCDH20	protocadherin 20
8173613	0.00544019	-0.47524059	RLIM	ring finger protein, LIM domain interacting
7904921	0.00548926	-0.41853402		
8075198	0.00552375	-0.38715775		
8149475	0.0055617	-0.40361036	CNOT7	CCR4-NOT transcription complex, subunit 7
7896417	0.00563782	-0.94617864		
7912361	0.0056567	-0.36774972	MASP2	mannan-binding lectin serine peptidase 2
8022404	0.0056903	-0.49151104	FAM210A	family with sequence similarity 210, member A
8173174	0.00570365	-0.44169143	USP51	ubiquitin specific peptidase 51
8019273	0.00572308	-0.4437143	ALYREF	Aly/REF export factor
8062782	0.00574316	-0.35107174	TOX2	TOX high mobility group box family member 2
8152092	0.00574696	-0.49306521		
7908496	0.00576171	-0.30036417	CFHR2	complement factor H-related 2
7935679	0.00584077	-0.59294195	CPN1	carboxypeptidase N, polypeptide 1
7898448	0.00586683	-0.32563272	PADI4	peptidyl arginine deiminase, type IV
7903474	0.00588765	-0.66252786		
8088167	0.00590185	-0.73221561	SELK	selenoprotein K
8053386	0.00593987	-0.42835305		
7896709	0.00595633	-0.54491053		
7977621	0.00596052	-0.31595099	NDRG2	NDRG family member 2
7970241	0.00599773	-0.47770509	F10	coagulation factor X
7930413	0.00605122	-0.59449389	DUSP5	dual specificity phosphatase 5
7895018	0.0060528	-0.76877776		
7904084	0.00607682	-0.42246545	AKR7A2P1	aldo-keto reductase family 7, member A2 pseudogene 1
8134452	0.00610284	-0.3608268	BHLHA15	basic helix-loop-helix family, member a15
8012891	0.00614412	-0.44763079		
7979886	0.00615054	-0.47851425		
7972745	0.00617206	-0.99279147	IRS2	insulin receptor substrate 2
7945688	0.00619404	-0.32391	INS-IGF2///INS///IGF2	INS-IGF2 readthrough///insulin///insulin-like growth factor 2 (somatomedin A)
8080960	0.00621401	-0.40331914		
8131475	0.00623208	-0.42100182	C1GALT1	core 1 synthase, glycoprotein-N-acetylgalactosamine 3-beta-galactosyltransfera
8035398	0.00623283	-0.60831376	RAB3A	RAB3A, member RAS oncogene family
7993185	0.00627444	-0.45327951	NUBP1///NUBP1	nucleotide binding protein 1///nucleotide binding protein 1
7978666	0.00630918	-0.40811759	MBIP	MAP3K12 binding inhibitory protein 1
8123763	0.00635391	-0.32196566		
8106976	0.00640806	-0.38056911	GPR150	G protein-coupled receptor 150
7905533	0.00646517	-0.42610209	IVL	involucrin
8082667	0.00652538	-0.42223065	NUDT16	nudix (nucleoside diphosphate linked moiety X)-type motif 16
7911138	0.00656876	-0.32565054	CNST	consortin, connexin sorting protein
8172022	0.00662795	-0.39992152	TMEM47	transmembrane protein 47
8061507	0.00665163	-0.39298354		
7905949	0.0067186	-0.41477061		

8172345	0.00671888	-0.3772574	ELK1	ELK1, member of ETS oncogene family
7898655	0.00672387	-0.60517746	CDA	cytidine deaminase
8132694	0.00672768	-2.42071729	IGFBP1	insulin-like growth factor binding protein 1
8135480	0.00675373	-0.58554821	DNAJB9	DnaJ (Hsp40) homolog, subfamily B, member 9
8141533	0.00678251	-0.40249095		
8111757	0.00680358	-0.47485865	C9	complement component 9
7991809	0.00681807	-0.43076631	PDIA2///ARHGDIG	protein disulfide isomerase family A, member 2///Rho GDP dissociation inhibitor
8052087	0.00687575	-0.46199213		
8043682	0.00687815	-0.59561521	LOC653924	glycerol-3-phosphate acyltransferase 2, mitochondrial pseudogene
8157264	0.00689371	-0.59903063	SLC31A2	solute carrier family 31 (copper transporters), member 2
7909142	0.00693518	-0.53564924	NUCKS1	nuclear casein kinase and cyclin-dependent kinase substrate 1
8019181	0.0069406	-0.4619242	LOC100130370	uncharacterized LOC100130370
8012344	0.00697218	-0.45144554	HES7	hairy and enhancer of split 7 (Drosophila)
7921014	0.00703173	-0.37471617	MEF2D///MEF2D	myocyte enhancer factor 2D///myocyte enhancer factor 2D
7894011	0.00705212	-0.64433672		
7920697	0.00708493	-0.38311175	GBA	glucosidase, beta, acid
8037737	0.00711773	-0.32678056	NOVA2	neuro-oncological ventral antigen 2
8036031	0.00717089	-0.47881442		
8023984	0.0071809	-0.3533444	HCN2	hyperpolarization activated cyclic nucleotide-gated potassium channel 2
8082605	0.00721481	-0.34669716		
7931556	0.00723762	-0.42116855	VENTX	VENT homeobox
7917741	0.00724415	-0.35159811	TMED5	transmembrane emp24 protein transport domain containing 5
8112613	0.00725973	-0.55011642		
8006562	0.00728147	-0.44878483	RASL10B	RAS-like, family 10, member B
8034514	0.00734294	-0.30934348	C19orf43	chromosome 19 open reading frame 43
7909610	0.00742968	-0.80696302	ATF3	activating transcription factor 3
8059026	0.00743657	-0.33410252	MIR375	microRNA 375
8014865	0.00748496	-0.30968903	NEUROD2	neuronal differentiation 2
7902687	0.00749592	-1.58929102	CYR61	cysteine-rich, angiogenic inducer, 61
8129666	0.00752051	-0.65162755	SLC2A12	solute carrier family 2 (facilitated glucose transporter), member 12
8079140	0.00753724	-0.41811603	SNRK	SNF related kinase
7929653	0.00753755	-0.41250631	ANKRD2	ankyrin repeat domain 2 (stretch responsive muscle)
7952408	0.00758054	-0.51254783	SIAE	sialic acid acetylesterase
7893679	0.00762347	-0.66557408		
8012000	0.00765775	-0.5342722	RNASEK	ribonuclease, RNase K
7951660	0.00766067	-0.31945717		
8101699	0.00767203	-0.76333399	PPM1K	protein phosphatase, Mg2+/Mn2+ dependent, 1K
8073960	0.0076739	-0.34498536	PIM3	pim-3 oncogene
8029693	0.00776588	-2.48951161	FOSB///FOSB	FBJ murine osteosarcoma viral oncogene homolog B///FBJ murine osteosarcom homolog B
8125919	0.00778632	-0.70085929	LOC285847///FKBP 5	uncharacterized LOC285847///FK506 binding protein 5
8124433	0.00780294	-0.39079902	HIST1H4G	histone cluster 1, H4g
7920047	0.00782009	-0.30044311	MRPL9	mitochondrial ribosomal protein L9
8005747	0.00782995	-0.40879915		
8070257	0.00784738	-0.42553747	PIGP	phosphatidylinositol glycan anchor biosynthesis, class P
8042335	0.00785852	-0.39836679	VDAC2	voltage-dependent anion channel 2
7896657	0.00790549	-0.36538957		
8063386	0.00791892	-0.45700192	CEBPB	CCAAT/enhancer binding protein (C/EBP), beta
7938748	0.00792251	-0.45622772		
7912207	0.00793853	-0.41925277		
7931926	0.00797927	-0.30257615		
8112570	0.00798736	-0.31578424	MRPS27	mitochondrial ribosomal protein S27
8099918	0.00808893	-0.39758671		
8099633	0.0080994	-0.93030989	PPARGC1A	peroxisome proliferator-activated receptor gamma, coactivator 1 alpha
7892679	0.00817767	-0.7803035		
8123463	0.00825871	-0.40715449	C6orf120///PHF10	chromosome 6 open reading frame 120///PHD finger protein 10
8168892	0.00828467	-0.30980017	TCEAL2	transcription elongation factor A (SII)-like 2
7895253	0.00832644	-0.7513525		
8164428	0.00833208	-0.31929364	COQ4///TRUB2	coenzyme Q4 homolog (S. cerevisiae)///TruB pseudouridine (psi) synthase hom
7896321	0.00834717	-0.63173595		
8098604	0.00836097	-1.0878421	ANKRD37///UFSP2	ankyrin repeat domain 37///UFM1-specific peptidase 2
8161610	0.00853768	-0.62339209	TMEM252	transmembrane protein 252

8146559	0.00854129	-0.4153998		
8013804	0.00855972	-0.46431045	DHRS13	dehydrogenase/reductase (SDR family) member 13
8079117	0.00856495	-0.70857495	CCBP2	chemokine binding protein 2
8038877	0.00857639	-0.50946137	SIGLEC5	sialic acid binding Ig-like lectin 5
8134415	0.0085817	-0.34670333	ACN9	ACN9 homolog (S. cerevisiae)
7934278	0.00861048	-1.41272271	P4HA1	prolyl 4-hydroxylase, alpha polypeptide I
8105151	0.00862206	-0.36808791		
7908488	0.00863954	-0.43377221	CFHR1	complement factor H-related 1
7895972	0.00864048	-0.57482767		
8149289	0.00865386	-0.43339143	SOX7	SRY (sex determining region Y)-box 7
8109732	0.0086566	-0.40228854	MAT2B	methionine adenosyltransferase II, beta
8116658	0.00866762	-0.37468245	FAM50B	family with sequence similarity 50, member B
8096489	0.00868943	-0.3952269	PDLIM5	PDZ and LIM domain 5
7970448	0.008704	-0.31183144	GJB6	gap junction protein, beta 6, 30kDa
8104499	0.00876472	-0.37895916	ANKRD33B	ankyrin repeat domain 33B
7936320	0.00877865	-0.43328263	RPL13AP6	ribosomal protein L13a pseudogene 6
7918437	0.00882881	-0.34185604	LAMTOR5	late endosomal/lysosomal adaptor, MAPK and MTOR activator 5
7936833	0.0088747	-0.64274924		
7895263	0.0088885	-0.38760549		
8133114	0.00889094	-0.32720993	VKORC1L1	vitamin K epoxide reductase complex, subunit 1-like 1
8104022	0.0089315	-0.59880096	PDLIM3	PDZ and LIM domain 3
7944006	0.00893599	-0.48927117	RBM7	RNA binding motif protein 7
8166382	0.00897159	-0.31889815	MBTPS2	membrane-bound transcription factor peptidase, site 2
7966389	0.00897588	-0.33924654	FAM109A	family with sequence similarity 109, member A
7995324	0.00897682	-0.58131206		
7945536	0.00897846	-0.4207714	CEND1	cell cycle exit and neuronal differentiation 1
7910790	0.00898445	-0.5331333		
7937465	0.00899656	-0.33036562	TALDO1	transaldolase 1
8053139	0.00903744	-0.32251651	C2orf81	chromosome 2 open reading frame 81
8115144	0.00903823	-0.40536169	ARSI	arylsulfatase family, member I
7985777	0.00904812	-0.35551268	ISG20	interferon stimulated exonuclease gene 20kDa
7919568	0.00905407	-0.44556348		
7965152	0.009072	-0.40563482		
8027402	0.00912961	-0.36855138	CCNE1	cyclin E1
8096533	0.00914464	-0.41241511		
8147566	0.00914732	-0.37727663	KCNS2	potassium voltage-gated channel, delayed-rectifier, subfamily S, member 2
7950644	0.00915194	-0.31693204	NDUFC2	NADH dehydrogenase (ubiquinone) 1, subcomplex unknown, 2, 14.5kDa
7975045	0.00915666	-0.40716591	MTHFD1	methylenetetrahydrofolate dehydrogenase (NADP+ dependent) 1, methenyltetra cyclohydrolase, formyltetrahydrofolate synthetase
7995332	0.00920364	-0.55891548		
7940005	0.00924711	-0.47656773	P2RX3	purinergic receptor P2X, ligand-gated ion channel, 3
8070689	0.00929776	-0.372955	HSF2BP	heat shock transcription factor 2 binding protein
8060741	0.00934063	-0.35615199		
8117696	0.00934483	-0.49963342	COX11	cytochrome c oxidase assembly homolog 11 (yeast)
7947828	0.00938372	-0.40675709	MYBPC3	myosin binding protein C, cardiac
8106473	0.00938475	-0.43605402		
8161829	0.00945475	-0.43462103	C9orf41	chromosome 9 open reading frame 41
8094874	0.0094803	-0.39952773		
8016320	0.00949417	-0.44895129	RPRML	reprimo-like
8044682	0.00951594	-0.44605661		
8132209	0.00953039	-0.4444967	ZNRF2P1	zinc and ring finger 2 pseudogene 1
7922754	0.00954886	-0.48114118		
7919314	0.00955327	-0.42479366	FMO5	flavin containing monooxygenase 5
7948369	0.00955503	-0.58428935		
7999387	0.00957671	-0.35731933	EMP2	epithelial membrane protein 2
7895181	0.00961533	-0.59036358		
8146837	0.00963234	-0.57234307		
7935855	0.00970267	-0.32919828	LBX1	ladybird homeobox 1
7995326	0.00970578	-0.39318939		
7917240	0.00972789	-0.57141755	CTBS	chitobiase, di-N-acetyl-
7999171	0.00977018	-0.46860413		
8170702	0.00983402	-0.36197817		

7894504	0.0098639	-0.81397023		
8150830	0.00986768	-0.47849016	LYPLA1	lysophospholipase I
8056943	0.00991212	-0.35405226	KIAA1715	KIAA1715
8098414	0.00993869	-0.56395089	SPCS3	signal peptidase complex subunit 3 homolog (S. cerevisiae)
8110604	0.00997563	-0.44555367		
8161238	0.01003471	-0.50454921	RAB1C	RAB1C, member RAS oncogene family pseudogene
8076655	0.01014197	-0.32891458	PNPLA5	patatin-like phospholipase domain containing 5
7980990	0.01014993	-0.55239339	C14orf142///UBR7	chromosome 14 open reading frame 142///ubiquitin protein ligase E3 componen (putative)
8147970	0.01015589	-0.30581758	EBAG9	estrogen receptor binding site associated, antigen, 9
8088908	0.01020996	-0.41134802		
7938756	0.01025138	-0.32092892	ST13P5	suppression of tumorigenicity 13 (colon carcinoma) (Hsp70 interacting protein) p
8106475	0.0103189	-0.3594368	ACTB	actin, beta
7977951	0.01036025	-0.34461725		
8148304	0.01039175	-1.18304529	TRIB1	tribbles homolog 1 (Drosophila)
7939902	0.01040063	-0.38828584	LOC646813	DEAH (Asp-Glu-Ala-His) box helicase 9 pseudogene
8097801	0.01042103	-0.72860338	FAM160A1	family with sequence similarity 160, member A1
8146118	0.01042813	-0.45186442		
8105104	0.0104285	-0.44920844	C5orf51	chromosome 5 open reading frame 51
8096457	0.01048316	-0.31630198		
8170882	0.01048448	-0.30836951	ATP6AP1	ATPase, H+ transporting, lysosomal accessory protein 1
7950471	0.01048504	-0.31612176	OR2AT4	olfactory receptor, family 2, subfamily AT, member 4
8120937	0.01053038	-0.31732211	RIPPLY2	ripply2 homolog (zebrafish)
8035435	0.01053185	-0.41787212	KIAA1683	KIAA1683
8117071	0.01053456	-0.38635547	FAM8A1	family with sequence similarity 8, member A1
8005473	0.01053554	-0.61759142	PAIP1	poly(A) binding protein interacting protein 1
7979725	0.01064551	-0.6167953	PLEKHH1///PIGH	pleckstrin homology domain containing, family H (with MyTH4 domain) member 1///phosphatidylinositol glycan anchor biosynthesis, class H
7895045	0.0106535	-0.3972872		
7895382	0.01067106	-0.43690162		
7959946	0.01067747	-0.36204361	MMP17	matrix metallopeptidase 17 (membrane-inserted)
8055862	0.01067783	-0.52379533	ARL5A	ADP-ribosylation factor-like 5A
8045075	0.01067908	-0.3331529	GPR17	G protein-coupled receptor 17
8149330	0.01076585	-0.32968311	CTSB	cathepsin B
8016433	0.01077936	-0.35821508	HOXB1	homeobox B1
8167165	0.01081851	-0.36529185	ARAF	v-raf murine sarcoma 3611 viral oncogene homolog
8133219	0.01082924	-0.34597685		
8037301	0.01085019	-0.36746609	LYPD3	LY6/PLAUR domain containing 3
7975779	0.01094785	-2.88929943	FOS	FBJ murine osteosarcoma viral oncogene homolog
8169709	0.01097268	-0.59147705	GLRX5	glutaredoxin 5
8103411	0.01107409	-0.51160094		
8169233	0.01107828	-0.89697503		
8159583	0.01108292	-0.30872508	GRIN1	glutamate receptor, ionotropic, N-methyl D-aspartate 1
7917599	0.01115141	-0.38245791	BARHL2	BarH-like homeobox 2
8002051	0.01122705	-0.4209698	AGRP	agouti related protein homolog (mouse)
8015273	0.01124124	-0.47729307	KRT31	keratin 31
7993126	0.01127186	-0.35256905	ABAT	4-aminobutyrate aminotransferase
8090872	0.01130951	-0.3586311	KY	kyphoscoliosis peptidase
8133690	0.01133111	-0.33750963	MDH2	malate dehydrogenase 2, NAD (mitochondrial)
8007471	0.01133115	-0.34387362	NBR1	neighbor of BRCA1 gene 1
7972808	0.01140737	-0.45470767	CARKD	carbohydrate kinase domain containing
8025375	0.01141417	-0.33462212	CCL25	chemokine (C-C motif) ligand 25
8020455	0.01142591	-0.32615767	GATA6	GATA binding protein 6
7970498	0.01143682	-0.32320218	LATS2	large tumor suppressor kinase 2
7959157	0.01148112	-0.38455019	GATC	glutamyl-tRNA(Gln) amidotransferase, subunit C
7893539	0.01148932	-0.89483126		
8083223	0.01149917	-0.61872419	C3orf58	chromosome 3 open reading frame 58
7894044	0.01156672	-0.62169782		
7976834	0.01159747	-0.33291697	MIR494	microRNA 494
8108483	0.01162163	-0.37284271	SLC4A9	solute carrier family 4, sodium bicarbonate cotransporter, member 9
8169240	0.01166785	-0.47839001	PRPS1	phosphoribosyl pyrophosphate synthetase 1
8039273	0.01169896	-0.36604803	CDC42EP5	CDC42 effector protein (Rho GTPase binding) 5
7960381	0.01172681	-0.78031434	EFCAB4B	EF-hand calcium binding domain 4B

7906469	0.01172837	-0.43181692	DUSP23	dual specificity phosphatase 23
8007208	0.01176499	-0.37747576	HSPB9	heat shock protein, alpha-crystallin-related, B9
8039504	0.01185048	-0.32685578	SHISA7	shisa homolog 7 (Xenopus laevis)
8172803	0.01185087	-0.35944288		
8127425	0.01187957	-0.33122812	LMBRD1	LMBR1 domain containing 1
8147687	0.01188765	-0.96720356		
8103706	0.0119034	-0.43042592	AADAT	aminoadipate aminotransferase
8151436	0.01191743	-0.40114317	PEX2	peroxisomal biogenesis factor 2
8037197	0.01199463	-0.35368453	CXCL17	chemokine (C-X-C motif) ligand 17
8148317	0.01213641	-1.53771242	MYC	v-myc myelocytomatosis viral oncogene homolog (avian)
7995007	0.01214603	-0.44895844	HSD3B7	hydroxy-delta-5-steroid dehydrogenase, 3 beta- and steroid delta-isomerase 7
8091485	0.01215067	-0.46352355	SIAH2	siah E3 ubiquitin protein ligase 2
8055992	0.01221026	-0.44396258	ACVR1C	activin A receptor, type IC
8013259	0.01225764	-0.37267665		
8045321	0.01226119	-0.34637321	POTEF///POTEE	POTE ankyrin domain family, member F///POTE ankyrin domain family, membe
7906978	0.01226135	-0.39136656	MGST3///MGST3	microsomal glutathione S-transferase 3///microsomal glutathione S-transferase
7989473	0.01226217	-0.46402123	C2CD4B	C2 calcium-dependent domain containing 4B
8175811	0.01230799	-0.38985992	FAM58A///FAM58A	family with sequence similarity 58, member A///family with sequence similarity 5
8073192	0.01233734	-0.33962969	UQCRFS1	ubiquinol-cytochrome c reductase, Rieske iron-sulfur polypeptide 1
8164883	0.01234507	-0.35384973	SURF4	surfeit 4
8129039	0.01241569	-0.43250449		
7901445	0.01248125	-0.34184383		
7937106	0.01249689	-0.40268783	NKX6-2	NK6 homeobox 2
8162624	0.01253841	-0.80813545	AAED1	AhpC/TSA antioxidant enzyme domain containing 1
7970096	0.01256054	-0.30243621	ING1	inhibitor of growth family, member 1
7931500	0.01258157	-0.35851563	GPR123	G protein-coupled receptor 123
8040949	0.01260771	-0.49050292	KRTCAP3	keratinocyte associated protein 3
7949995	0.01263317	-0.37894332	MRPL21	mitochondrial ribosomal protein L21
8070900	0.01265558	-0.3728143		
8088820	0.01270739	-0.39483186	RYBP	RING1 and YY1 binding protein
7929947	0.01280099	-0.3864066	TLX1	T-cell leukemia homeobox 1
8024623	0.01280121	-0.36112096	NFIC	nuclear factor I/C (CCAAT-binding transcription factor)
7949894	0.01280713	-0.38023445		
7893236	0.01281341	-0.46729035		
7972973	0.01282642	-0.31533021	SETD8	SET domain containing (lysine methyltransferase) 8
8108050	0.01286117	-0.38233943	TCF7	transcription factor 7 (T-cell specific, HMG-box)
7909225	0.0128639	-0.39847863	DYRK3	dual-specificity tyrosine-(Y)-phosphorylation regulated kinase 3
8052676	0.01291357	-0.35226701		
8113413	0.01297933	-0.44238759	NUDT12	nudix (nucleoside diphosphate linked moiety X)-type motif 12
8067201	0.01299057	-0.4433533		
8059965	0.01299385	-0.32936562	KLHL30-AS1	KLHL30 antisense RNA 1
8012349	0.01301791	-0.61080484	PER1	period circadian clock 1
8001108	0.01307271	-0.45434015		
7950128	0.01307978	-0.40380926	LRTOMT///ANAPC15	leucine rich transmembrane and 0-methyltransferase domain containing///anaph complex subunit 15
7922646	0.01310747	-0.52034567	TOR1AIP2	torsin A interacting protein 2
8107468	0.0131189	-0.43346861		
7896094	0.01311953	-0.46778485		
8162276	0.01318523	-1.27354794	NFIL3	nuclear factor, interleukin 3 regulated
7931810	0.01321711	-1.08633018	KLF6	Kruppel-like factor 6
7893850	0.01322589	-0.61197901		
8123651	0.01326686	-0.34933522	TUBB2B	tubulin, beta 2B class IIb
7908525	0.01329628	-0.35267747	C1orf53	chromosome 1 open reading frame 53
7938100	0.01338751	-0.40413009	SMPD1	sphingomyelin phosphodiesterase 1, acid lysosomal
8149685	0.0134127	-0.31159078	LGI3	leucine-rich repeat LGI family, member 3
7924910	0.0134202	-0.33775024	ACTA1	actin, alpha 1, skeletal muscle
7980001	0.01352574	-0.42469421		
8159249	0.01354097	-0.38676713	MRPS2	mitochondrial ribosomal protein S2
7933209	0.01354222	-0.302417	C10orf25///RASSF4///ZNF22	chromosome 10 open reading frame 25///Ras association (RalGDS/AF-6) doma 4///zinc finger protein 22
7995322	0.01356053	-0.50750183		
8153409	0.01361469	-0.43716573	MAFA	v-maf musculoaponeurotic fibrosarcoma oncogene homolog A (avian)
7898721	0.01365553	-0.39126966		

7978093	0.01365727	-0.36393444	JPH4	junctophilin 4
7989708	0.01371619	-0.3938201	MTFMT	mitochondrial methionyl-tRNA formyltransferase
8063796	0.01375761	-0.30485353	CDH4	cadherin 4, type 1, R-cadherin (retinal)
7940662	0.01379246	-0.30687787	ROM1	retinal outer segment membrane protein 1
7996331	0.01379648	-0.34469461	CA7	carbonic anhydrase VII
8096281	0.01380044	-0.3148774	IBSP	integrin-binding sialoprotein
7992145	0.01384314	-0.3655483	SSTR5	somatostatin receptor 5
7978838	0.01387614	-0.39360271	DNAAF2	dynein, axonemal, assembly factor 2
7920971	0.01389666	-0.44245375	C1orf85	chromosome 1 open reading frame 85
7934178	0.0139363	-0.3468346	PCBD1	pterin-4 alpha-carbinolamine dehydratase/dimerization cofactor of hepatocyte nu alpha
8141643	0.01394108	-0.34059854	UFSP1	UFM1-specific peptidase 1 (non-functional)
7893685	0.01395807	-0.36791291		
7992191	0.01396418	-0.36515952	TPSD1	tryptase delta 1
7893344	0.01398267	-0.41858942		
8145047	0.01398749	-0.35209255	SFTPC	surfactant protein C
7944401	0.01399267	-0.3230911	HMBS	hydroxymethylbilane synthase
8095139	0.01419659	-0.49530176	SRD5A3	steroid 5 alpha-reductase 3
8158147	0.01429382	-1.03344562	SLC25A25	solute carrier family 25 (mitochondrial carrier; phosphate carrier), member 25
7893196	0.01431305	-0.48386921		
8023920	0.01441801	-0.49887911	TXNL4A	thioredoxin-like 4A
7892916	0.01442825	-0.39090428		
8027854	0.01458923	-0.38329854	FFAR1	free fatty acid receptor 1
7997861	0.01459896	-0.35865965		
8165508	0.0146273	-0.36157331	NRARP	NOTCH-regulated ankyrin repeat protein
7999718	0.01465169	-0.3490034	FOPNL	FGFR1OP N-terminal like
8121727	0.01467365	-0.33059573	BRD7P3	bromodomain containing 7 pseudogene 3
7956287	0.01468388	-0.3676406	NAB2	NGFI-A binding protein 2 (EGR1 binding protein 2)
8062864	0.01470981	-0.32015008	WISP2	WNT1 inducible signaling pathway protein 2
8118824	0.01475188	-0.43480547		
8085287	0.0147641	-0.43712628	BRK1	BRICK1, SCAR/WAVE actin-nucleating complex subunit
8176263	0.01480253	-0.31743686	TAF9B	TAF9B RNA polymerase II, TATA box binding protein (TBP)-associated factor, 3
8073612	0.01481086	-0.51790703	TSPO	translocator protein (18kDa)
8029870	0.01488137	-0.32385895	NPAS1	neuronal PAS domain protein 1
8142671	0.01490459	-0.30949337	WASL	Wiskott-Aldrich syndrome-like
8001178	0.01512553	-0.43219834	C16orf87	chromosome 16 open reading frame 87
8110920	0.01512884	-0.38773368	FASTKD3	FAST kinase domains 3
8019046	0.01516639	-0.3651434	EIF4A3	eukaryotic translation initiation factor 4A3
8124134	0.01517148	-0.30223801	TPMT	thiopurine S-methyltransferase
7894881	0.0152645	-0.3581052		
7905329	0.0152858	-0.6738789	MLLT11	myeloid/lymphoid or mixed-lineage leukemia (trithorax homolog, Drosophila); tra
7896637	0.01537938	-0.39231734		
7903281	0.01539254	-0.41256119	SLC35A3	solute carrier family 35 (UDP-N-acetylglucosamine (UDP-GlcNAc) transporter),
8003425	0.01545441	-0.336718	CBFA2T3	core-binding factor, runt domain, alpha subunit 2; translocated to, 3
8158666	0.01547562	-0.49568416	HMCN2	hemicentin 2
7931764	0.01547816	-0.34974081	ADARB2	adenosine deaminase, RNA-specific, B2 (non-functional)
8089112	0.01556802	-0.69116131	FILIP1L	filamin A interacting protein 1-like
8149612	0.01558939	-0.35665093	LZTS1	leucine zipper, putative tumor suppressor 1
7939424	0.01564802	-0.36768455	API5	apoptosis inhibitor 5
7942774	0.01567066	-0.40242264	AQP11	aquaporin 11
8035234	0.01576141	-0.39597498		
8165453	0.01605512	-0.39955056	LRRC26	leucine rich repeat containing 26
7896533	0.01609657	-0.67037838		
7981078	0.01613337	-0.49110393	SERPINA11	serpin peptidase inhibitor, clade A (alpha-1 antiproteinase, antitrypsin), member
7909332	0.01614287	-0.57211101	CD55	CD55 molecule, decay accelerating factor for complement (Cromer blood group
8172471	0.01618281	-0.35593395	PIM2	pim-2 oncogene
8037267	0.01618553	-0.474422	PSG2	pregnancy specific beta-1-glycoprotein 2
8042701	0.01621342	-0.36762858	EMX1	empty spiracles homeobox 1
8116859	0.01621874	-0.33113292	TMEM14C	transmembrane protein 14C
8024373	0.01626396	-0.32987556	IZUMO4	IZUMO family member 4
8110708	0.01627093	-0.47987818	TPPP	tubulin polymerization promoting protein
8171837	0.01630449	-0.54013801	KLHL15	kelch-like family member 15

7895971	0.01630642	-0.54769836		
8030578	0.01637273	-0.31031437	FLJ26850	FLJ26850 protein
8040249	0.01640558	-0.31062974	ATP6V1C2///PDIA6	ATPase, H+ transporting, lysosomal 42kDa, V1 subunit C2///protein disulfide isc member 6
8055688	0.0164527	-0.83364087	RND3///RND3	Rho family GTPase 3///Rho family GTPase 3
8101992	0.01652567	-0.37992405	SLC39A8	solute carrier family 39 (zinc transporter), member 8
8139421	0.01654418	-0.36508112	H2AFV	H2A histone family, member V
8067167	0.01655575	-0.60701203	AURKA	aurora kinase A
8155508	0.01655871	-0.75226649		
8055672	0.01658109	-0.35416777	MMADHC	methylmalonic aciduria (cobalamin deficiency) cblD type, with homocystinuria
8125843	0.01659299	-0.31380661	SPDEF	SAM pointed domain containing ets transcription factor
7955624	0.01666015	-0.41859108	KRT86///KRT83///KRT81	keratin 86///keratin 83///keratin 81
8035868	0.01668323	-0.304017		
8169465	0.01674931	-0.37569538		
7978644	0.01675481	-0.43907969	NFKBIA	nuclear factor of kappa light polypeptide gene enhancer in B-cells inhibitor, alph
7956395	0.01675569	-0.37918514	NXPH4	neurexophilin 4
7895752	0.01680823	-0.55872325		
8080958	0.0170633	-0.54267042	GPR27	G protein-coupled receptor 27
7896519	0.01708722	-0.58062185		
8037949	0.01717769	-0.41832376	SULT2A1	sulfotransferase family, cytosolic, 2A, dehydroepiandrosterone (DHEA)-preferrin
8097687	0.01718892	-0.38931962	POU4F2	POU class 4 homeobox 2
8158902	0.01724479	-0.40478951	C9orf171	chromosome 9 open reading frame 171
7981084	0.01724911	-0.35802564	SERPINA9	serpin peptidase inhibitor, clade A (alpha-1 antiproteinase, antitrypsin), member
7898537	0.01728462	-0.31245777	PAX7	paired box 7
8156240	0.01728631	-0.30924988	CTSL3P	cathepsin L family member 3, pseudogene
8024228	0.0173331	-0.31886935	MIDN	midnolin
7957551	0.0174208	-1.02415093	SOCS2	suppressor of cytokine signaling 2
8110427	0.01744307	-0.32370395		
8110166	0.01744636	-0.41437139	HIGD2A	HIG1 hypoxia inducible domain family, member 2A
8063970	0.01746431	-0.30210449	COL9A3	collagen, type IX, alpha 3
8058866	0.01748739	-0.31716286	TNP1	transition protein 1 (during histone to protamine replacement)
7895902	0.01750909	-0.57093101		
8030706	0.01751678	-0.37022035	EMC10	ER membrane protein complex subunit 10
7981013	0.01757047	-0.31638017	PRIMA1	proline rich membrane anchor 1
8025028	0.01759601	-0.3261772	CLPP	ClpP caseinolytic peptidase, ATP-dependent, proteolytic subunit homolog (E. co
7902930	0.01760699	-0.39332551	HSP90B3P	heat shock protein 90kDa beta (Grp94), member 3, pseudogene
8119102	0.01761731	-0.44535647		
7925161	0.0176747	-0.42738364	IRF2BP2	interferon regulatory factor 2 binding protein 2
7912968	0.0177088	-0.43397222	TAS1R2	taste receptor, type 1, member 2
8027920	0.0177103	-0.32199904	ETV2	ets variant 2
7969975	0.01777618	-0.43521291		
7893026	0.01777863	-0.33833864		
8112422	0.01790304	-0.33107496		
7966746	0.01796364	-0.42326506	HRK	harakiri, BCL2 interacting protein (contains only BH3 domain)
7978586	0.01802709	-0.5384399	CFL2	cofilin 2 (muscle)
7997158	0.0181073	-0.34428531	MARVELD3	MARVEL domain containing 3
8073544	0.01813965	-0.31870155	MIR33A	microRNA 33a
8065603	0.01814678	-0.35227612	TSPY26P	testis specific protein, Y-linked 26, pseudogene
8028380	0.01815791	-0.30438397	PSMD8	proteasome (prosome, macropain) 26S subunit, non-ATPase, 8
8157605	0.01818415	-0.6823413		
7892776	0.01819091	-0.4954715		
8113551	0.01819237	-0.40308953	MCC	mutated in colorectal cancers
8138337	0.01821486	-0.42728155	AGMO	alkylglycerol monooxygenase
7966621	0.01822571	-0.89783926	SDS	serine dehydratase
7893339	0.01824485	-0.52709092		
8115664	0.01826251	-0.3860378	GLRX	glutaredoxin (thioltransferase)
8084275	0.01827394	-0.30541854	HTR3C	5-hydroxytryptamine (serotonin) receptor 3C, ionotropic
8022674	0.01831479	-0.38186196	CDH2	cadherin 2, type 1, N-cadherin (neuronal)
7896378	0.01834395	-0.73322051		
8161747	0.01838533	-0.79970969	ZFAND5	zinc finger, AN1-type domain 5
7894827	0.01840224	-0.38072453		
7893962	0.01843417	-0.70487892		

8119620	0.01844262	-1.15973477	GNMT	glycine N-methyltransferase
8027385	0.0184487	-0.449968	VSTM2B	V-set and transmembrane domain containing 2B
8030128	0.01847241	-0.81531956	PPP1R15A	protein phosphatase 1, regulatory subunit 15A
7927146	0.01850802	-0.36234914	CSGALNACT2	chondroitin sulfate N-acetylgalactosaminyltransferase 2
7895096	0.01859161	-0.46518114		
8083826	0.01859301	-0.40926291	SEC62	SEC62 homolog (S. cerevisiae)
7895127	0.01859667	-0.62104955		
7995342	0.01859732	-0.57088018		
8069633	0.01859803	-0.32686666	ATP5J	ATP synthase, H+ transporting, mitochondrial Fo complex, subunit F6
8098240	0.01865334	-0.53738251		
8103023	0.01866578	-0.51929891		
7971345	0.01870527	-0.40222941		
8021484	0.01870848	-0.32247486	CDH20	cadherin 20, type 2
7893624	0.01875201	-0.54683872		
7893458	0.01876127	-0.50923216		
8056728	0.01878338	-0.32988846		
8083136	0.01890196	-0.56952413	ATP1B3	ATPase, Na+/K+ transporting, beta 3 polypeptide
8037166	0.01894193	-0.32733753	ERF	Ets2 repressor factor
7925342	0.01896059	-0.55168933	ERO1LB	ERO1-like beta (S. cerevisiae)
8005233	0.01902083	-0.65109102		
8035445	0.01903955	-0.88262482	JUND	jun D proto-oncogene
8025968	0.01922158	-0.40112981	ZNF69	zinc finger protein 69
8118667	0.01926325	-0.49673901	MYL12B	myosin, light chain 12B, regulatory
8156196	0.01930364	-0.31685026	C9orf170	chromosome 9 open reading frame 170
8104369	0.01938669	-0.55158501	SRD5A1	steroid-5-alpha-reductase, alpha polypeptide 1 (3-oxo-5 alpha-steroid delta 4-de alpha 1)
8050763	0.019394	-0.33115268	PTRHD1	peptidyl-tRNA hydrolase domain containing 1
7926979	0.01944806	-0.85024179		
8170009	0.01945979	-0.42042031	FAM127A	family with sequence similarity 127, member A
8135080	0.01946657	-0.37253209	AP1S1	adaptor-related protein complex 1, sigma 1 subunit
8136801	0.01949629	-0.51674739	PRSS3P2///PRSS3///PF	protease, serine, 3 pseudogene 2///protease, serine, 3///protease, serine, 2 (tryp
8046564	0.01951697	-0.32019429	HOXD1	homeobox D1
7893003	0.01952961	-0.58047125		
8038815	0.01955853	-0.36868431	LIM2	lens intrinsic membrane protein 2, 19kDa
7915841	0.01964684	-0.30094815	KNCN	kinocilin
8119712	0.01965196	-0.37958133	SRF	serum response factor (c-fos serum response element-binding transcription fact
8010113	0.0197047	-0.30616097	MGAT5B	mannosyl (alpha-1,6-)-glycoprotein beta-1,6-N-acetyl-glucosaminyltransferase, i
7972291	0.01980484	-0.36077884	SOX21	SRY (sex determining region Y)-box 21
8172358	0.01981566	-0.48876675	UXT	ubiquitously-expressed, prefoldin-like chaperone
7898176	0.01986291	-0.3436589	CELA2A	chymotrypsin-like elastase family, member 2A
7979269	0.0198885	-0.33773096	GCH1	GTP cyclohydrolase 1
8163930	0.01989117	-0.39999006	NDUFA8	NADH dehydrogenase (ubiquinone) 1 alpha subcomplex, 8, 19kDa
7997228	0.01989639	-0.30765144		
7965606	0.01995563	-0.83535876	HAL	histidine ammonia-lyase
8109475	0.02002595	-0.41059635	MRPL22	mitochondrial ribosomal protein L22
8148194	0.02003972	-0.32845115		
8099200	0.02011903	-0.31126488	JAKMIP1	janus kinase and microtubule interacting protein 1
7982868	0.02012026	-1.370095	CHAC1	ChaC, cation transport regulator homolog 1 (E. coli)
7969533	0.02014075	-0.35027102	SLAIN1	SLAIN motif family, member 1
7892972	0.02014133	-0.45522981		
8038109	0.02017002	-0.47087379	FAM83E	family with sequence similarity 83, member E
8180317	0.02021308	-0.65916847	TGIF1	TGFB-induced factor homeobox 1
8037872	0.02022134	-0.38847186	BBC3	BCL2 binding component 3
7914000	0.02023854	-1.01535393	NR0B2	nuclear receptor subfamily 0, group B, member 2
8118804	0.0202519	-0.31237845	PACSIN1	protein kinase C and casein kinase substrate in neurons 1
8047372	0.02028188	-0.47967441	NDUFB3	NADH dehydrogenase (ubiquinone) 1 beta subcomplex, 3, 12kDa
7963970	0.02030429	-0.33986864	PMEL	premelanosome protein
8069532	0.02036576	-0.62754457	HSPA13	heat shock protein 70kDa family, member 13
8052669	0.02037158	-0.37371098	SERTAD2	SERTA domain containing 2
8093074	0.02051172	-0.36131904	ZDHHC19	zinc finger, DHHC-type containing 19
8130009	0.02059968	-0.48249909		
8115895	0.02060427	-0.37564097	KIAA1191	KIAA1191

8062873	0.02065539	-0.51050214	KCNK15	potassium channel, subfamily K, member 15
7907351	0.02066828	-0.31229037		
7894834	0.02080351	-0.53986824		
7954794	0.02081112	-0.30518875	C12orf40	chromosome 12 open reading frame 40
7969544	0.02084114	-0.36246368	NDFIP2	Nedd4 family interacting protein 2
8136067	0.0210401	-0.38319586	TSPAN33	tetraspanin 33
8134880	0.02107828	-0.37714677	MOSPD3	motile sperm domain containing 3
8076072	0.02110278	-0.41070952	KCNJ4	potassium inwardly-rectifying channel, subfamily J, member 4
7898653	0.02114532	-0.46350768	FAM43B	family with sequence similarity 43, member B
8050790	0.02120541	-0.32776396	DNAJC27	DnaJ (Hsp40) homolog, subfamily C, member 27
7923596	0.02122208	-0.51949514	ETNK2	ethanolamine kinase 2
8168466	0.02123332	-0.34970423	MAGT1	magnesium transporter 1
8175119	0.02123455	-0.30932291		
8110055	0.02124143	-0.31113424	CPEB4	cytoplasmic polyadenylation element binding protein 4
8055404	0.02126076	-0.38070137	UBXN4	UBX domain protein 4
8052733	0.02134874	-0.33095114		
7912031	0.02135698	-0.35676742	HES2	hairy and enhancer of split 2 (Drosophila)
7985233	0.02137948	-0.4244739	RASGRF1	Ras protein-specific guanine nucleotide-releasing factor 1
8010783	0.02139915	-0.36987111	UTS2R	urotensin 2 receptor
8035539	0.02142694	-0.32391473	CERS1///GDF1	ceramide synthase 1///growth differentiation factor 1
8112726	0.02142732	-0.30984653		
8084880	0.02149923	-0.78783537	HES1	hairy and enhancer of split 1, (Drosophila)
8047217	0.02156229	-0.51903807	COQ10B	coenzyme Q10 homolog B (S. cerevisiae)
8054831	0.02160232	-0.30893561	EN1	engrailed homeobox 1
7892953	0.0216039	-0.5953891		
8088480	0.02161502	-0.40173939	ID2B///ID2	inhibitor of DNA binding 2B, dominant negative helix-loop-helix protein (pseudog DNA binding 2, dominant negative helix-loop-helix protein
8012140	0.02162173	-0.42865541	YBX2	Y box binding protein 2
8145660	0.02166305	-0.33575994	DCTN6	dynactin 6
7892720	0.02175788	-0.55387632		
8138289	0.02180788	-0.42911811	ETV1	ets variant 1
8180280	0.02182658	-0.37147413	PCDHA7	protocadherin alpha 7
8129677	0.02183814	-0.52353047	SGK1	serum/glucocorticoid regulated kinase 1
7925448	0.02184787	-0.36054589		
8081055	0.02190184	-0.3660887	CHMP2B	charged multivesicular body protein 2B
8007141	0.02192513	-0.33319703	EIF1	eukaryotic translation initiation factor 1
8120194	0.02208171	-0.30428824	TFAP2B	transcription factor AP-2 beta (activating enhancer binding protein 2 beta)
7986327	0.02215396	-0.39860426		
8128429	0.02218067	-0.42964211	CCNC	cyclin C
7892583	0.0221809	-0.76878003		
7970716	0.02219094	-0.35595354	LNX2	ligand of numb-protein X 2
7944876	0.02224067	-0.43067392	NRGN	neurogranin (protein kinase C substrate, RC3)
8049567	0.02239918	-0.76011616	RAMP1	receptor (G protein-coupled) activity modifying protein 1
7955184	0.02239971	-0.38865949	PRPH	peripherin
8077450	0.02246795	-0.33853098	ARL8B	ADP-ribosylation factor-like 8B
8008540	0.02248531	-0.3707805	FLJ42842	uncharacterized FLJ42842
7967870	0.02249265	-0.50442104	TERF1	telomeric repeat binding factor (NIMA-interacting) 1
7969665	0.0225117	-0.31785763	HS6ST3	heparan sulfate 6-O-sulfotransferase 3
7893778	0.02252415	-0.30331615		
7950671	0.0225325	-0.32449008	GAB2	GRB2-associated binding protein 2
7900146	0.02256338	-0.50669604	ZC3H12A	zinc finger CCCH-type containing 12A
7894004	0.02261292	-0.57197977		
7918869	0.02272015	-0.31672532	NGF	nerve growth factor (beta polypeptide)
7929840	0.02275819	-0.34138901	PAX2	paired box 2
7955719	0.02278816	-0.5853758	HIGD1A	HIG1 hypoxia inducible domain family, member 1A
7987792	0.02280139	-0.30623845	PLA2G4D	phospholipase A2, group IVD (cytosolic)
7991772	0.02283536	-0.37135292	HBQ1	hemoglobin, theta 1
7910387	0.02284822	-0.41487135	RHOU	ras homolog family member U
7928746	0.02288075	-0.42850412		
7896398	0.02289499	-0.56234786		
8016463	0.02305445	-0.33959836	HOXB6	homeobox B6
8049598	0.02306453	-0.41366036	ESPNL	espin-like

8042251	0.02313198	-0.33084638	OTX1	orthodenticle homeobox 1
8083333	0.02317573	-0.30834586	EIF2A	eukaryotic translation initiation factor 2A, 65kDa
8141303	0.02318773	-0.39082838		
8099172	0.02322339	-0.37595106	CRMP1	collapsin response mediator protein 1
7976496	0.02323646	-0.34662107	SERPINA3	serpin peptidase inhibitor, clade A (alpha-1 antiproteinase, antitrypsin), member
7953697	0.02331522	-0.33217722		
7896324	0.02342616	-0.41711882		
7947221	0.02345421	-0.46365485	LIN7C	lin-7 homolog C (C. elegans)
8003840	0.02346158	-0.42210102	EMC6	ER membrane protein complex subunit 6
7937016	0.02350475	-0.386841	CLRN3	clarin 3
8088889	0.02363846	-0.3373212		
8019263	0.02366396	-0.39120489	ARHGDIA	Rho GDP dissociation inhibitor (GDI) alpha
7894502	0.02371148	-0.57231416		
7894862	0.02371227	-0.35613105		
8152512	0.02377635	-0.44395978	TNFRSF11B	tumor necrosis factor receptor superfamily, member 11b
7920256	0.02378071	-0.52521306		
8023727	0.02382188	-0.54358887	DSEL	dermatan sulfate epimerase-like
7903765	0.02388648	-2.80657645	GSTM1	glutathione S-transferase mu 1
8091863	0.02395895	-1.44659388	SLITRK3	SLIT and NTRK-like family, member 3
7914923	0.02400623	-0.3883317	OSCP1	organic solute carrier partner 1
8026163	0.02400683	-0.83125325	IER2	immediate early response 2
7893087	0.02401063	-0.35864595		
8066391	0.02421891	-0.45539776		
8102779	0.02436202	-0.31416575		
8122343	0.02436402	-0.37770049	HECA	headcase homolog (Drosophila)
7980425	0.02437771	-0.31825705	ISM2	isthmin 2
7892697	0.02443476	-0.52723697		
8022488	0.02448474	-0.41883731	ABHD3	abhydrolase domain containing 3
8072488	0.02472195	-0.31448667	DRG1	developmentally regulated GTP binding protein 1
8140140	0.02474001	-0.63393463	CLDN3	claudin 3
8025402	0.02475447	-1.0299977	ANGPTL4	angiopoietin-like 4
8105111	0.02477418	-0.39150814	FBXO4	F-box protein 4
7935270	0.02479891	-0.51852086	BLNK	B-cell linker
8130403	0.02482936	-0.36519141		
8004521	0.02493475	-0.39030054	MPDU1	mannose-P-dolichol utilization defect 1
8170965	0.02496213	-0.31350077	CTAG1A///CTAG2///CT	cancer/testis antigen 1A///cancer/testis antigen 2///cancer/testis antigen 1B
8110872	0.02500576	-0.3790684	IRX2	iroquois homeobox 2
7957611	0.02502437	-0.30675515		
7979033	0.02504748	-0.44091821	SAV1	salvador homolog 1 (Drosophila)
8067820	0.02511803	-0.44436672	IQSEC3	IQ motif and Sec7 domain 3
8133155	0.0251423	-0.37952273	TPST1///TPST1	tyrosylprotein sulfotransferase 1///tyrosylprotein sulfotransferase 1
8148265	0.02514553	-0.32541619	RNF139	ring finger protein 139
8135601	0.02514937	-0.42875094	MET	met proto-oncogene (hepatocyte growth factor receptor)
8128716	0.02515417	-0.36886794	CD164	CD164 molecule, sialomucin
8045229	0.025186	-0.42299716	ARHGEF4///ARHGEF4	Rho guanine nucleotide exchange factor (GEF) 4///Rho guanine nucleotide exch (GEF) 4
7997556	0.02522968	-0.34025101	DNAAF1///TAF1C	dynein, axonemal, assembly factor 1///TATA box binding protein (TBP)-associat polymerase I, C, 110kDa
8019183	0.02522978	-0.33072592	ACTG1	actin, gamma 1
8147375	0.02526453	-0.46175394	DPY19L4	dpy-19-like 4 (C. elegans)
7892688	0.02537948	-0.56750676		
7975390	0.02538631	-0.41441156	SMOC1	SPARC related modular calcium binding 1
8032312	0.02551534	-0.31898879	ATP8B3	ATPase, aminophospholipid transporter, class I, type 8B, member 3
8068593	0.02552488	-0.71143207	ETS2	v-ets erythroblastosis virus E26 oncogene homolog 2 (avian)
8022418	0.02553354	-0.45049931		
8137485	0.02555227	-0.33073436	DPP6	dipeptidyl-peptidase 6
8169210	0.02568072	-0.56449138	RIPPLY1///CLDN2	ripply1 homolog (zebrafish)///claudin 2
8150908	0.02570623	-0.39409707	IMPAD1	inositol monophosphatase domain containing 1
8102594	0.02570979	-0.37260471	TNIP3	TNFAIP3 interacting protein 3
8056977	0.02572337	-0.3593071	NFE2L2	nuclear factor (erythroid-derived 2)-like 2
8066590	0.02577605	-0.36891177	TNNC2	troponin C type 2 (fast)
8033162	0.02578024	-0.30152477	KHSRP	KH-type splicing regulatory protein
8079163	0.02580835	-0.58638954		

8100306	0.02590369	-0.37449119		
7895217	0.02592048	-0.4714582		
7896310	0.02593443	-0.30808722		
7894704	0.02594183	-0.38018161		
8083415	0.02598718	-0.44414187	AADAC	arylacetamide deacetylase
8061944	0.02600145	-0.34539848	ACTL10	actin-like 10
7893173	0.02601082	-0.69304519		
7991898	0.02606118	-0.4740994	NHLRC4	NHL repeat containing 4
8144378	0.0261092	-0.43548758	AGPAT5	1-acylglycerol-3-phosphate O-acyltransferase 5
8079170	0.02614056	-0.33178241	TCAIM	T cell activation inhibitor, mitochondrial
8156848	0.02615146	-0.95555334	NR4A3	nuclear receptor subfamily 4, group A, member 3
8099506	0.02625425	-0.3595168	TAPT1	transmembrane anterior posterior transformation 1
8146717	0.02626105	-0.32853884	SGK3	serum/glucocorticoid regulated kinase family, member 3
8149720	0.02639784	-0.53197671	EGR3	early growth response 3
7893619	0.0264725	-0.50591131		
8036133	0.02651955	-0.32277986	UPK1A	uroplakin 1A
8062539	0.02652947	-0.32068848	SLC32A1	solute carrier family 32 (GABA vesicular transporter), member 1
7914354	0.02656147	-0.34405917	PEF1	penta-EF-hand domain containing 1
8042962	0.02658871	-0.42156346	MRPL19	mitochondrial ribosomal protein L19
7903162	0.02660328	-0.31385927	TMEM56	transmembrane protein 56
7895973	0.02661055	-0.34212364		
8073007	0.02671792	-0.57984919	MAFF	v-maf musculoaponeurotic fibrosarcoma oncogene homolog F (avian)
8111788	0.02673459	-0.38484986	TTC33	tetratricopeptide repeat domain 33
8044301	0.02674857	-0.30485791	SOWAHC	sosondowah ankyrin repeat domain family member C
8131803	0.0268214	-0.89782804	IL6	interleukin 6 (interferon, beta 2)
7896255	0.0268285	-0.49141501		
7913146	0.02684534	-0.30739874	AKR7A3	aldo-keto reductase family 7, member A3 (aflatoxin aldehyde reductase)
8064779	0.0268465	-0.34906901	ADRA1D	adrenoceptor alpha 1D
7911376	0.02686542	-0.31042638	HES4	hairy and enhancer of split 4 (Drosophila)
7941172	0.02693658	-0.36190574	SPDYC	speedy/RINGO cell cycle regulator family member C
8138527	0.0269443	-0.34457007	STEAP1B	STEAP family member 1B
8172030	0.02694978	-0.30162403		
7969479	0.02704771	-0.31087773	BTF3P11	basic transcription factor 3 pseudogene 11
7975626	0.02706253	-0.45496525	ELMSAN1	ELM2 and Myb/SANT-like domain containing 1
7997712	0.02712303	-0.72653936	IRF8	interferon regulatory factor 8
7976858	0.02733543	-0.35806974	DIO3	deiodinase, iodothyronine, type III
8052698	0.02736741	-0.3432308	C1D	C1D nuclear receptor corepressor
7963760	0.02745965	-0.34943116	NFE2	nuclear factor (erythroid-derived 2), 45kDa
8142697	0.0275065	-0.38058452	POT1	protection of telomeres 1
7894355	0.02752803	-0.47717593		
7995438	0.02755705	-0.39120457		
7930398	0.02760936	-0.31817982	MXI1	MAX interactor 1, dimerization protein
8177046	0.02779921	-0.55366392		
7897034	0.02784002	-0.31623434	GABRD	gamma-aminobutyric acid (GABA) A receptor, delta
8171823	0.02789586	-0.34248416	APOO	apolipoprotein O
8032834	0.02793904	-0.60454653	LRG1	leucine-rich alpha-2-glycoprotein 1
8065353	0.02795063	-0.46532419	THBD	thrombomodulin
7896690	0.0280276	-0.50665589		
8001798	0.02805468	-0.31075312		
7913850	0.02810734	-0.33194813	LOC646471///MTFR1L	uncharacterized LOC646471///mitochondrial fission regulator 1-like
8002999	0.02810917	-0.31232508	GCSHP3///LOC729080	glycine cleavage system protein H (aminomethyl carrier) pseudogene 3///glycine system protein H (aminomethyl carrier) pseudogene///glycine cleavage system p (aminomethyl carrier)
7941269	0.02816762	-0.39682246		
8123728	0.0281749	-0.35133147	LYRM4	LYR motif containing 4
8078435	0.02818281	-0.32867305	TRIM71	tripartite motif containing 71, E3 ubiquitin protein ligase
7965040	0.02819495	-0.9639456	PHLDA1	pleckstrin homology-like domain, family A, member 1
7917728	0.02825363	-0.38428366	FAM69A	family with sequence similarity 69, member A
8010237	0.02831182	-0.40665404	C17orf99	chromosome 17 open reading frame 99
8023871	0.02831187	-0.31651338	ZADH2	zinc binding alcohol dehydrogenase domain containing 2
7895334	0.02831804	-0.40671984		
8061357	0.02832728	-0.41737689	PAX1	paired box 1

7955441	0.02841787	-0.34617998	METTL7A	methyltransferase like 7A
7922051	0.02846687	-0.36141561	CREG1	cellular repressor of E1A-stimulated genes 1
7894304	0.02854155	-0.43810697		
8016540	0.02857595	-0.38617005	PHOSPHO1	phosphatase, orphan 1
7901802	0.02859746	-0.31103064	MGC34796	sepiapterin reductase (7,8-dihydrobiopterin:NADP+ oxidoreductase) pseudogen
8121144	0.02862334	-0.53181855	MANEA	mannosidase, endo-alpha
8168578	0.0286449	-0.32061114	UBE2DNL	ubiquitin-conjugating enzyme E2D N-terminal like (pseudogene)
7968236	0.02879759	-0.32860821	RASL11A	RAS-like, family 11, member A
8076677	0.02881079	-0.32440831	PHF21B	PHD finger protein 21B
7915329	0.02889301	-0.35165665		
7980523	0.02894642	-0.36038494	GTF2A1	general transcription factor IIA, 1, 19/37kDa
8010036	0.02915004	-0.31136209	ZACN///EXOC7///EXOC	zinc activated ligand-gated ion channel///exocyst complex component 7///exocys component 7
8151125	0.02920851	-0.38130249	TCF24	transcription factor 24
7936826	0.0293103	-0.49470972	IKZF5	IKAROS family zinc finger 5 (Pegasus)
8141066	0.0293129	-0.34087125	PON3	paraoxonase 3
8083324	0.02931723	-0.44598425	TSC22D2	TSC22 domain family, member 2
7984174	0.02934602	-0.36266321	SNX22///PPIB	sorting nexin 22///peptidylprolyl isomerase B (cyclophilin B)
8106336	0.02935051	-0.32301615	SV2C	synaptic vesicle glycoprotein 2C
8065403	0.02937605	-0.34332977	CST3	cystatin C
7935692	0.02946431	-0.34669087	ERLIN1	ER lipid raft associated 1
8166569	0.02947284	-0.38794584		
8075118	0.02950802	-0.37285849	CRYBB1	crystallin, beta B1
7893082	0.02963252	-0.72359235		
7893928	0.02963398	-0.44527055		
8099073	0.02966075	-0.36510382	LRPAP1	low density lipoprotein receptor-related protein associated protein 1
8112592	0.02969395	-0.30322489	FOXD1	forkhead box D1
7914974	0.02974117	-0.31862742	GRIK3	glutamate receptor, ionotropic, kainate 3
7990090	0.02983301	-0.30991691		
8024934	0.02984721	-0.30359383	ZNRF4	zinc and ring finger 4
8037003	0.02989863	-0.34628531		
8086729	0.02990948	-0.34223589	KIF9	kinesin family member 9
7914180	0.03003791	-0.31162767	SPCS2	signal peptidase complex subunit 2 homolog (S. cerevisiae)
8175288	0.03006719	-0.49348638	MOSPD1	motile sperm domain containing 1
8142307	0.03007847	-0.46495251	PNPLA8	patatin-like phospholipase domain containing 8
7974207	0.03022414	-0.33246294	MGAT2	mannosyl (alpha-1,6-)-glycoprotein beta-1,2-N-acetylglucosaminyltransferase
8109505	0.03025007	-0.3168818	PPP1R2P3	protein phosphatase 1, regulatory (inhibitor) subunit 2 pseudogene 3
7956613	0.03028358	-0.32320653	TSPAN31	tetraspanin 31
8114778	0.03032904	-0.31923659	LOC729080///GCSH	glycine cleavage system protein H (aminomethyl carrier) pseudogene///glycine c protein H (aminomethyl carrier)
8015376	0.03035113	-0.35383165	KRT16	keratin 16
8060594	0.03039813	-0.31677192	GNRH2	gonadotropin-releasing hormone 2
7974531	0.03044569	-0.40690066	RPL13AP3	ribosomal protein L13a pseudogene 3
8042283	0.03045036	-0.4313904	LGALSL	lectin, galactoside-binding-like
7924526	0.03052556	-0.5730035	TP53BP2	tumor protein p53 binding protein, 2
8037205	0.03060711	-0.37469774	CEACAM1	carcinoembryonic antigen-related cell adhesion molecule 1 (biliary glycoprotein)
8085116	0.03069795	-0.4270489	EDEM1	ER degradation enhancer, mannosidase alpha-like 1
8041000	0.0308347	-0.34092652	GPN1	GPN-loop GTPase 1
8157246	0.03093764	-0.30004733	KIAA1958	KIAA1958
8162848	0.03102888	-0.46982795		
7893259	0.03106309	-0.45965939		
7975268	0.03108553	-0.67223504	VTI1B///ARG2	vesicle transport through interaction with t-SNAREs 1B///arginase 2
7969414	0.03118009	-0.75072228	KLF5	Kruppel-like factor 5 (intestinal)
7896667	0.03119811	-0.30314426		
8166202	0.03140884	-0.31081949	GRPR	gastrin-releasing peptide receptor
7910001	0.03146211	-0.34819306	DEGS1	delta(4)-desaturase, sphingolipid 1
7974229	0.03148209	-0.32930146	KLHDC2	kelch domain containing 2
7945781	0.0315067	-0.32735019	PHLDA2	pleckstrin homology-like domain, family A, member 2
8119609	0.03162741	-0.43975818	CNPY3	canopy 3 homolog (zebrafish)
8154163	0.03165353	-0.36892988	RCL1	RNA terminal phosphate cyclase-like 1
7924553	0.03173748	-0.37378922		
8148559	0.03178579	-0.3286659	THEM6	thioesterase superfamily member 6
8153322	0.03181092	-0.32572281	ARC	activity-regulated cytoskeleton-associated protein

7997569	0.03183536	-0.3593739	ADAD2	adenosine deaminase domain containing 2
7989365	0.03184464	-0.35315308	RORA	RAR-related orphan receptor A
8096905	0.03194318	-0.3484977	AP1AR	adaptor-related protein complex 1 associated regulatory protein
7894138	0.0319447	-0.41249327		
8112072	0.03205433	-0.32973633	CCNO	cyclin O
7919582	0.03215064	-0.45153478		
8062461	0.0321613	-0.4378055	LBP	lipopolysaccharide binding protein
7909127	0.03217148	-0.30164741	MFSD4	major facilitator superfamily domain containing 4
8004241	0.03218767	-0.30138601	RNASEK///C17orf49	ribonuclease, RNase K///chromosome 17 open reading frame 49
7925950	0.03226732	-0.44792722	UCN3	urocortin 3
7905929	0.03228423	-0.46237758	EFNA1	ephrin-A1
8131406	0.03229614	-0.43798212	RAC1	ras-related C3 botulinum toxin substrate 1 (rho family, small GTP binding protei
8029701	0.03231542	-0.56255539	PPM1N	protein phosphatase, Mg2+/Mn2+ dependent, 1N (putative)
7950032	0.03231706	-0.32374714	FGF4	fibroblast growth factor 4
7895685	0.03232665	-0.38863908		
7901883	0.03239727	-0.30073131	ANGPTL3	angiopoietin-like 3
7916609	0.032456	-1.19924629	JUN	jun proto-oncogene
8157139	0.03247628	-0.39821883		
8174891	0.03251936	-0.34442849		
8015037	0.0326976	-0.4437154		
7918379	0.03271243	-1.06526659	GSTM3	glutathione S-transferase mu 3 (brain)
7912670	0.03271953	-0.41278526	UQCRHL///UQCRH	ubiquinol-cytochrome c reductase hinge protein-like///ubiquinol-cytochrome c re protein
8089013	0.03272423	-0.44129858		
8129254	0.03277701	-0.31788096	MAN1A1	mannosidase, alpha, class 1A, member 1
8161648	0.03279122	-0.58184507	KLF9	Kruppel-like factor 9
7990729	0.03282401	-0.32144785	CHRNB4	cholinergic receptor, nicotinic, beta 4 (neuronal)
8128001	0.03287032	-0.36487137	CGA	glycoprotein hormones, alpha polypeptide
7997733	0.03289396	-0.39153926	FOXC2	forkhead box C2 (MFH-1, mesenchyme forkhead 1)
8013509	0.03292713	-0.30154468	C17orf103	chromosome 17 open reading frame 103
7894927	0.03314685	-0.49501761		
8144505	0.03314709	-0.31133007	CLDN23	claudin 23
7994804	0.03315019	-0.30419955	MYLPF	myosin light chain, phosphorylatable, fast skeletal muscle
7961507	0.0331577	-0.41364629	ART4	ADP-ribosyltransferase 4 (Dombrock blood group)
8076561	0.03322706	-0.37209892	KIAA1654	KIAA1654 protein
8066031	0.033325	-0.30769332	SCAND1	SCAN domain containing 1
8048699	0.03339672	-0.37034553		
7989915	0.03350831	-0.35760344	TIPIN	TIMELESS interacting protein
7979179	0.03356123	-0.49963529	ERO1L	ERO1-like (S. cerevisiae)
8076128	0.0336813	-0.40784078	JOSD1	Josephin domain containing 1
8070169	0.03371285	-0.32026315		
8096538	0.03381924	-0.39575948	RAP1GDS1	RAP1, GTP-GDP dissociation stimulator 1
8129637	0.03384934	-0.71846815	VNN2	vanin 2
8034578	0.03392588	-0.44430408	KLF1	Kruppel-like factor 1 (erythroid)
8172573	0.03396907	-0.42796571	SYP	synaptophysin
8043718	0.0340294	-0.35804576	COX5B	cytochrome c oxidase subunit Vb
7895873	0.03416901	-0.54949333		
8154848	0.03420829	-0.38688874	PRSS3///PRSS2	protease, serine, 3///protease, serine, 2 (trypsin 2)
8038782	0.03425367	-0.34151532	CTU1	cytosolic thiouridylase subunit 1
7892808	0.03429172	-0.35178188		
8046086	0.03432726	-0.47280196	CERS6	ceramide synthase 6
7930311	0.03451604	-0.38494613	GSTO2	glutathione S-transferase omega 2
7956668	0.03452285	-0.35508016		
7943760	0.03458118	-0.32568226	SIK2	salt-inducible kinase 2
8139889	0.03473559	-0.57016099		
8066513	0.03475014	-0.50765406	SDC4	syndecan 4
8071809	0.03475814	-1.11041942	GSTT2B///GSTT2	glutathione S-transferase theta 2B (gene/pseudogene)///glutathione S-transfera
8156058	0.03477317	-0.3385584		
7932794	0.03479717	-0.43998284		
8070863	0.03481119	-0.32447879	SSR4P1	signal sequence receptor, delta pseudogene 1
7926674	0.03486934	-0.39434239	PTF1A	pancreas specific transcription factor, 1a
7898673	0.03489448	-0.38741235		

7992678	0.03498186	-0.43720439	LOC652276	potassium channel tetramerisation domain containing 5 pseudogene
7894599	0.03506526	-0.8500798		
8100994	0.03521137	-0.89961072	CXCL2	chemokine (C-X-C motif) ligand 2
7896079	0.03523457	-0.78866393		
7945101	0.03531058	-0.33274163	DCPS	decapping enzyme, scavenger
8105302	0.03539902	-1.07895136	FST	follistatin
8039892	0.03575151	-0.31856104	KIR2DS5///KIR2DS3	killer cell immunoglobulin-like receptor, two domains, short cytoplasmic tail, 5///k immunoglobulin-like receptor, two domains, short cytoplasmic tail, 3
7907859	0.03583894	-0.36042964		
8170633	0.03585005	-0.41274458		
8175773	0.03585005	-0.41274458		
8084963	0.03587451	-0.5106764	PAK2	p21 protein (Cdc42/Rac)-activated kinase 2
8000467	0.03590794	-0.33572319	GSG1L	GSG1-like
7893500	0.03604075	-0.36131196		
8040547	0.03609127	-0.36165176		
8011990	0.03610252	-0.3392767	TEKT1	tektin 1
8034565	0.03613846	-0.35546524	DNASE2	deoxyribonuclease II, lysosomal
7924758	0.03615374	-0.68660195		
8143788	0.0362049	-0.31173326		
7941122	0.03622614	-0.42196295	SAC3D1	SAC3 domain containing 1
7968734	0.03622724	-0.430126	SLC25A15	solute carrier family 25 (mitochondrial carrier; ornithine transporter) member 15
8166455	0.03628888	-0.37811587	PRDX4	peroxiredoxin 4
8135392	0.03634644	-0.31292591	HBP1	HMG-box transcription factor 1
8018864	0.03637402	-0.97614025	SOCS3	suppressor of cytokine signaling 3
8130715	0.03637743	-0.31640538	PRR18	proline rich 18
8107100	0.03637959	-0.52635217	RGMB	RGM domain family, member B
7919600	0.0364701	-1.18776629		
8180277	0.03649965	-0.41422308	PCDHA3	protocadherin alpha 3
7970563	0.03653589	-0.3664252		
8107671	0.03656598	-0.49789462		
8111216	0.03662959	-0.31002799		
7999360	0.03669984	-0.35232371	RPL21P28///RPL21	ribosomal protein L21 pseudogene 28///ribosomal protein L21
8005097	0.03674099	-0.41900767	HS3ST3B1	heparan sulfate (glucosamine) 3-O-sulfotransferase 3B1
8024728	0.03680636	-0.4029797	NMRK2	nicotinamide riboside kinase 2
8108066	0.03683949	-0.30291868	UBE2B	ubiquitin-conjugating enzyme E2B
8166049	0.03687075	-0.31750506	PRPS2	phosphoribosyl pyrophosphate synthetase 2
8040516	0.0369157	-0.5051371	MFSD2B	major facilitator superfamily domain containing 2B
7974387	0.03694516	-0.31008798	STYX	serine/threonine/tyrosine interacting protein
8161190	0.03703269	-0.49644051		
8077441	0.03709841	-0.47519167	BHLHE40	basic helix-loop-helix family, member e40
8049187	0.0372187	-0.83626207	EFHD1	EF-hand domain family, member D1
7896070	0.03722737	-0.33076845		
8069676	0.03736156	-0.85879656	ADAMTS1	ADAM metallopeptidase with thrombospondin type 1 motif, 1
8090291	0.03743618	-0.41555263	ALG1L	ALG1, chitobiosyldiphosphodolichol beta-mannosyltransferase-like
7893424	0.03747201	-0.53942236		
8048705	0.03747287	-0.31537828		
7896239	0.03748422	-0.82097306		
7978748	0.03748752	-0.46587441	FBXO33	F-box protein 33
8142912	0.03752103	-0.36271778	TMEM209	transmembrane protein 209
8042788	0.03757364	-0.51907	ACTG2	actin, gamma 2, smooth muscle, enteric
8032525	0.03760865	-0.30075297	SLC39A3	solute carrier family 39 (zinc transporter), member 3
8000323	0.03761989	-0.31043876	NDUFAB1	NADH dehydrogenase (ubiquinone) 1, alpha/beta subcomplex, 1, 8kDa
8143040	0.03762051	-0.33487517	SLC35B4	solute carrier family 35, member B4
8042115	0.03765576	-0.31046491		
7974253	0.03766438	-0.36563707		
7896544	0.03767489	-0.42552135		
7980098	0.0377386	-0.3229128	CCDC176///ALDH6A1//	coiled-coil domain containing 176///aldehyde dehydrogenase 6 family, member A dehydrogenase 6 family, member A1
8151056	0.03776473	-0.44895028	CYP7B1	cytochrome P450, family 7, subfamily B, polypeptide 1
8162610	0.03790572	-0.31454809	CDC14B	cell division cycle 14B
8046680	0.03792176	-0.37746179	PLEKHA3	pleckstrin homology domain containing, family A (phosphoinositide binding spec
8148553	0.03792385	-0.33180889	LY6K	lymphocyte antigen 6 complex, locus K
7893640	0.03796471	-0.47023799		

7895180	0.0380123	-0.39490714		
7915084	0.03802175	-0.41401087	YRDC	yrdC domain containing (E. coli)
8131539	0.03805652	-0.42472604	TMEM106B	transmembrane protein 106B
7965510	0.03818661	-0.37599997	TMCC3	transmembrane and coiled-coil domain family 3
7892839	0.03828469	-0.52130725		
8086462	0.03828507	-0.34427825	GTDC2	glycosyltransferase-like domain containing 2
8146930	0.03831349	-0.37505013	TMEM70	transmembrane protein 70
7981309	0.03833545	-0.37944993	BEGAIN	brain-enriched guanylate kinase-associated
8157818	0.03840628	-0.34990148	WDR38	WD repeat domain 38
7896230	0.03847837	-0.32376766		
7998910	0.03849053	-0.3726705	CCDC64B	coiled-coil domain containing 64B
8088745	0.03856495	-0.40317011	FRMD4B	FERM domain containing 4B
8117045	0.0385961	-0.42829137	RBM24	RNA binding motif protein 24
7922717	0.03870875	-0.40204553	RGS16	regulator of G-protein signaling 16
8036557	0.0387583	-0.44289261		
8006569	0.03883207	-0.32168146	C17orf50	chromosome 17 open reading frame 50
7894519	0.0389427	-0.45007921		
7965508	0.03895378	-0.43266683		
8167880	0.03902056	-0.30822552	PAGE5	P antigen family, member 5 (prostate associated)
7892661	0.0390339	-0.34842873		
8136215	0.03911033	-0.33587842		
8013747	0.03911946	-0.30577509	PROCA1	protein interacting with cyclin A1
8151296	0.03918597	-0.44884649	LACTB2	lactamase, beta 2
8146115	0.03926141	-0.70187996	C8orf4	chromosome 8 open reading frame 4
7936242	0.03927188	-0.32557283	ITPRIP	inositol 1,4,5-trisphosphate receptor interacting protein
7917088	0.03939231	-0.47481236	PIGK	phosphatidylinositol glycan anchor biosynthesis, class K
7969651	0.03940047	-0.42909617	DNAJC3	DnaJ (Hsp40) homolog, subfamily C, member 3
7957467	0.03940386	-0.33457218	C12orf29///CEP290	chromosome 12 open reading frame 29///centrosomal protein 290kDa
7939465	0.0394497	-0.32307716	HSD17B12	hydroxysteroid (17-beta) dehydrogenase 12
8125316	0.03948778	-0.31327916	FKBPL	FK506 binding protein like
8043320	0.03967198	-0.42123852	LOC400965	uncharacterized LOC400965
7902074	0.03978258	-0.53527499	LEPROT///LEPR	leptin receptor overlapping transcript///leptin receptor
8139879	0.04009814	-0.40630081	SKP1	S-phase kinase-associated protein 1
8043022	0.0402328	-0.3720733		
7898693	0.04023794	-0.57118973	ALPL	alkaline phosphatase, liver/bone/kidney
8072113	0.04024057	-0.3599734	SRRD	SRR1 domain containing
7892682	0.04028159	-0.61767811		
8132897	0.04031903	-0.38316288	LANCL2	LanC lantibiotic synthetase component C-like 2 (bacterial)
7895149	0.04033131	-0.35104922		
8021707	0.04036137	-0.40527748	SOCS6	suppressor of cytokine signaling 6
7960253	0.04036618	-0.40279901	NINJ2	ninjurin 2
8180373	0.04044063	-0.30530173	SUMO1	small ubiquitin-like modifier 1
8131881	0.04050256	-0.51546753	FAM221A	family with sequence similarity 221, member A
7909888	0.04055082	-0.39481768		
7895876	0.04064224	-0.51776048		
7894830	0.04078726	-0.38072844		
8133704	0.04086501	-0.31752423	SRRM3///SRRM3	serine/arginine repetitive matrix 3///serine/arginine repetitive matrix 3
8143949	0.04092381	-0.31269606	CRYGN	crystallin, gamma N
8026292	0.04102516	-0.33918384	EEF1D	eukaryotic translation elongation factor 1 delta (guanine nucleotide exchange pr
8051215	0.04106882	-0.34905397	BRE-AS1///RBKS	BRE antisense RNA 1///ribokinase
7892603	0.04119487	-0.57770842		
7893641	0.04123141	-0.41225582		
8042532	0.04131916	-0.31021714	VAX2	ventral anterior homeobox 2
8090891	0.04135466	-0.33407575	EPHB1	EPH receptor B1
8114572	0.04145722	-0.69304903	HBEGF	heparin-binding EGF-like growth factor
7930304	0.04152995	-0.44213784	GSTO1	glutathione S-transferase omega 1
7894542	0.04163326	-0.45839945		
7978628	0.04169152	-0.303697	PPP2R3C	protein phosphatase 2, regulatory subunit B", gamma
8097461	0.04169451	-0.94018506	CCRN4L///CCRN4L	CCR4 carbon catabolite repression 4-like (S. cerevisiae)///CCR4 carbon catabol like (S. cerevisiae)
7910494	0.04171778	-0.38933035	ARV1	ARV1 homolog (S. cerevisiae)
8096733	0.04175978	-0.38660729	SGMS2	sphingomyelin synthase 2

7933872	0.0418679	-0.67145235	EGR2	early growth response 2
8000998	0.04187791	-0.3586624	VKORC1	vitamin K epoxide reductase complex, subunit 1
8105852	0.0419086	-0.32586931	MRPS36	mitochondrial ribosomal protein S36
7982574	0.04192064	-0.35892474	FAM98B	family with sequence similarity 98, member B
7978846	0.04198855	-0.41409048	POLE2	polymerase (DNA directed), epsilon 2, accessory subunit
7984405	0.04211497	-0.46112505	C15orf61	chromosome 15 open reading frame 61
8156761	0.04219894	-0.3833524	NANS	N-acetylneuraminic acid synthase
8038899	0.04239774	-0.51731989	FPR1	formyl peptide receptor 1
8065327	0.04247344	-0.43658117	NKX2-4	NK2 homeobox 4
7896060	0.04249677	-0.40557897		
8051949	0.04278211	-0.4063265	SIX2	SIX homeobox 2
7919564	0.04299338	-0.53504869		
7984103	0.04300036	-0.33968794	LACTB	lactamase, beta
8008980	0.04302428	-0.41815642	C17orf82	chromosome 17 open reading frame 82
8067111	0.04316854	-0.34170788		
7894165	0.04336137	-0.43868054		
8113369	0.04337134	-0.85935617	SLCO4C1	solute carrier organic anion transporter family, member 4C1
8037179	0.04340699	-0.36773145	CNFN	cornifelin
7964660	0.04343101	-1.04348582	AVPR1A	arginine vasopressin receptor 1A
7944623	0.04345925	-0.30698576	TBCEL	tubulin folding cofactor E-like
8067812	0.04353198	-0.33554639	C20orf201	chromosome 20 open reading frame 201
8154135	0.04367493	-0.48780871	SLC1A1	solute carrier family 1 (neuronal/epithelial high affinity glutamate transporter, sys member 1
8160531	0.04367916	-0.46596527	C9orf72	chromosome 9 open reading frame 72
7896581	0.04376155	-0.60576349		
8119161	0.04379688	-0.3655529	PIM1	pim-1 oncogene
7898594	0.04380584	-0.31414433	HTR6	5-hydroxytryptamine (serotonin) receptor 6, G protein-coupled
7953032	0.04385456	-0.31093702	LRTM2	leucine-rich repeats and transmembrane domains 2
8054154	0.0439285	-0.31709247	KIAA1211L	KIAA1211-like
8039269	0.04396328	-0.33332001	LENG8///LENG9	leukocyte receptor cluster (LRC) member 8///leukocyte receptor cluster (LRC) m
7930208	0.0439735	-0.32327182	INA	internexin neuronal intermediate filament protein, alpha
8023246	0.04427122	-0.44347621	C18orf32	chromosome 18 open reading frame 32
7962884	0.04428387	-0.91955532	RND1	Rho family GTPase 1
7935011	0.04430029	-0.37042566	CPEB3	cytoplasmic polyadenylation element binding protein 3
8057045	0.04431619	-0.35951489	FKBP7	FK506 binding protein 7
7897424	0.0443265	-0.31869502		
7975284	0.04434487	-0.37654479	RDH12	retinol dehydrogenase 12 (all-trans/9-cis/11-cis)
7892526	0.04444113	-0.54199907		
8103166	0.04454597	-0.36943995	SH3D19	SH3 domain containing 19
8162833	0.04468221	-0.33186974	ERP44	endoplasmic reticulum protein 44
7994961	0.04472426	-0.30552266	CTF1	cardiotrophin 1
7894119	0.04474271	-0.51751825		
8156043	0.04480562	-0.33093067	PSAT1	phosphoserine aminotransferase 1
7967660	0.04498187	-0.33108713	RIMBP2	RIMS binding protein 2
8064502	0.04504349	-0.34076308	SNRPB///SNRPB	small nuclear ribonucleoprotein polypeptides B and B1///small nuclear ribonucle polypeptides B and B1
8179221	0.04504621	-0.34468993	DPCR1	diffuse panbronchiolitis critical region 1
8122013	0.04529034	-0.43236609	L3MBTL3	l(3)mbt-like 3 (Drosophila)
7896278	0.04530243	-0.31632531		
8103892	0.04534194	-0.31818744		
8039389	0.0454938	-0.53296458	PTPRH	protein tyrosine phosphatase, receptor type, H
7894788	0.04554422	-0.44019559		
8154305	0.04564674	-0.32248636	SELT	selenoprotein T
7964832	0.04565144	-0.51531905		
8139460	0.04567281	-0.30409919	NACAD	NAC alpha domain containing
8080184	0.04572773	-0.43406508	ALAS1	aminolevulinate, delta-, synthase 1
8030749	0.0458141	-0.34302471		
8112327	0.04585459	-0.32325777	CKS1B	CDC28 protein kinase regulatory subunit 1B
8006634	0.04585563	-0.38575586	PIGW	phosphatidylinositol glycan anchor biosynthesis, class W
8144685	0.04588065	-0.46600653		
8028719	0.04588984	-0.30297679	DLL3	delta-like 3 (Drosophila)
8019074	0.04590943	-0.30784858	NPTX1	neuronal pentraxin I
8110237	0.04599519	-0.32463613	UNC5A	unc-5 homolog A (C. elegans)

8103399	0.0460248	-0.34168137	PDGFC	platelet derived growth factor C
8040270	0.04604606	-0.30668553	C2orf50	chromosome 2 open reading frame 50
8037502	0.04608252	-0.30936894	NKPD1	NTPase, KAP family P-loop domain containing 1
8138922	0.04609038	-0.43977166	KBTBD2	kelch repeat and BTB (POZ) domain containing 2
7984660	0.04614986	-0.59772748		
8109697	0.04618032	-0.34160251	CCNG1	cyclin G1
8056763	0.04626457	-0.50138702	RPS15	ribosomal protein S15
8175177	0.04644161	-0.40455334	MBNL3	muscleblind-like splicing regulator 3
7932227	0.04654376	-0.37299962	NMT2	N-myristoyltransferase 2
7947649	0.04664147	-0.33839254	CHRM4	cholinergic receptor, muscarinic 4
7936916	0.04666062	-0.37132291	FLJ40536	FLJ40536 protein
8021470	0.04669698	-0.30660694	PMAIP1	phorbol-12-myristate-13-acetate-induced protein 1
8073992	0.0467102	-0.31520528	PANX2	pannexin 2
7992732	0.04676855	-0.3732518	ZG16B	zymogen granule protein 16B
7895246	0.04695187	-0.58685476		
8139828	0.04705725	-0.3096443		
8137931	0.04714298	-0.31127236	MMD2	monocyte to macrophage differentiation-associated 2
8169920	0.04718826	-0.38944057	RBMX2	RNA binding motif protein, X-linked 2
7981783	0.0472862	-0.41832815	OR4N4	olfactory receptor, family 4, subfamily N, member 4
8106962	0.04735951	-0.38628844	ARSK	arylsulfatase family, member K
7940022	0.04739637	-0.43655	RTN4RL2	reticulon 4 receptor-like 2
7961626	0.04744029	-0.66688432	SLCO1A2	solute carrier organic anion transporter family, member 1A2
8175537	0.04757382	-0.49592705	SPANXA2-OT1	SPANXA2 overlapping transcript 1 (non-protein coding)
8074063	0.04763452	-0.39919584	ADM2	adrenomedullin 2
8090639	0.04775727	-0.33510458	PIK3R4	phosphoinositide-3-kinase, regulatory subunit 4
8092095	0.04777602	-0.39039726	TNIK	TRAF2 and NCK interacting kinase
8092314	0.04788819	-0.3010854	DNAJC19	DnaJ (Hsp40) homolog, subfamily C, member 19
7893652	0.04789673	-0.53847207		
7922472	0.04793304	-0.32057647		
7924603	0.04798643	-0.30569892	LBR	lamin B receptor
7945371	0.0480214	-0.31510022	IFITM3	interferon induced transmembrane protein 3
8023710	0.04803044	-0.47750003	CDH19	cadherin 19, type 2
8060418	0.04807919	-0.4299071	SIRPA	signal-regulatory protein alpha
7895267	0.04813092	-0.65876524		
7968670	0.04813242	-0.37148649	UFM1	ubiquitin-fold modifier 1
7988426	0.04815445	-0.37502611	SLC30A4	solute carrier family 30 (zinc transporter), member 4
8162825	0.04823702	-0.43122287		
8056730	0.04828219	-0.34111728	LOC440925	uncharacterized LOC440925
8049435	0.04832363	-0.3644272	SH3BP4	SH3-domain binding protein 4
7925043	0.04833157	-0.36887144	EXOC8///SPRTN	exocyst complex component 8///SprT-like N-terminal domain
8086949	0.04843583	-0.34862771	CCDC51	coiled-coil domain containing 51
8171161	0.04844577	-0.4643664	ARSE	arylsulfatase E (chondrodysplasia punctata 1)
7995866	0.04845392	-0.30480636	MIR138-2	microRNA 138-2
8080998	0.04845937	-0.42463023		
8110865	0.04848899	-0.31198208	IRX4	iroquois homeobox 4
7992716	0.04856993	-0.4012807	PRSS41	protease, serine, 41
8100202	0.04863039	-0.59941823	LOC280665///CNGA1	anti-CNG alpha 1 cation channel translation product-like///cyclic nucleotide gate
8033458	0.04865324	-0.31934509	LOC388499///LYPLA2	lysophospholipase II pseudogene///lysophospholipase II
8146427	0.04868957	-0.49228482	PCMTD1	protein-L-isoaspartate (D-aspartate) O-methyltransferase domain containing 1
8123936	0.04878114	-0.48467684	NEDD9///NEDD9	neural precursor cell expressed, developmentally down-regulated 9///neural pre expressed, developmentally down-regulated 9
7916120	0.04884725	-0.43140927	TXNDC12	thioredoxin domain containing 12 (endoplasmic reticulum)
7961865	0.04898419	-0.34980162	LYRM5///KRAS	LYR motif containing 5///v-Ki-ras2 Kirsten rat sarcoma viral oncogene homolog
8059731	0.04901827	-0.33575194	PDE6D	phosphodiesterase 6D, cGMP-specific, rod, delta
8003344	0.04902658	-0.33401686	SNAI3	snail family zinc finger 3
7987472	0.04908388	-0.32549584	C15orf56///C15orf56	chromosome 15 open reading frame 56///chromosome 15 open reading frame 5
8131600	0.04909259	-0.82742201	TSPAN13	tetraspanin 13
8052940	0.04913736	-0.34259164	PAIP2B	poly(A) binding protein interacting protein 2B
7896707	0.04927863	-0.396316		
7949843	0.04941305	-0.39256652	CABP2	calcium binding protein 2
8006433	0.04957766	-0.80150668	CCL2	chemokine (C-C motif) ligand 2
7923659	0.04970296	-0.30852482	PPP1R15B	protein phosphatase 1, regulatory subunit 15B

7983763	0.04971166	-0.46361643	MAPK6	mitogen-activated protein kinase 6
7941469	0.04977356	-0.36473252	TSGA10IP	testis specific, 10 interacting protein
8169699	0.04985667	-0.33899633		
8016841	0.04990781	-0.41095366	TMEM100	transmembrane protein 100
7902036	0.04997828	-0.34125517		

Comparison of *PTEN* expression in livers between 9 normal and 24 NAFLD/NASH individuals (female).

Probe ID	p-value	Log (Fold Change)	Gene Symbol	Gene Description
7928959	0.88502	-0.06754	PTEN	phosphatase and tensin homolog

Supplementary Table 2. 219 potential target genes of miR-21

miRNA	Gene Name	TargetScan Sites	PicTar Sites
hsa-miR-21-5p	KLHL15	1[18,912]	6[24,6206]
hsa-miR-21-5p	TNPO1	1[6,2277]	6[10,13308]
hsa-miR-21-5p	KLHDC5	1[7,161]	5[9,250]
hsa-miR-21-5p	PLAG1	3[7,512]	5[8,579]
hsa-miR-21-5p	UBE2K	0[0,0]	4[5,104]
hsa-miR-21-5p	YOD1	2[9,3030]	4[11,3172]
hsa-miR-21-5p	HNRNPU	1[5,110]	3[9,114]
hsa-miR-21-5p	CNOT6	1[2,21]	3[8,1002]
hsa-miR-21-5p	RASA1	1[7,212]	3[7,295]
hsa-miR-21-5p	SUZ12	0[0,0]	3[6,1166]
hsa-miR-21-5p	ITGB8	1[4,151]	3[6,1126]
hsa-miR-21-5p	SCML2	1[2,416]	3[5,439]
hsa-miR-21-5p	MAP3K1	1[5,195]	3[5,326]
hsa-miR-21-5p	PURA	0[0,0]	3[5,238]
hsa-miR-21-5p	ACBD5	0[0,0]	3[5,187]
hsa-miR-21-5p	POM121	1[1,1]	3[5,121]
hsa-miR-21-5p	MTAP	1[4,132]	3[4,290]
hsa-miR-21-5p	MTMR12	1[4,35]	3[4,286]
hsa-miR-21-5p	RPS6KA3	1[1,61]	3[4,145]
hsa-miR-21-5p	SLC7A6	1[1,4]	3[3,154]
hsa-miR-21-5p	ZNF367	2[22,8223]	3[22,8379]
hsa-miR-21-5p	RP2	0[0,0]	3[2,53]
hsa-miR-21-5p	TNRC6B	2[15,1113]	3[15,1160]
hsa-miR-21-5p	PURB	1[1,30]	3[12,1575]
hsa-miR-21-5p	CUX1	2[10,536]	3[11,752]
hsa-miR-21-5p	NFIB	1[9,662]	3[11,1028]
hsa-miR-21-5p	LEMD3	1[8,395]	2[9,400]
hsa-miR-21-5p	FRS2	1[1,113]	2[9,392]
hsa-miR-21-5p	YAP1	1[8,191]	2[9,287]
hsa-miR-21-5p	C17orf39	1[1,19]	2[9,227]
hsa-miR-21-5p	SMAD7	1[7,476]	2[8,499]
hsa-miR-21-5p	CPEB3	1[7,562]	2[7,625]
hsa-miR-21-5p	FCHO2	0[0,0]	2[7,533]
hsa-miR-21-5p	PBRM1	1[7,336]	2[7,355]
hsa-miR-21-5p	RMND5A	1[5,1139]	2[7,1393]
hsa-miR-21-5p	DNAJC16	1[3,97]	2[7,106]
hsa-miR-21-5p	AKIRIN1	0[0,0]	2[7,1054]
hsa-miR-21-5p	SPRY2	1[1,35]	2[6,77]
hsa-miR-21-5p	RBPJ	1[1,149]	2[6,686]
hsa-miR-21-5p	ZNF704	0[0,0]	2[6,40]
hsa-miR-21-5p	FAM46A	0[0,0]	2[6,3417]
hsa-miR-21-5p	SATB1	2[6,116]	2[6,116]
hsa-miR-21-5p	PPP1R3B	2[5,64]	2[5,64]

hsa-miR-21-5p	HBP1	0[0,0]	2[5,207]
hsa-miR-21-5p	RNF111	0[0,0]	2[5,189]
hsa-miR-21-5p	PLEKHA1	1[3,514]	2[4,583]
hsa-miR-21-5p	TGFBR2	1[2,3562]	2[4,3696]
hsa-miR-21-5p	EPHA4	1[3,28]	2[4,34]
hsa-miR-21-5p	CSRNP3	1[1,18]	2[4,154]
hsa-miR-21-5p	FBXO11	1[3,1]	2[4,14]
hsa-miR-21-5p	PIK3R1	2[4,108]	2[4,108]
hsa-miR-21-5p	MATR3	0[0,0]	2[3,78]
hsa-miR-21-5p	THRB	2[3,66]	2[3,66]
hsa-miR-21-5p	MKRN1	0[0,0]	2[3,45]
hsa-miR-21-5p	MEF2A	0[0,0]	2[3,279]
hsa-miR-21-5p	POM121C	1[2,7]	2[3,20]
hsa-miR-21-5p	RBMS3	1[2,60]	2[2,68]
hsa-miR-21-5p	IMPAD1	0[0,0]	2[2,66]
hsa-miR-21-5p	STAT3	1[2,168]	2[2,407]
hsa-miR-21-5p	CD47	0[0,0]	2[2,36]
hsa-miR-21-5p	PVRL3	0[0,0]	2[2,354]
hsa-miR-21-5p	ZSWIM6	1[3,395]	2[2,332]
hsa-miR-21-5p	MEF2C	1[1,17]	2[2,25]
hsa-miR-21-5p	RSBN1	0[0,0]	2[2,16]
hsa-miR-21-5p	SOX7	1[2,109]	2[2,109]
hsa-miR-21-5p	GLCCI1	1[16,1845]	2[17,2071]
hsa-miR-21-5p	ZCCHC3	1[10,1917]	2[17,1997]
hsa-miR-21-5p	SKI	1[10,643]	2[13,1587]
hsa-miR-21-5p	ADNP	1[10,455]	2[11,478]
hsa-miR-21-5p	CDC25A	1[10,123]	2[11,292]
hsa-miR-21-5p	GATAD2B	2[10,1633]	2[10,1633]
hsa-miR-21-5p	SYT14	0[0,0]	1[8,333]
hsa-miR-21-5p	BTG2	1[8,2272]	1[8,2272]
hsa-miR-21-5p	FAM63B	1[8,214]	1[8,214]
hsa-miR-21-5p	KIAA1468	0[0,0]	1[7,79]
hsa-miR-21-5p	BTBD3	0[0,0]	1[7,3161]
hsa-miR-21-5p	BCL2	1[7,276]	1[7,276]
hsa-miR-21-5p	E2F3	0[0,0]	1[7,259]
hsa-miR-21-5p	PITX2	1[7,175]	1[7,175]
hsa-miR-21-5p	MSL1	1[7,138]	1[7,138]
hsa-miR-21-5p	ATXN10	0[0,0]	1[6,924]
hsa-miR-21-5p	RAB6A	1[6,64]	1[6,64]
hsa-miR-21-5p	MRPL49	1[6,58]	1[6,58]
hsa-miR-21-5p	SPG20	1[6,286]	1[6,286]
hsa-miR-21-5p	TIMP3	1[6,136]	1[6,136]
hsa-miR-21-5p	KRIT1	1[6,124]	1[6,124]
hsa-miR-21-5p	IL12A	1[6,105]	1[5,96]
hsa-miR-21-5p	UBR3	1[5,93]	1[5,93]
hsa-miR-21-5p	PCBP1	1[5,92]	1[5,92]

hsa-miR-21-5p	TAF5	0[0,0]	1[5,87]
hsa-miR-21-5p	RHOB	1[5,5598]	1[5,5598]
hsa-miR-21-5p	ASF1A	1[5,49]	1[5,49]
hsa-miR-21-5p	SMARCD1	1[5,36]	1[5,36]
hsa-miR-21-5p	CHD7	1[5,3304]	1[5,3304]
hsa-miR-21-5p	LRRC57	1[4,79]	1[4,79]
hsa-miR-21-5p	BCL11A	1[4,43]	1[4,43]
hsa-miR-21-5p	PAN3	1[4,42]	1[4,42]
hsa-miR-21-5p	BRD1	0[0,0]	1[4,163]
hsa-miR-21-5p	TRIM33	1[4,155]	1[4,155]
hsa-miR-21-5p	AP1AR	1[3,75]	1[3,75]
hsa-miR-21-5p	PDZD2	1[3,73]	1[3,73]
hsa-miR-21-5p	SCRN1	1[3,70]	1[3,70]
hsa-miR-21-5p	NFIA	1[3,55]	1[3,55]
hsa-miR-21-5p	GLYR1	1[3,428]	1[3,428]
hsa-miR-21-5p	ALX1	1[3,33]	1[3,33]
hsa-miR-21-5p	ZDHHC17	0[0,0]	1[3,178]
hsa-miR-21-5p	RECK	1[3,161]	1[3,161]
hsa-miR-21-5p	DLX2	1[3,146]	1[3,146]
hsa-miR-21-5p	KIAA2026	0[0,0]	1[3,108]
hsa-miR-21-5p	CBX4	1[22,2569]	1[22,2569]
hsa-miR-21-5p	SPIN1	0[0,0]	1[2,94]
hsa-miR-21-5p	TGFBI	1[2,930]	1[2,930]
hsa-miR-21-5p	MBTPS2	0[0,0]	1[2,8]
hsa-miR-21-5p	PPP3CA	1[2,497]	1[2,497]
hsa-miR-21-5p	PER2	1[2,484]	1[2,484]
hsa-miR-21-5p	C11orf95	1[2,48]	1[2,48]
hsa-miR-21-5p	PPARA	1[2,40]	1[2,40]
hsa-miR-21-5p	JHDM1D	1[2,39]	1[2,39]
hsa-miR-21-5p	SOS2	0[0,0]	1[2,33]
hsa-miR-21-5p	SLC9A6	0[0,0]	1[2,288]
hsa-miR-21-5p	PCSK6	1[2,232]	1[2,232]
hsa-miR-21-5p	EHD1	1[2,228]	1[2,228]
hsa-miR-21-5p	TESK2	0[0,0]	1[2,20]
hsa-miR-21-5p	PCBP2	1[2,171]	1[2,171]
hsa-miR-21-5p	PSRC1	0[0,0]	1[2,171]
hsa-miR-21-5p	CRIM1	0[0,0]	1[2,1621]
hsa-miR-21-5p	KLF6	1[2,137]	1[2,137]
hsa-miR-21-5p	WWP1	1[2,132]	1[2,132]
hsa-miR-21-5p	ARHGAP24	1[2,13]	1[2,13]
hsa-miR-21-5p	TSHZ1	0[0,0]	1[2,115]
hsa-miR-21-5p	UBE2D3	1[2,105]	1[2,105]
hsa-miR-21-5p	STK40	1[2,0]	1[2,0]
hsa-miR-21-5p	XKR6	1[2,0]	1[2,0]
hsa-miR-21-5p	PELI1	1[19,4917]	1[19,4917]
hsa-miR-21-5p	EIF2C2	0[0,0]	1[19,1480]

hsa-miR-21-5p	PDCD4	1[18,1672]	1[18,1672]
hsa-miR-21-5p	MBNL1	1[15,3279]	1[15,3279]
hsa-miR-21-5p	STAG2	1[14,394]	1[14,394]
hsa-miR-21-5p	KLF3	1[11,4344]	1[11,4344]
hsa-miR-21-5p	EIF1AX	1[10,269]	1[10,269]
hsa-miR-21-5p	DAZL	0[0,0]	1[1,9]
hsa-miR-21-5p	NAA50	0[0,0]	1[1,6]
hsa-miR-21-5p	RASGRP1	1[1,5]	1[1,5]
hsa-miR-21-5p	SETD1B	1[1,47]	1[1,47]
hsa-miR-21-5p	NIPBL	0[0,0]	1[1,212]
hsa-miR-21-5p	SSFA2	0[0,0]	1[1,1996]
hsa-miR-21-5p	ELF2	1[1,19]	1[1,19]
hsa-miR-21-5p	MATN2	1[2,30]	1[1,17]
hsa-miR-21-5p	GLIS2	1[1,125]	1[1,125]
hsa-miR-21-5p	JPH1	1[1,12]	1[1,12]
hsa-miR-21-5p	MAPRE1	0[0,0]	1[1,11]
hsa-miR-21-5p	VCL	2[7,576]	0[0,0]
hsa-miR-21-5p	RAB22A	2[6,2476]	0[0,0]
hsa-miR-21-5p	PTPN9	1[9,425]	0[0,0]
hsa-miR-21-5p	FBXO28	1[9,137]	0[0,0]
hsa-miR-21-5p	ZNF217	1[8,1458]	0[0,0]
hsa-miR-21-5p	BRWD1	1[7,682]	0[0,0]
hsa-miR-21-5p	GNG12	1[6,587]	0[0,0]
hsa-miR-21-5p	LRP6	1[6,345]	0[0,0]
hsa-miR-21-5p	PTPN14	1[6,1660]	0[0,0]
hsa-miR-21-5p	ZFP36L2	1[6,115]	0[0,0]
hsa-miR-21-5p	DNAJA2	1[5,96]	0[0,0]
hsa-miR-21-5p	GAB1	1[5,831]	0[0,0]
hsa-miR-21-5p	CHIC1	1[5,50]	0[0,0]
hsa-miR-21-5p	SC5DL	1[5,245]	0[0,0]
hsa-miR-21-5p	SESTD1	1[5,164]	0[0,0]
hsa-miR-21-5p	DCUN1D3	1[4,69]	0[0,0]
hsa-miR-21-5p	GTPBP1	1[4,62]	0[0,0]
hsa-miR-21-5p	PRKCE	1[4,45]	0[0,0]
hsa-miR-21-5p	MAP2K3	1[4,37]	0[0,0]
hsa-miR-21-5p	PFKM	1[4,336]	0[0,0]
hsa-miR-21-5p	EIF4EBP2	1[4,303]	0[0,0]
hsa-miR-21-5p	SNTB2	1[4,214]	0[0,0]
hsa-miR-21-5p	RFFL	1[3,84]	0[0,0]
hsa-miR-21-5p	EIF2C4	1[3,6]	0[0,0]
hsa-miR-21-5p	PAG1	1[3,50]	0[0,0]
hsa-miR-21-5p	PGRMC2	1[3,469]	0[0,0]
hsa-miR-21-5p	S100A10	1[3,381]	0[0,0]
hsa-miR-21-5p	GXYLT1	1[3,336]	0[0,0]
hsa-miR-21-5p	LIFR	1[3,3256]	0[0,0]
hsa-miR-21-5p	FOXP2	1[3,32]	0[0,0]

hsa-miR-21-5p	5-Mar	1[3,14]	0[0,0]
hsa-miR-21-5p	BCL7A	1[21,973]	0[0,0]
hsa-miR-21-5p	UBN2	1[2,99]	0[0,0]
hsa-miR-21-5p	TNFRSF11B	1[2,91]	0[0,0]
hsa-miR-21-5p	KLF5	1[2,823]	0[0,0]
hsa-miR-21-5p	ARMCX1	1[2,78]	0[0,0]
hsa-miR-21-5p	DUSP8	1[2,66]	0[0,0]
hsa-miR-21-5p	TOPORS	1[2,61]	0[0,0]
hsa-miR-21-5p	TET1	1[2,38]	0[0,0]
hsa-miR-21-5p	AIM1L	1[2,37]	0[0,0]
hsa-miR-21-5p	MBLAC2	1[2,35]	0[0,0]
hsa-miR-21-5p	MSH2	1[2,325]	0[0,0]
hsa-miR-21-5p	SLC10A7	1[2,26]	0[0,0]
hsa-miR-21-5p	COL4A1	1[2,2419]	0[0,0]
hsa-miR-21-5p	GPR64	1[2,24]	0[0,0]
hsa-miR-21-5p	BMPR2	1[2,210]	0[0,0]
hsa-miR-21-5p	ZBTB47	1[2,2042]	0[0,0]
hsa-miR-21-5p	MCTP2	1[2,20]	0[0,0]
hsa-miR-21-5p	C5orf41	1[2,137]	0[0,0]
hsa-miR-21-5p	SESN1	1[2,132]	0[0,0]
hsa-miR-21-5p	C17orf75	1[2,13]	0[0,0]
hsa-miR-21-5p	FAM3C	1[2,12]	0[0,0]
hsa-miR-21-5p	ARHGEF12	1[2,11]	0[0,0]
hsa-miR-21-5p	CCR7	1[2,108]	0[0,0]
hsa-miR-21-5p	C10orf12	1[2,10]	0[0,0]
hsa-miR-21-5p	BRD2	1[17,667]	0[0,0]
hsa-miR-21-5p	CDK6	1[13,1469]	0[0,0]
hsa-miR-21-5p	KBTBD6	1[11,635]	0[0,0]
hsa-miR-21-5p	ARHGAP31	1[1,8]	0[0,0]
hsa-miR-21-5p	FAM126B	1[1,70]	0[0,0]
hsa-miR-21-5p	HSDL2	1[1,6]	0[0,0]
hsa-miR-21-5p	MBNL3	1[1,5]	0[0,0]
hsa-miR-21-5p	DAG1	1[1,213]	0[0,0]
hsa-miR-21-5p	PIKFYVE	1[1,21]	0[0,0]
hsa-miR-21-5p	TNS1	1[1,189]	0[0,0]
hsa-miR-21-5p	RALGPS2	1[1,13]	0[0,0]
hsa-miR-21-5p	FAM13A	1[1,13]	0[0,0]
hsa-miR-21-5p	LMBR1	1[1,107]	0[0,0]

Supplementary Table 3. Thirteen down-regulated genes in livers of human NAFLD/NASH that have binding motifs for miR-21.

P Value	Log FC/Fatty liver/Normal)	Gene symbol	Gene Name	miRNA	TargetScan Sites	PicTar Sites
0.01630449	-0.54013801	KLHL15	kelch-like family member 15	hsa-miR-21-5p	1[18,912]	6[24,6206]
0.04430029	-0.37042566	CPEB3	cytoplasmic polyadenylation element binding protein 3	hsa-miR-21-5p	1[7,562]	2[7,625]
0.03634644	-0.31292591	HBP1	HMG-box transcription factor 1	hsa-miR-21-5p	0[0,0]	2[5,207]
0.02570623	-0.39409707	IMPAD1	inositol monophosphatase domain containing 1	hsa-miR-21-5p	0[0,0]	2[2,66]
0.00491062	-0.34885596	PVRL3	poliovirus receptor-related 3	hsa-miR-21-5p	0[0,0]	2[2,354]
0.00865386	-0.43339143	SOX7	SRY (sex determining region Y)-box 7	hsa-miR-21-5p	1[2,109]	2[2,109]
0.00260512	-0.71029488	RHOB	ras homolog family member B	hsa-miR-21-5p	1[5,5598]	1[5,5598]
0.03194318	-0.3484977	AP1AR	adaptor-related protein complex 1 associated regulatory protein	hsa-miR-21-5p	1[3,75]	1[3,75]
0.00897159	-0.31889815	MBTPS2	membrane-bound transcription factor peptidase, site 2	hsa-miR-21-5p	0[0,0]	1[2,8]
0.01321711	-1.08633018	KLF6	Kruppel-like factor 6	hsa-miR-21-5p	1[2,137]	1[2,137]
0.02377635	-0.44395978	TNFRSF11B	tumor necrosis factor receptor superfamily, member 11b	hsa-miR-21-5p	1[2,91]	0[0,0]
0.03118009	-0.75072228	KLF5	Kruppel-like factor 5 (intestinal)	hsa-miR-21-5p	1[2,823]	0[0,0]
0.04644161	-0.40455334	MBNL3	muscleblind-like splicing regulator 3	hsa-miR-21-5p	1[1,5]	0[0,0]

Supplementary Table 4. qRT-PCR primers used in this study

Gene Name	Forward primer	Reverse primer
Human *HBP1*	GAGTGAACCAGCCTTCCCTCAT	ACAGTGCCAGACAGTTGAAGGC
Moue *Hbp1*	TGGCTTGCTCACTGTAGAGTGC	CAGGAGGTAGACATACGTCACC
Human *p53*	CCTCAGCATCTTATCCGAGTGG	TGGATGGTGGTACAGTCAGAGC
Mouse *p53*	CACGTACTCTCCTCCCCTCAAT	AACTGCACAGGGCACGTCTT
Human *SREBP1C*	ACTTCTGGAGGCATCGCAAGCA	AGGTTCCAGAGGAGGCTACAAG
Mouse *Srebp1c*	CGACTACATCCGCTTCTTGCAG	CCTCCATAGACACATCTGTGCC
Human *FASN*	TTCTACGGCTCCACGCTCTTCC	GAAGAGTCTTCGTCAGCCAGGA
Mouse *Fasn*	CACAGTGCTCAAAGGACATGCC	CACCAGGTGTAGTGCCTTCCTC
Human *SCD1*	CCTGGTTTCACTTGGAGCTGTG	TGTGGTGAAGTTGATGTGCCAGC
Mouse *Scd1*	GCAAGCTCTACACCTGCCTCTT	CGTGCCTTGTAAGTTCTGTGGC
Human *GPAT*	TTGTGGCTTGCCTGCTCCTCTA	AATCACGAGCCAGGACTTCCTC
Mouse *Gpat*	GCAAGCACTGTTACCAGCGATC	TGCAATCAGCCTTCGTCGGAAG
Human *CCND1*	TCTACACCGACAACTCCATCCG	TCTGGCATTTTGGAGAGGAAGTG
Mouse *Ccnd1*	GCAGAAGGAGATTGTGCCATCC	AGGAAGCGGTCCAGGTAGTTCA
Human *CCNB1*	GACCTGTGTCAGGCTTTCTCTG	GGTATTTTGGTCTGACTGCTTGC
Mouse *Ccnb1*	AGAGGTGGAACTTGCTGAGCCT	GCACATCCAGATGTTTCCATCGG

Supplementary Table 5. miRNAs that are highly and specifically expressed in hepatocytes.

	Ct		ΔCt		$2^{-\Delta Ct}$		Ct		ΔCt		$2^{-\Delta Ct}$		Ave. $2^{-\Delta Ct}$		Fold Change
miRNA ID	**WT1**	**WT2**	**WT1**	**WT2**	**WT1**	**WT2**	**DKO1**	**DKO2**	**DKO1**	**DKO2**	**DKO1**	**DKO2**	**WT**	**DKO**	**DKO/WT**
mmu-miR-21	25.504	23.928	8.516	6.348	0.00273167	0.0122761	33.838	26.752	17.688	11.300	4.7357E-06	0.00039661	0.007503905	0.000200672	0.026742
mmu-miR-122	22.365	21.345	5.377	3.765	0.02406367	0.0735567	26.180	24.536	10.030	9.084	0.00095646	0.00184265	0.048810186	0.001399559	0.028674
mmu-miR-192	23.378	22.054	6.390	4.474	0.0119239	0.0449978	26.303	24.690	10.153	9.238	0.0008783	0.00165609	0.028460862	0.001267196	0.044524
mmu-miR-30c	23.793	22.661	6.805	5.081	0.00894316	0.0295438	26.099	25.122	9.949	9.670	0.0010117	0.00122755	0.019243496	0.001119627	0.058182
hsa-miR-30a-3p	23.769	24.231	6.781	6.651	0.00909318	0.0099506	25.672	26.853	9.522	11.401	0.00136017	0.00036979	0.00952189	0.000864979	0.090841
mmu-miR-19b	24.509	22.691	7.521	5.111	0.00544444	0.0289358	27.076	24.557	10.926	9.105	0.00051398	0.00181603	0.017190126	0.001165003	0.067772
mmu-miR-30b	24.212	23.308	7.224	5.728	0.00668897	0.0188669	26.802	25.150	10.652	9.698	0.00062148	0.00120396	0.012777924	0.00091272	0.071429
mmu-let-7g	26.364	25.287	9.376	7.707	0.00150502	0.0047859	28.757	27.006	12.607	11.554	0.00016029	0.00033258	0.00314545	0.000246438	0.078347
mmu-miR-30e	25.973	24.847	8.985	7.267	0.00197354	0.0064925	27.878	27.017	11.728	11.565	0.0002948	0.00033006	0.004233042	0.000312426	0.073806
mmu-miR-29a	24.430	22.458	7.442	4.878	0.00575088	0.0340076	26.324	24.590	10.174	9.138	0.00086561	0.00177496	0.019879228	0.001320282	0.066415
mmu-miR-26b	26.134	24.538	9.146	6.958	0.00176514	0.0080433	28.187	26.264	12.037	10.812	0.00023796	0.00055624	0.004904211	0.0003971	0.080971
mmu-miR-26a	25.490	23.226	8.502	5.646	0.00275831	0.0199703	27.288	24.873	11.138	9.421	0.00044374	0.0014588	0.011364307	0.000951271	0.083707
mmu-miR-17	25.260	24.397	8.272	6.817	0.00323504	0.0088691	26.815	25.722	10.665	10.270	0.00061591	0.00080988	0.006052062	0.000712895	0.117794
mmu-miR-106a	26.483	25.696	9.495	8.116	0.00138586	0.0036045	27.867	27.027	11.717	11.575	0.00029705	0.00032778	0.002495164	0.000312414	0.125208
mmu-miR-484	25.192	25.251	8.204	7.671	0.00339117	0.0049068	26.622	26.389	10.472	10.937	0.00070407	0.00051008	0.004148991	0.000607072	0.146318
mmu-miR-125b-5p	27.341	26.233	10.353	8.653	0.0007646	0.0024842	28.758	27.099	12.608	11.647	0.00016018	0.00031182	0.001624405	0.000236001	0.145285
mmu-miR-191	23.274	23.119	6.286	5.539	0.0128152	0.0215078	24.210	24.156	8.060	8.704	0.00374713	0.00239792	0.017161476	0.003072524	0.179036
mmu-miR-24	23.695	22.427	6.707	4.847	0.00957176	0.0347462	24.886	22.981	8.736	7.529	0.00234532	0.00541433	0.022158993	0.003879826	0.17509
mmu-miR-16	22.631	22.048	5.643	4.468	0.02001187	0.0451854	23.136	22.835	6.986	7.383	0.00788868	0.00599095	0.03259862	0.006939818	0.212887
mmu-miR-2134	16.977	18.260	-0.011	0.680	1.00765426	0.6241652	17.246	18.971	1.096	3.519	0.46781165	0.08723188	0.815909718	0.277521769	0.340138
mmu-miR-2146	20.563	21.864	3.575	4.284	0.0839108	0.0513319	21.240	22.102	5.090	6.650	0.02936009	0.00995751	0.067621352	0.0196588	0.290719
mmu-miR-142-3p	28.469	27.431	11.481	9.851	0.00034984	0.0010828	29.132	27.100	12.982	11.648	0.0001236	0.0003116	0.000716329	0.000217603	0.303776
mmu-miR-126-3p	21.265	20.774	4.277	3.194	0.05158161	0.1092723	21.934	20.262	5.784	4.810	0.01814857	0.03564889	0.080426962	0.026898731	0.334449
mmu-miR-139-5p	27.021	26.326	10.033	8.746	0.00095448	0.0023291	27.314	26.078	11.164	10.626	0.00043581	0.00063278	0.001641798	0.000534299	0.325435

mmu-miR-1937b	18.374	18.697	1.386	1.117	0.38262405	0.4610514	18.818	18.287	2.668	2.835	0.15734456	0.1401457	0.421837722	0.148745128	0.352612
mmu-miR-145	27.880	25.955	10.892	8.375	0.00052624	0.0030121	28.442	25.423	12.292	9.971	0.00019941	0.00099639	0.001769184	0.000597899	0.337952
mmu-miR-486	26.424	26.279	9.436	8.699	0.00144371	0.0024062	26.161	26.332	10.011	10.880	0.00096915	0.00053063	0.00192498	0.000749889	0.389557
mmu-miR-126-5p	25.840	24.903	8.852	7.323	0.00216413	0.0062454	26.368	24.118	10.218	8.666	0.00083961	0.00246192	0.004204742	0.001650763	0.392596
mmu-miR-805	23.583	24.462	6.595	6.882	0.01034444	0.0084784	23.665	23.949	7.515	8.497	0.00546713	0.00276789	0.009411399	0.004117508	0.437502
mmu-miR-146a	25.255	24.807	8.267	7.227	0.00324627	0.0066751	25.608	24.004	9.458	8.552	0.00142186	0.00266435	0.004960677	0.002043108	0.411861
mmu-miR-1937c	21.345	21.400	4.357	3.820	0.04879918	0.0708053	21.443	20.826	5.293	5.374	0.02550633	0.02411375	0.05980222	0.02481004	0.414868
mmu-miR-721	22.005	24.120	5.017	6.540	0.03088394	0.0107464	23.009	22.368	6.859	6.916	0.0086146	0.00828088	0.020815179	0.00844774	0.405845
mmu-miR-223	27.620	26.374	10.632	8.794	0.00063016	0.0022529	27.790	25.456	11.640	10.004	0.00031334	0.00097386	0.001441529	0.000643598	0.446469
mmu-miR-150	27.367	27.284	10.379	9.704	0.00075095	0.001199	27.315	26.413	11.165	10.961	0.00043551	0.00050166	0.000974954	0.000468586	0.480624

Supplementary Table 6. Comparison of mice treated with miR-21-ASO or miR-21-MM-ASO for 4 weeks

Parameter	miR-21-MM-ASO treated mice	miR-21-ASO treated mice
Body weight (g)	34±3	32±4
Liver weight	1.9±0.3	1.7±0.5
Liver cholesterol concentration (mg/g)	3.8±0.7	4.0±0.7
Total plasma cholesterol(mg/dl)	140±19	129±16.2
Total plasma triglycerides (mg/dl)	113±20.3	105±10.3

Supplementary Table 7. Comparison of mice treated with miR-21-ASO or miR-21-MM-ASO for 8 weeks

Parameter	miR-21-MM-ASO treated mice	miR-21-ASO treated mice
Body weight (g)	43±4	41±3.4
Liver weight (g)	2.4±0.4	1.9±0.38*
Liver cholesterol concentration (mg/g)	4.5±0.6	4.3±0.5
Liver triglyceride concentration (mg/g)	142±16	75±8.1*
Total plasma cholesterol(mg/dl)	191±21	179±14.6
Total plasma triglycerides (mg/dl)	143±15.2	136±9.8

Supplementary Table 8. Comparison of serum chemistries of mice treated with miR-21-ASO or miR-21-MM-ASO

ASO	ASO treatment (weeks)	Albumin (g/dL)	Total Bilirubin (mg/dL)	ALP (U/L)	ALT (U/L)	AST (U/L)
miR-21-MM-ASO (control)	4	3.21+0.15	0.37+0.08	56.8+9.3	52.1+2.4	326.6+19.7
miR-21-ASO	4	3.28+0.18	0.31+0.14	45.0+15.8	40.7+2.3*	261.8+23.8*
miR-21-MM-ASO (control)	8	3.45+0.17	0.28+0.03	74.75+6.7	55.3+7.8	337.8+30.8
miR-21-ASO	8	3.61+0.29	0.23+0.05	58.6+23.27	48.8+5.60	231.16+24.1*

Table 1. 1219 down-regulated probes in livers of human patients with NAFLD/NASH.

Table 2. 219 potential target genes of miR-21.

Table 3. Thirteen down-regulated genes in livers of human NAFLD/NASH that have binding motifs for miR-21.

Table 4. RT-PCR primers used in this study

Table 5. miRNAs that are highly expressed in hepatocytes. Highly-expressed miRNAs were identified by comparing miRNA profiles of livers between wild-type and *Dicer1* knockout mice. Internal control is U6 nuclear small RNA and U6 was measured five times in each sample. The average Ct value of U6: WT1: 16.998; WT2: 17.58; DKO1: 16.150; and DKO2: 15.452. WT: Wild type; and DKO: *Dicer1* knockout.

Table 6. Comparison of mice treated with miR-21-ASO and miR-21-MM-ASO for four weeks. Data represent mean ± SD. Mann-Whitney was used for statistical analysis.

Table 7. Comparison of mice treated with miR-21-ASO and miR-21-MM-ASO for eight weeks. Data represent mean ± SD. Mann-Whitney was used for statistical analysis. *$p < 0.05$.

Table 8. Comparison of serum chemistry of mice treated with miR-21-ASO and miR-21-MM-ASO. Data represent mean ± SD. Mann-Whitney was used for statistical analysis. *$p < 0.05$.